UCRL-ID-122436

Evaluated cross-sections libraries and kerma factors for neutrons up to 100 MeV on ^{16}O and ^{14}N

M. B. Chadwick
Nuclear Data Group, Lawrence Livermore National Laboratory, Livermore, CA 94551-0808

P.G. Young
Theoretical Division, Los Alamos National Laboratory, Los Alamos, NM 87545

July, 1995

This is an informal report intended primarily for internal or limited external distribution. The opinions and conclusions stated are those of the author and may or may not be those of the Laboratory.
Work performed under the auspices of the U.S. Department of Energy by the Lawrence Livermore National Laboratory under Contract W-7405-Eng-48.

Available to DOE and DOE contractors from the
Office of Scientific and Technical Information
P.O. Box 62, Oak Ridge, TN 37831
Prices available from (615) 576-8401, FTS 626-8401

Available to the public from the
National Technical Information Service
U.S. Department of Commerce
5285 Port Royal Rd.,
Springfield, VA 22161

Lawrence Livermore National Laboratory
UCRL-ID-??????
July 1995

Evaluated cross-section libraries and kerma factors for neutrons up to 100 MeV on ^{16}O and ^{14}N

M. B. Chadwick
P. G. Young

TABLE OF CONTENTS

Evaluated cross section libraries and kerma factors for neutrons up to 100 MeV on ^{16}O and ^{14}N

M. B. Chadwick
University of California, Nuclear Data Group,
Lawrence Livermore National Laboratory, Livermore, CA 94550

P. G. Young
University of California, Theoretical Division,
Los Alamos National Laboratory, Los Alamos, NM 87545

We present evaluations of the interaction of 20 to 100 MeV neutrons with oxygen and nitrogen nuclei, which follows on from our previous work on carbon [1]. Our aim is to accurately represent integrated cross sections, inclusive emission spectra, and kerma factors, in a data library which can be used in radiation transport calculations. We apply the FKK-GNASH nuclear model code, which includes Hauser-Feshbach, preequilibrium, and direct reaction mechanisms, and use experimental measurements to optimize the calculations. We determine total, elastic, and nonelastic cross sections, angle-energy correlated emission spectra for light ejectiles with $A \leq 4$ and gamma-rays, and average energy depositions. Our results for charged-particle emission spectra agree well with the measurements of Subramanian *et al.* [2]. We compare kerma factors derived from our evaluated cross sections with experimental data, providing an integral benchmarking of our work. The evaluated data libraries are available as electronic files.

I. INTRODUCTION

A number of new applications, such as radiation transport simulations of fast neutron and proton cancer radiotherapy and the accelerator-driven transmutation of waste, require evaluated nuclear data libraries when modeling the interaction of neutrons above 20 MeV. In a previous paper [1] we described the calculation and evaluation of neutron cross sections on carbon up to 100 MeV. The present work, for oxygen and nitrogen, uses the same evaluation techniques as described in our carbon paper. We therefore provide here only a summary of the methods employed, and refer the reader to Ref. [1] for full details.

When calculating absorbed dose in the body from a fast-neutron radiotherapy beam, the most important energy-deposition mechanisms are nuclear reactions with hydrogen, oxygen, carbon and nitrogen nuclei, since these elements account (by mass) for 10%, 65%, 18%, and 3% of the body, respectively. Neutrons, being uncharged, deposit energy in matter by first undergoing nuclear interactions which result in secondary charged nuclear ejectiles. These ejectiles then deposit their kinetic energy via electromagnetic interactions. In the case of hydrogen, it is elastic neutron-proton collisions that result in a substantial energy transfer from the incident neutrons to recoil protons. The higher mass of carbon, nitrogen and oxygen nuclei results in elastic scattering being a less important mechanism for energy deposition than for hydrogen. However, these nuclei may undergo inelastic scattering processes where nuclear fragmentation occurs. Indeed, for neutrons above about 70 – 80 MeV, the relatively large abundance of oxygen results in neutron-oxygen reactions giving the dominant contribution to absorbed dose in tissue.

Since only a limited number of experiments for neutron reactions on nitrogen and oxygen have been performed for energies between 20 and 100 MeV, we have based our evaluations mainly on the results of nuclear model calculations, benchmarked to the measurements where they exist. These calculations include direct, preequilibrium, and compound nucleus decay using Hauser-Feshbach theory. Our theoretical efforts, described in Sec. III and in more detail in Ref. [1], have concentrated on improvements to the modeling of reaction processes that become important at higher energies, particularly in preequilibrium emission and level densities. The light mass of oxygen and nitrogen, and consequently the relatively wide-spacing of their nuclear levels, presents a particular challenge to model calculations which rely on statistical assumptions in their derivations. However, our calculations in most cases provide a good description of the experimental data because our implementation of Hauser-Feshbach theory uses experimental nuclear level schemes for low excitation energies where a statistical level-density model is not applicable. Also, even in these light nuclei the density of nuclear states above about 10 MeV excitation energy becomes large enough for non-statistical effects to become less important.

These evaluations are available as electronic databases in the Lawrence Livermore National Laboratory (LLNL) Evaluated Nuclear Data Library (ENDL) format, and we plan to translate the library into the ENDF format. They can be used together with existing evaluations for neutrons below 20 MeV, such as the ENDL evaluation by Howerton [3] or the ENDF/B-VI evaluation by Hale *et al.* [4] for oxygen and Young *et al.* [5] for nitrogen. Table I contains a summary of the quantities evaluated.

In Sec. II we describe our evaluation methods and compare them to those of previous analyses. Section. III describes the nuclear theory and models we use. In Sec. IV we give a detailed description of our results compared with experimental cross sections, and in Sec. V we compare kerma factors derived from our evaluated cross sections with measurements, and with other calculations. A summary and a description of directions and needs for future work are given in Sec. VI.

II. EVALUATION METHODS

The evaluation represents inclusive emission spectra of the secondary particles which need to be transported in radiation transport calculations (neutrons, gammas, and light charged particles with A $\leq$ 4), as well as the total kinetic energy given to heavier charged particles, which is assumed to be deposited locally. This representation of the data is adequate for calculations of transport and absorbed dose. The libraries are fully angle-energy correlated, and describe the emission spectra at various angles, all in the laboratory frame of reference. We have omitted triton and helium-3 emission reactions since measurements [2] show these cross sections to be small.

The evaluations are based mainly on model calculations using the FKK-GNASH code system [6], benchmarked to available experimental data. But other reaction model codes were also used in this work: spherical optical model calculations were performed with the SCAT2 code [7]; and when evaluating preequilibrium cross sections we also considered hybrid model results from the ALICE code [8] and exciton model results from the GNASH code [6]. There are a number of advantages to using nuclear theory and model calculations to produce evaluated cross section libraries. The model input parameters can be adjusted (within the uncertainty ranges to which they are known) to optimize agreement with experimental data at incident energies where measurements have been made. The calculations then provide a useful way to interpolate and extrapolate to other energies. Also, model calculations enable evaluated libraries to be generated for all reaction products in a fully consistent way, automatically conserving energy, unitarity, spin, and parity.

Table II summarizes the experimental data used in the evaluations, in some cases pointing to other places in this paper where the data are shown in more detail. We show these various experimental data sets compared with our evaluations in Sec. IV. Some of the major steps involved in this evaluation are: (1) Optical model analyses for n, p, d, α particles to generate elastic and nonelastic cross sections, and transmission coefficients; (2) Build a database of low-lying nuclear levels for all product nuclides for use in Hauser-Feshbach and preequilibrium calculations. (3) Match a statistical level density on to the experimental low-lying levels; (4) Perform preequilibrium calculations using Feshbach-Kerman-Koonin (FKK) [9, 10] quantum multistep theory, exciton, and hybrid models for comparison purposes. On the basis of these calculations, and measured cross sections, evaluate the primary preequilibrium spectra; (5) Use the FKK-GNASH code to generate inclusive cross sections based on primary and multiple preequilibrium emission, equilibrium decay, and direct reactions; (6) Use the Kalbach systematics [11] to give continuum angular distributions, and transform the double-differential cross sections to the laboratory frame assuming 2-body kinematics; and (7) Generate ENDL-format library files.

It is useful to compare the calculation methods used here with those of previous works. In addition to the present work, Refs. [12–15] used preequilibrium models with Hauser-Feshbach compound nucleus decay to study neutron reactions on biologically-important nuclei. Dimbylow [13] used an early version of the GNASH code, and his model calculations were compared against the UC-Davis cross section and kerma measurements. Even though details of the preequilibrium spectral shapes were not described very well (since early preequilibrium algorithms were utilized) the resulting kerma factors accounted for the data fairly accurately.

Intranuclear cascade (INC) calculations with either evaporation or a Fermi breakup compound nucleus decay have been described in Refs. [16–21]. While the physical assumptions made in these models do not hold well below 100 MeV, some analyses [16] have shown that they can provide a reasonable description of experimental measurements at these energies. It is only the comprehensive work by Brenner and Prael [16] which makes comparisons with experimental charged-particle spectra. Brenner and Prael did not include elastic or inelastic coupled-channels scattering in their analyses, and did not present results for gamma-ray production. A failing of many INC-type calculations for reactions on biologically-important nuclei is that they do not account for the large numbers of high-energy preequilibrium deuterons, and they largely underpredict the production of alpha particles [21, 22].

Finally, Caswell *et al.* [23] extended the evaluated ENDF libraries from 20 MeV to 30 MeV, using optical model results to obtain the total, elastic, and reaction cross sections. But extrapolations of partial cross sections beyond 20 MeV with this method are not always reliable. More recently, the latest ENDF/B-VI evaluation for nitrogen was extended to 40 MeV [5]. However, this evaluation was intended primarily for use in neutron transport calculations, and not all charged-particle decay channels are explicitly described. The present evaluation is unique in that experimental measurements have been utilized to optimize the model calculations, and extensive comparisons with experimental data have been made to validate our results.

III. NUCLEAR THEORY AND MODELS

We determine total, elastic, and nonelastic scattering cross sections using optical model analyses, which are also needed for generating transmission coefficients and wavefunctions in the equilibrium and preequilibrium calculations. Our work implements the spherical optical potential developed by Islam and Finlay of Ohio University [24], from 20 to 50 MeV (to 60 MeV for nitrogen). Above this energy we use the global potential developed by Madland [25], based on the earlier work of Schwandt *et al.* [26], and below 20 we use the Los Alamos spherical potential [27]. In addition to neutrons, optical potentials are also needed for the other ejectiles for calculating transmission coefficients for their decay. Proton potentials were obtained from the neutron potentials using the Lane model isospin transformation, namely $(N-Z)/A \rightarrow -(N-Z)/A$, with a Coulomb correction to the real central potential of $0.4Z/A^{1/3}$. Potentials for deuterons and alphas up to high energies were obtained using the method of Watanabe, as implemented by Madland [25].

Preequilibrium nucleon emission was obtained mainly from the FKK quantum mechanical theory, and preequilibrium deuteron and alpha clusters were obtained from the semiclassical model of Kalbach [28]. In some cases we modified the calculations to agree better with experimental measurements where they exist. Preequilibrium gamma-ray emission through the Giant Resonance is modeled using a semiclassical exciton model [6]. Contributions from multiple preequilibrium emission (MPE) processes (where more than one particle is emitted through a preequilibrium mechanism) were included using the theory of Ref. [29]. Full details of these theories are given in Ref. [1].

We use Hauser-Feshbach theory to calculate equilibrium emission of particles and gamma rays, conserving angular momentum and parity in an open-ended sequence of decay chains. We performed trial calculations to determine the most important reaction pathways and ignore paths that contain < 1 mb of cross section. Gamma, neutron, proton, deuteron, and alpha particle decay channels were included. Transmission coefficients for equilibrium particle decay were obtained using the optical potentials described above, and gamma-ray transmission coefficients were obtained from the generalized Lorentzian model of Kopecky and Uhl [30]

Nuclear level densities were determined using the Ignatyuk model [31], as implemented by Arthur *et al.* [14]. Pairing energies were obtained from the Cook systematics with the Los Alamos extensions to light nuclei from Ref. [27]. This continuum level density formulation is matched continuously onto discrete low-lying levels at the lower excitation energies. Discrete level information (energy, spin, parity, gamma-ray branching ratios) is tabulated for each nuclide in an input file, which is based on a number of different sources including the Ajzenberg-Selove compilations [32]. For each nucleus we performed a level-density analysis and determined the excitation energy at which we judged the level data complete. Table III below lists the number of discrete levels used, and the matching energy, for the residual nuclides that can be produced (many of which are unstable). As an example of our results, in Fig. 1 we show the experimental cumulative number of levels matched on to our continuum statistical description for ^{15}N. We show this example since this nucleus is produced following high-energy deuteron emission in the $^{16}\mathrm{O}(n,xd)$ reaction, and our evaluated spectra show structure corresponding to the gap of over 5 MeV between the ground and first excited states.

IV. RESULTS AND COMPARISONS WITH EXPERIMENTS

A. Total, Elastic, and Reaction Cross Sections

Table IV shows the evaluated total, elastic, and reaction (nonelastic) cross sections for oxygen and nitrogen, based on our optical model calculations. Between 20 and 100 MeV, the optical models we use provide a reasonably good description of measured reaction cross section data (see the dashed lines in Figs. 2 and 3). But since an accurate description of the reaction cross section is important for determining secondary particle spectra, we slightly modify the calculated results to better describe the experimental data to give the full lines shown in Fig. 2 and 3, and renormalize the calculated transmission coefficients accordingly. No measurements for the neutron reaction cross section on oxygen or nitrogen exist above about 50 MeV. However, systematics have been determined from a number of target element at 95 MeV by DeJuren [33], and for 100 MeV protons by Kirby and Link [34] (at this energy the proton and neutron reaction cross sections would be expected to be very similar). We have, therefore, used these systematics to guide our evaluated reaction cross sections. Additionally, below 50 MeV we have also been guided by the proton-induced reaction cross sections of Carlson *et al.* [35]. The data points of Islam *et al.*, Olsson *et al.*, and Petler *et al.* shown in Figs 2. and 3 were obtained by subtracting their angle-integrated elastic data from the evaluated total cross sections (see below).

The evaluated total cross section was obtained by slightly modifying the optical model results to agree with data, principally the new high-accuracy results of Finlay *et al.* [36]. The results are shown in Figs. 4 and 5 compared with measurements taken from the Brookhaven National Nuclear Data Center CSISRS file. In the case of nitrogen, we use the ENDF/B-VI total cross section below 40 MeV [5].

The elastic scattering cross sections were obtained from our optical model calculations, renormalized to the difference between evaluated total and reaction cross sections. The results are compared against experimental total elastic scattering data in Fig. 6. The angle-integrated data from Olsson *et al.* were taken from Ref. [37]. A legendre-fit to the Petler *et al.* nitrogen data [38] yielded elastic cross sections of 1020 ± 19 mb and 1062 ± 9 mb at 20 and 25 MeV, respectively. Measured angle-integrated elastic cross sections on oxygen between 18 and 28 MeV were obtained from the legendre -fits of Islam *et al.* [39]. As an illustrative example of the differential elastic scattering, we show in Fig. 7 the elastic angular distributions at 20 and 26 MeV, compared with the differential cross section data of Islam *et al.* [24] in the center-of-mass frame.

Since direct inelastic neutron scattering to low-lying levels in oxygen has been shown to be important [39], we use the DWBA results from Ref. [39] for neutron scattering to the 3^- (6.13 MeV), 2^+ (6.92 MeV), and 1^- (7.12 MeV) states in ^{16}O. No such direct DWBA contributions were included for nitrogen.

B. Inclusive production cross sections and spectra

Table V shows the calculated production cross sections and average kinetic energies for the light ejectiles. In Figs. 8 and 9 we show the variation of these cross sections as a function of incident neutron energy. The tight binding of alpha particles along with the high probability of alpha clustering in light nuclei results in the alpha production cross section being large. Even though the multiplicities for particle production increase with increasing energy, the production cross sections do not generally show a large increase with energy because the nonelastic cross sections fall by about a factor of two between 20 and 100 MeV for oxygen and nitrogen.

An important test of the accuracy of the data libraries is that the evaluated emission spectra of light particles ($A \leq 4$) should be consistent with the measurements by Subramanian *et al.* [2] of UC-Davis. Figs. 10 and 11 show our calculated (lab frame) angle-integrated emission spectra of protons, deuterons, and alphas, compared with these measurements for oxygen and nitrogen. The structure seen at high emission energies is due to the inclusion of discrete nuclear levels in our calculations. Noteworthy features of the emission spectra seen in Fig. 10 and 11 are: (1) preequilibrium fast particle emission is particularly important and, except for alpha-emission, is large in magnitude compared to equilibrium decay (unlike reactions on heavier nuclei [42]); (2) preequilibrium deuteron emission is significant; and (3) alpha production cross sections at low emission energies are large. In general our calculations and those of Brenner and Prael [16], shown by the dashed line in Fig. 10, account for these features equally well, except for deuteron emission where our results describe the measurements more accurately.

For the UC-Davis data at 60 MeV, we have performed a new angle-integration of their double-differential data, and show our results in Fig. 10. The original UC-Davis angle-integrated results were kindly provided us by Dr. Romero who used them to obtain kerma factors [40, 41]. However, the partial kerma from proton emission [41] appeared too high to us, suggesting that the angle-integrated proton spectrum may have been overestimated. For oxygen and nitrogen the measurements were only made at angles forward of 65-degrees, and consequently there are uncertainties in deriving angle-integrated spectra. The original approach of Subramanian *et al.* was to assume a constant cross section from 65-degrees back to 180-degrees. However, this overestimates the angle-integrated cross section since continuum angular distributions decrease significantly at back-angles. Our procedure instead was to use the shape of our calculated angular distribution to extrapolate the data from 65-degrees to 180-degrees. As can be seen in Fig. 10, this resulted in a significantly lower experimental angle-integrated spectrum for proton emission, in better agreement with the model calculations. The experimental 60 MeV angle-integrated $^{14}N(n, xp)$ cross section in Fig. 11 is also probably overestimated due to the angle-integration procedure employed, as described above. Thus, we expect that much of the discrepancy seen between calculation and experiment here will vanish when a more accurate angle-integration technique is used, and we plan to check this in the future.

Figure 12 compares our calculated double-differential alpha, proton, and deuteron emission spectra against the UC-Davis measurements at 60 MeV. A dramatic example of the influence of nuclear structure is seen in the $^{16}O(n, xd)$ spectra, where the first excited ^{15}N state lies at 5.27 MeV (see Fig. 1). Our calculations account for the angular variations seen in the data, showing that the phenomenological systematics of Kalbach provide a good representation of angular distributions. At the higher emission energies the spectra show a dramatic forward peaking, typical of preequilibrium and direct reactions, since the incident projectile's direction of motion is partially preserved. At the lowest energies, the particles are emitted from compound nucleus reactions. In the center-of-mass these are emitted with angular distributions symmetric about 90-degrees (and almost isotropic), but in the laboratory some forward-peaking remains. Our calculations also clearly show how discrete structure effects in the spectra track with emission angle and energy due to kinematics.

C. Neutron Emission Compared With (p,xp) Data

There are no measurements of (n, xn) emission spectra with which we can compare our calculations. However, Bertrand and Peelle have measured $^{16}O(p, xp)$ cross sections at 40 and 60 MeV [42]. It would be expected that $^{12}O(p, xp)$ and $^{16}O(n, xn)$ spectra should be similar, particularly for the higher emission energies where Coulomb effects are negligible. Some differences would be expected due, for instance, to different Q-values in the competing channels in the two cases, but we expect such effects to have a small impact. Therefore we have used the Bertrand and Peelle measurements to benchmark our neutron emission calculations, as shown in Fig. 13, where we compare our results against the 40 and 60 MeV data. At 40 MeV the calculated emission spectrum agrees with data except at the lowest energies, where it lies below the measurements. At 60 MeV the calculations underpredict the data by about 15% between emission energies of 20 and 40 MeV. Our calculations agree better with these data than those of Brenner and Prael [16], which are also shown for comparison. Our evaluated (n, xn) spectra are approximately a factor of two larger than the (n, xp) spectra in the preequilibrium region, which is consistent with the systematics observed by Kalend *et al.* [43].

D. Comparison with exclusive measurements

Although our evaluation represents inclusive, and not exclusive, cross sections it is useful to compare our calculated excitation functions against exclusive measurements where they exist, as a further check on the evaluations.

The partial cross sections for the $(n, 2n)$ reactions on nitrogen and oxygen are shown in Fig. 14, compared with the measurements by Brill [44]. Our calculations are seen to agree reasonably well with these data. At the higher energies the calculated $(n, 2n)$ cross section does not become very small because of the presence of multiple preequilibrium processes which provide a mechanism for the emission of two high-energy particles.

Although experimental data for the $^{16}O(n,p)$ and $^{14}N(n,p)$ reactions do not exist above 20 MeV, measurements have been made at lower energies. In Fig. 15 we show our calculations together with these data. The trends of the calculated excitation functions above 20 MeV are consistent with the lower-energy measurements. Likewise, the variation of our calculated $(n,d)+(n,np)$ cross section on oxygen above 20 MeV is consistent with experimental point at 14 MeV, as seen in Fig. 16.

V. KERMA FACTORS

Kerma factors are a measure of the kinetic of secondary charged-particles following a neutron reaction, and are important for determining absorbed dose in radiotherapy, and heating effects when neutrons interact with matter. We partition the calculated kerma factors into contributions from light charged particle ejectiles with $A \leq 4$ (obtained from lab-frame emission spectra), elastic recoils (obtained from elastic scattering angular distributions), and non-elastic heavy recoils (from the calculated recoil production cross sections along with energy-balance). Full details of the methods we use are given in Ref. [1].

The partial kerma factor for a certain secondary charged-particle type is obtained from the product of the cross section (in b) and the average energy (in MeV), in units of b.MeV/atom. To convert to the SI unit of Gy.m^2 (where 1 Gray (Gy) = 1J/1Kg) we multiply by 0.603225 $\times 10^{-15}$ for oxygen and 0.689045 $\times 10^{-15}$ for nitrogen, which are the product of three factors: the number of atoms per Kg of ^{16}O (6.0221367 / M_A) $\times$ 10^{26} (where M_A=15.994915 for oxygen, 14.003074 for nitrogen); J/MeV (1.60217733 $\times 10^{-13}$); and m^2/b (10^{-28}).

A. Oxygen

In Table VI we show our calculated partial and total kerma factors based on our evaluated cross section libraries. At the lowest energies, the total kerma factor is dominated by the alpha contribution, due to the large production cross section for alpha particles at these energies. The increasing proton and deuteron partial kerma factors are due to the importance of preequilibrium emission with increasing incident energy. The elastic recoil kerma factor, on the other hand, decreases with increasing incident energy because the elastic angular distributions becomes increasingly forward-peaked, resulting in a reduced recoil kinetic energy.

In Fig. 17 we show our evaluated total kerma factor from 20-100 MeV, derived from our microscopic cross section libraries, compared with experimental measurements [13, 41, 45, 46], and we compare our result with other calculations and evaluations in Fig. 18. Below 20 MeV the histogram line shows the Howerton [3] result for the total kerma factor from the Livermore ENDL database. Our calculated kerma factor is consistent with the measurements, which provides an important benchmark for our cross sections. However, the variation seen among the experimental measurements requires some comments.

Direct kerma measurements have been recently reported by Schrewe *et al.* [46], for incident energies between 30 and 70 MeV. However, there are some uncertainties involved in obtaining kerma factors from these proportional-counter measurements due to uncertainties in gas-to-wall absorbed dose conversion factors. Kerma factors derived from measured cross sections have been presented by the UC-Davis group [40, 41]. To obtain total kerma factors from their data, angle-integrated spectra need to be inferred from the double-differential measurements, the cross sections have to be extrapolated from the threshold emission energy measured to zero energy, elastic recoil kerma have to be added; and the (unmeasured) contributions from nonelastic recoil fragments have to be estimated. A range of total kerma factors based upon the UC-Davis measurements have been reported in the literature (see Fig. 17 and Refs. [13, 40, 41]). As discussed earlier, we had an expectation that the UC-Davis kerma factors reported at 60 MeV were too high, due primarily to an overestimate of the angle-integrated proton emission spectrum. Therefore we re-angle-integrated the UC-Davis data using our calculated angular distribution shapes to extrapolate the measurements from 65-degrees to backward angles (see our results in Fig. 10). In addition, we added low-emission energy threshold contributions, and elastic and non-elastic recoil contributions, from our calculations. This yielded a total experimental kerma factor at 60 MeV of 4.31 ± 0.70 f Gy m^2, which is significantly smaller than previous estimates, but in good agreement with our evaluation, and with the Schrewe data.

B. Nitrogen

Figure 19 shows our evaluated total kerma factor from 20-100 MeV compared with UC-Davis experimental measurements [13]. Our results are seen to agree well with these data. Because of the uncertainties in angle-integrating the UC-Davis double-differential cross sections, as discussed above, we believe that the experimental data point at 60.7 MeV is too high. Our result are compared with other calculations and evaluations in Fig. 20. It is evident that there is a considerable variation in the predictions of different calculations.

In the absence of detailed nuclear structure effects, the total kerma factor for elements with similar Coulomb barriers (such as nitrogen and oxygen) would be expected to vary approximately as $A^{-1/3}$ (1/A from the normalization constant in the kerma definition, and $A^{2/3}$ from the non-elastic cross section), which gives a ratio of 1.05 for nitrogen to oxygen. However, the total kerma factor above 20 MeV for nitrogen exceeds that for oxygen by a larger amount due to differences in the detailed nuclear structure of these elements and the residual nuclei produced. One such example is the large differences in Q-values for proton emission, +0.63 MeV for nitrogen, -9.64 MeV for oxygen, which leads to higher partial proton kerma factors for nitrogen.

VI. CONCLUSIONS

We have produced evaluated nuclear data bases for neutrons incident on nitrogen and oxygen. The preequilibrium model calculations were optimized to account for experimental measurements, particularly those of Subramanian *et al.*, and this technique resulted in evaluated emission spectra which generally account for the experimental data well. Compared to Brenner and Prael's model calculations, which represent the most detailed and well-benchmarked calculations prior to the present work, our results are more accurate for deuteron emission and the quality is comparable for proton and alpha emission. Furthermore, total kerma factors derived from our calculations describe the experimental measurements well. We found that a new angle-integration of the UC-Davis oxygen data at 60 MeV, using our model calculations to extrapolated to unmeasured angles, resulted in a lower experimental total kerma factor than originally reported. We plan to repeat this analysis for the other energies and other target nuclei measured at UC-Davis.

These evaluated data, together with our result for carbon [1], can be used in radiation transport calculations of absorbed dose in fast neutron radiotherapy. The libraries can be updated when new experimental measurements, such as the 60 MeV ^{16}O+n data currently being analyzed at Louvain-la-Neuve [49], become available.

VII. ACKNOWLEDGMENTS

We are grateful to Larry Cox for generating the appendix tables from our evaluated files. We wish to thank H. Barschall, S. Benck, M. Blann, W. Chandler, V. Corcalciuc, L. Cox, P. DeLuca, R. Finlay, C. Hartmann-Siantar, R. Howerton, J.P. Meulders, A. Kerman, J. Rathkopf, G. Reffo, D. Resler, J. Romero, and R. White, for many useful discussions. This work was performed under the auspices of the U.S. Department of Energy by the Lawrence Livermore National Laboratory under contract no. W-7405-ENG-48, and by the Los Alamos National Laboratory under contract no. W-7405-ENG-36.

REFERENCES

[1] M.B. Chadwick, M. Blann, L.J. Cox, P.G. Young, and A.S. Meigooni, submitted to Nuclear Science and Engineering, and Lawrence Livermore National Laboratory report UCRL-JC- (1995); M.B. Chadwick, M. Blann, L.J. Cox, P.G. Young, and A.S. Meigooni, Lawrence Livermore National Laboratory report UCRL-ID-120829 (1995).

[2] (update) T.S. Subramanian, J.L. Romero, F.P. Brady, J.W. Watson, D.H. Fitzgerald, R. Garrett, G.A. Needham, J.L. Ullmann, C.I. Zanelli, D.J. Brenner, and R.E. Prael, Phys. Rev. C **28**, 521 (1983); J.L. Romero, private communication to MBC (1994).

[3] R.J. Howerton, Lawrence Livermore National Laboratory document UCRL-50400 **27** (1986)*revised.*

[4] G.M. Hale, P.G. Young, M.B. Chadwick, and Z.P. Chen, in *Proceedings of the International Conference on Nuclear Data for Science and Technology*, Julich, Germany, 13-17 May 1991, edited by S.M. Qaim (Springer Verlag, 1992) p. 921; Brookhaven National Nuclear Data Center ENDF/B-VI evaluation.

[5] G.M. Hale, P.G. Young, M.B. Chadwick, in *Proceedings of the International Conference on Nuclear Data for Science and Technology*, Gatlinburg, Tennessee, May 9-13 1994, edited by K. Dickens (American Nuclear Society, 1994) p. 607; Brookhaven National Nuclear Data Center ENDF/B-VI ^{14}N, Rev. 3, evaluation.

[6] P.G. Young, E.D. Arthur, and M.B. Chadwick, Los Alamos National Laboratory document LA-MS-12343 (1992); M.B. Chadwick and P.G. Young, Phys. Rev. C **47**, 2255 (1993).

[7] O. Bersillon, Bruyeres-le-Chatel progress report CEA-N-2037, p. 111 (1978).

[8] M. Blann, Lawrence Livermore National Laboratory document UCRL-JC-109052 (1991).

[9] H. Feshbach, A. Kerman, and S. Koonin, Ann. Phys. (N.Y.) **125**, 429 (1980).

[10] P.E. Hodgson and M.B. Chadwick, invited paper to the *International Conference on Nuclear Data for Science and Technology*, Gatlinburg, Tennessee, May 9-13 1994, edited by K. Dickens (American Nuclear Society, 1994) p. 519.

[11] C. Kalbach, Phys. Rev. C **37**, 2350 (1988).

[12] M.B. Chadwick, M. Blann, P.G. Young, and G. Reffo, in *Proceedings of the International Conference on Nuclear Data for Science and Technology*, Gatlinburg, Tennessee, May 9-13 1994, edited by K. Dickens (American Nuclear Society, 1994) p. 658.

[13] P.J. Dimbylow, Phys. Med. Biol. **27**, 989 (1982).

[14] P.G. Young, E.D. Arthur, M. Bozoian, T.R. England, G.M. Hale, R.J. LaBauve, R.C. Little, R.E. MacFarlane, D.G. Madland, R.T. Perry, and W.B. Wilson, Los Alamos National Laboratory document LA-11753-MS (1990).

[15] G.H. Herling, R.H. Bassel, J.H. Adams, and W.A. Frazer, Naval Research Report 8441, Washington, D.C., (1981).
[16] D.G. Brenner and R.E. Prael, At. Data and Nucl. Data Tables **41**, 71 (1989).
[17] R.G. Alsmiller Jr., and J. Barish, Health Physics **33**, 98 (1977).
[18] M.A. Behrooz and D.E. Watt, in *Proc. 4th Symp. on Neutron Dosimetry,* EUR-7448 (Luxembourg, CEC) 353-360 (1981).
[19] K. Morstin, A. Dydejczyk, and J. Booz, Rad. Prot. Dos. **23**, 35 (1988).
[20] A.H. Wells, Radiat. Res. **80**, 1 (1979).
[21] S. Mashnik, private communication to MBC (1995).
[22] K. Morstin, A. Dydejczyk, J. Booz, in *Nuclear and Atomic Data for Radiotherapy and Related Radiobiology*, International Atomic Energy Agency report STI/PUB/741 (IAEA, Vienna, 1987).
[23] R.S. Caswell, J.J. Coyne, M.L. Randolph, Radiat. Res. **83**, 217 (1980).
[24] M.S. Islam, R.W. Finlay, J.S. Petler, J. Rapaport, R. Alarcon, and J. Wierzbicki, Phys. Med. Biol. **33**, 315 (1988).
[25] D.G. Madland, in *Proceedings of a Specialists' Meeting on Preequilibrium Reactions*, Semmering, Austria, 10-12 Feb. 1988, edited by B. Strohmaier (NEA Report NEANDC-245, 1988) p. 103.
[26] P. Schwandt, *et al.* Phys. Rev. C **26**, 55 (1982).
[27] E.D. Arthur, Los Alamos National Laboratory progress report LA-9841-PR (1983).
[28] C. Kalbach, Z. Phys. **A 283**, 401 (1977).
[29] M.B. Chadwick, P.G. Young, D.C. George, and Y. Watanabe, Phys. Rev. C **50**, 996 (1994).
[30] J. Kopecky and M. Uhl, Phys. Rev. C **41**, 1941 (1990).
[31] A.V. Ignatyuk, G.N. Smirenkin, and A.S. Tishin, Sov. J. Nucl. Phys. **21**, 255 (1975).
[32] F. Ajzenberg-Selove, Nucl. Phys. **A449**, 1 (1986); Nucl. Phys. **A375**, 1 (1982).
[33] J. Dejuren and N. Knable, Phys. Rev. **77**, 606 (1950).
[34] P. Kirby and W.T. Link, Can. J. Phys. **44**, 1847 (1966).
[35] R.F. Carlson, A.J. Cox, T.N. Nasr, M.S. De Jong, D.L. Ginther, D.K. Hasell, A.M. Sourkes, W.T.H. Van Oers, and D.J. Margaziotis, Nucl. Phys. **A445**, 57 (1985); R.F. Carlson, A.J. Cox, J.R. Nimmo, N.E. Davidson, S.A. Elbakr, J.L. Horton, A. Houdayer, A.M. Sourkes, W.T.H. Van Oers, and D.J. Margaziotis, Phys. Rev. C **12**, 1167 (1975).
[36] R.W. Finlay, W.P. Abfalterer, G. Fink, E. Montei, T. Adami, P.W. Lisowski, G.L. Morgan, and R.C. Haight, Phys. Rev. C **47**, 237 (1993).
[37] N. Olsson, E. Ramstrom, and B. Trostell, Phys. Med. Biol. **35**, 1255 (1990).
[38] J.S. Petler, M.S. Islam, R.W. Finlay, and F.S. Dietrich, **32**, 673 (1985).
[39] M.S. Islam and R.W. Finlay, Nuclear Data and Atomic Data Tables **58**, 245 (1994).
[40] F.P. Brady and J.L. Romero, *Final Report to the National Cancer Institute,*

University of California, Davis, (1979).

[41] J.L. Romero, F.P. Brady, and T.S. Subramanian, in *Nuclear Data for Basic and Applied Sciences*, Santa Fe, New Mexico, 13-17 May, 1985, edited by P.G. Young (Gordon and Breach, 1986) p. 687.

[42] F.E. Bertrand and R.W. Peelle, Phys. Rev. C **8**, 1045 (1973).

[43] A.M. Kalend *et al.*, Phys. Rev. C **28**, 105 (1983).

[44] O.D. Brill, N.A. Vlasov, S.P. Kalinin, L.S. Sokolov, Sov. Phys. Dokl. **6**, 24 (1961).

[45] C.L. Hartmann, P.M. DeLuca Jr., and D.W. Pearson, Radiat. Prot. Dosim. **44**, 25 (1992).

[46] U.J. Schrewe, W.D. Newhauser, H. J. Brede, V. Dangendorf, P.M. DeLuca, Jr., S. Gerdung, R. Nolte, P. Schmelzbach, H. Schuhmacher, and T. Lim, in Chalk River Conference, 1994, to be published in Rad. Prot. Dos.; private communication to M.B. Chadwick (1995).

[47] D.G. Brenner and R.E. Prael, in *Nuclear and Atomic Data for Radiotherapy and Related Radiobiology*, ed. K. Okamoto (IAEA, Vienna, 1985) p. 205.

[48] R.M. White *et al.*, invited paper to the *Seventh Symposium on Neutron Dosimetry*, Berlin, Germany, October 14-18 (1992); Rad. Prot. Dos. **44**, 11 (1992).

[49] S. Benck, V. Corcalciuc, and J.P. Meulders, private communication to MBC (1995).

TABLES

TABLE I. Contents of Evaluated Data Library for ^{12}C+n.

Reaction type	Cross section	Angle-energy correlated lab spectra	Average lab energy deposition
n,total	X		
n,nonelastic	X		
n,elastic	X	(c.m. angular distributions)	X
n,xn	X	X	X
n,xp	X	X	X
n,xd	X	X	X
n,xα	X	X	X
n,xγ	X	(isotropic)	X
n,nonelastic recoils			X

TABLE II. Summary of experimental cross section data guiding these evaluations

Reaction type	Citation to experimental measurement
Nonelastic	See Figs. 2 and 3
Total	See Figs. 4 and 5
Elastic	See Figs. 6 and 7
Inelastic neutron scattering	See Islam and Finlay [39]
p, d, α production	27, 40, 61 MeV UC-Davis data [2], see Figs. 10-12
$(n, 2n)$	Brill (1961), see Fig. 14
(n, p)	Martin (1954) and Dejuren (1962), and Felber (1976), see Fig. 15
(n, d)	Lillie (1952), see Fig. 16
(p, xp)	Bertrand and Peelle [42], see Fig. 13 (guide for ^{16}O(n, xn) calcs.)

TABLE III. The number of low-lying discrete levels included, along with the matching excitation energy (in MeV) above which we used the Ignatyuk continuum level density description. For nuclides with $Z \leq 6$, see Table III in Ref. [1].

Nucleus (1000Z+A)	Number of levels	Matching energy	Nucleus (1000Z+A)	Number of levels	Matching energy
9017	20	7.479	7016	18	5.255
9016	10	5.104	7015	22	10.855
9015	2	1.950	7014	9	6.565
9014	1	0.000	7013	13	10.637
9013	1	0.000	7012	7	3.740
9012	1	0.000	7011	1	0.000
9011	1	0.000	7010	1	0.000
8017	45	10.026	6015	16	7.479
8016	24	13.327	6014	18	11.762
8015	13	9.741	6013	10	9.190
8014	6	6.890	6012	8	12.162
8013	4	6.925	6011	12	8.724
8012	1	0.000	6010	5	7.180
8011	1	0.000	6009	2	3.330

TABLE IV. Evaluated total, elastic, and nonelastic (reaction) cross sections (in mb) for n+^{16}O and ^{14}N, for various laboratory neutron energies.

	^{16}O+n			^{14}N+n		
Energy (MeV)	Total	Elastic	Nonelastic	Total	Elastic	Nonelastic
20	1640	1020	620	1550	1019	531
23	1646	1054	592	1465	961	504
27	1594	1071	523	1436	954	482
30	1559	1059	500	1394	929	465
35	1479	1012	467	1321	884	437
40	1402	967	435	1249	839	410
50	1211	815	396	1067	702	365
60	1050	680	370	924	597	327
70	912	573	339	788	490	298
80	807	489	318	693	410	283
90	721	421	300	611	340	271
100	637	340	297	550	288	262

TABLE V. Evaluated production cross sections (in mb) and average energies (in MeV) in the n+^{16}O and ^{14}N reactions, for various laboratory neutron energies (in MeV).

^{16}O+n										
Energy	$\sigma(n)$	$E_{av}(n)$	$\sigma(p)$	$E_{av}(p)$	$\sigma(d)$	$E_{av}(d)$	$\sigma(\alpha)$	$E_{av}(\alpha)$	$\sigma(\gamma)$	$E_{av}(\gamma)$
20	558	6.5	54	5.2	25	5.2	403	5.1	402	4.5
23	512	7.8	70	5.9	35	6.1	397	5.6	361	4.7
27	480	8.8	122	6.8	50	7.4	389	4.5	322	4.8
30	460	10.0	129	7.7	55	9.6	415	4.4	308	4.9
35	437	11.8	150	9.2	57	13.3	424	4.4	287	4.9
40	413	13.4	162	10.5	61	16.5	392	4.8	264	4.9
50	403	17.3	192	13.0	67	20.2	290	5.3	253	4.8
60	407	19.7	223	15.8	66	22.2	249	6.0	231	4.7
70	396	22.3	227	18.4	68	25.4	228	6.5	207	4.6
80	395	24.8	231	19.7	68	27.7	219	6.9	187	4.5
90	400	26.6	242	21.7	68	27.8	219	7.3	165	4.5
100	419	28.7	256	23.2	72	28.3	221	7.6	158	4.5
^{14}N+n										
Energy	$\sigma(n)$	$E_{av}(n)$	$\sigma(p)$	$E_{av}(p)$	$\sigma(d)$	$E_{av}(d)$	$\sigma(\alpha)$	$E_{av}(\alpha)$	$\sigma(\gamma)$	$E_{av}(\gamma)$
20	424	6.6	209	4.0	45	6.5	214	5.3	320	3.6
23	448	7.2	210	4.8	54	7.5	213	6.3	296	3.3
27	511	7.5	232	5.6	68	8.6	228	5.0	249	3.0
30	520	8.3	234	6.3	73	10.1	262	4.9	230	3.0
35	507	9.2	232	7.9	80	12.5	329	4.6	194	3.1
40	498	10.4	231	9.0	86	15.2	369	4.6	169	3.1
50	475	13.2	235	11.9	84	19.5	382	4.6	134	3.2
60	450	16.0	237	14.9	74	23.0	358	5.0	120	3.3
70	419	18.4	228	17.6	69	26.5	336	5.8	102	3.3
80	425	20.0	242	18.9	70	28.7	336	6.1	90	3.3
90	429	21.9	251	20.4	69	30.2	319	6.5	84	3.3
100	430	23.7	258	21.5	71	30.5	310	6.8	74	3.3

TABLE VI. Evaluated partial and total kerma factors (in units of f Gy m^2) for oxygen and nitrogen, for various laboratory neutron energies (in MeV). Contributions from protons, deuterons, alphas, non-elastic recoils, and elastic recoils, are given.

	^{16}O+n						^{14}N+n					
E_n	p	d	α	non. rec.	elas. rec.	Total	p	d	α	non. rec.	elas. rec.	Total
20	0.17	0.08	1.24	0.22	0.28	1.99	0.58	0.20	0.79	0.44	0.41	2.42
23	0.25	0.13	1.33	0.29	0.27	2.27	0.70	0.28	0.92	0.47	0.37	2.74
27	0.50	0.22	1.06	0.36	0.27	2.41	0.89	0.41	0.79	0.47	0.35	2.90
30	0.60	0.32	1.10	0.39	0.26	2.67	1.02	0.51	0.88	0.47	0.33	3.21
35	0.84	0.45	1.13	0.39	0.24	3.05	1.27	0.69	1.04	0.42	0.30	3.72
40	1.02	0.61	1.13	0.37	0.23	3.36	1.44	0.90	1.18	0.41	0.28	4.21
50	1.51	0.82	0.94	0.33	0.19	3.78	1.93	1.13	1.21	0.40	0.23	4.90
60	2.12	0.89	0.90	0.30	0.15	4.35	2.43	1.17	1.24	0.40	0.20	5.45
70	2.52	1.03	0.89	0.29	0.12	4.86	2.75	1.27	1.33	0.37	0.14	5.87
80	2.74	1.14	0.91	0.27	0.10	5.17	3.15	1.39	1.42	0.34	0.12	6.41
90	3.17	1.14	0.96	0.26	0.09	5.63	3.54	1.43	1.44	0.31	0.09	6.80
100	3.58	1.23	1.01	0.25	0.07	6.14	3.82	1.49	1.46	0.28	0.08	7.13

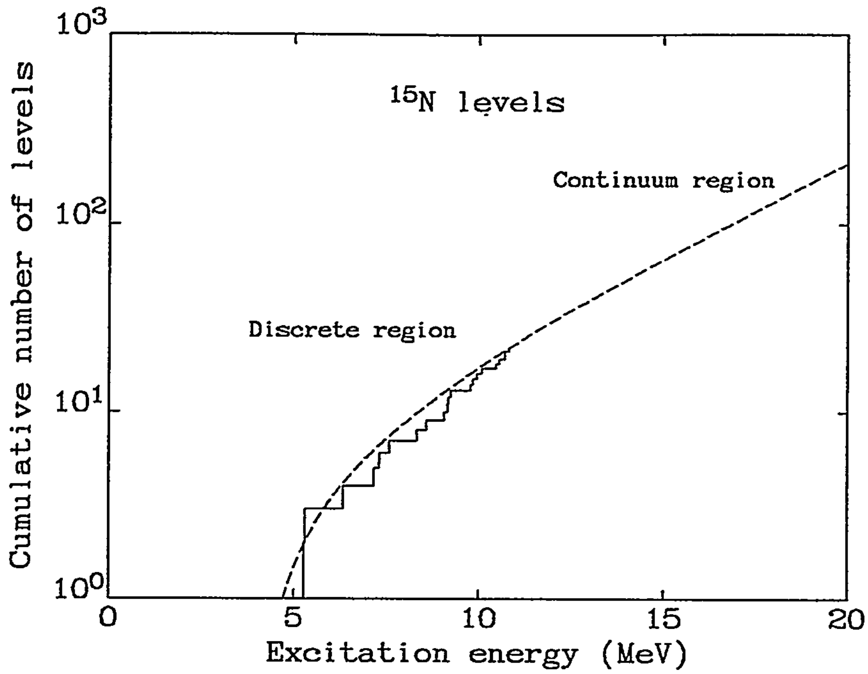

Fig. 1. An illustrative example of a level density analysis, for ^{15}N. Below 10.8 MeV experimental levels are used, and above this energy we use a statistical description, given by the dashed line.

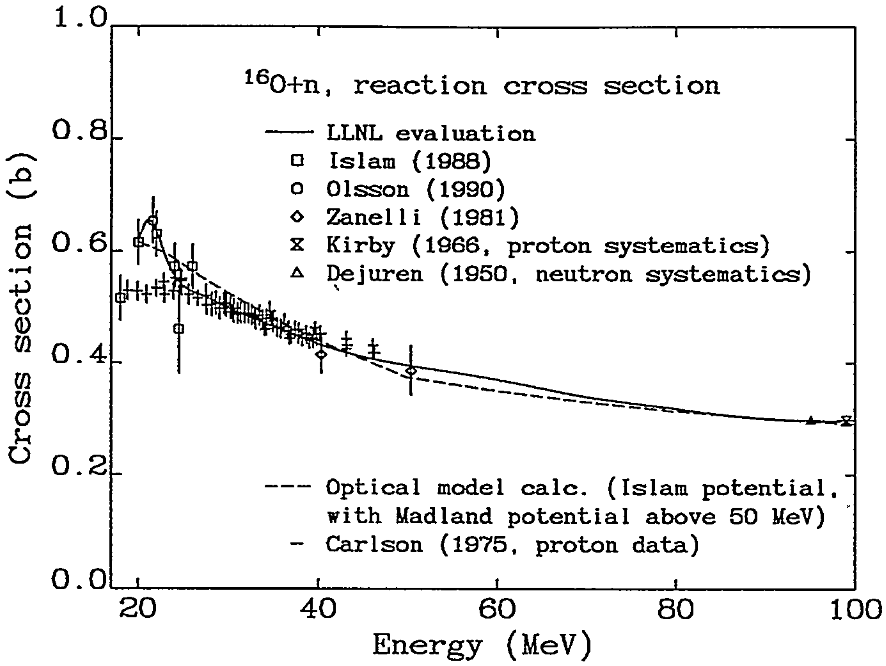

Fig. 2. Nonelastic cross section for neutrons on oxygen. The experimental data were taken from the Brookhaven NNDC CSISRS file.

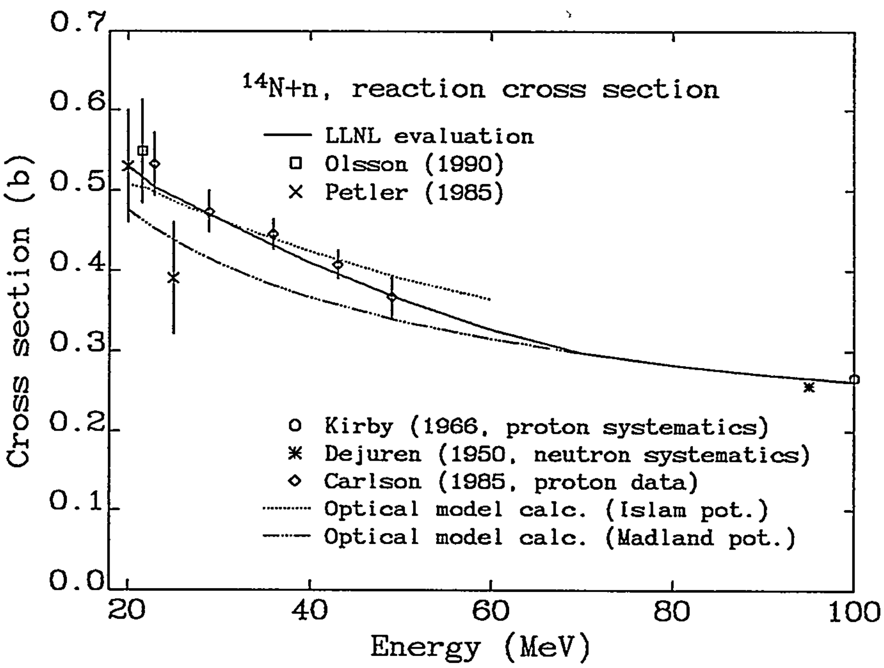

Fig. 3. Nonelastic cross section for neutrons on nitrogen. The experimental data were taken from the Brookhaven NNDC CSISRS file.

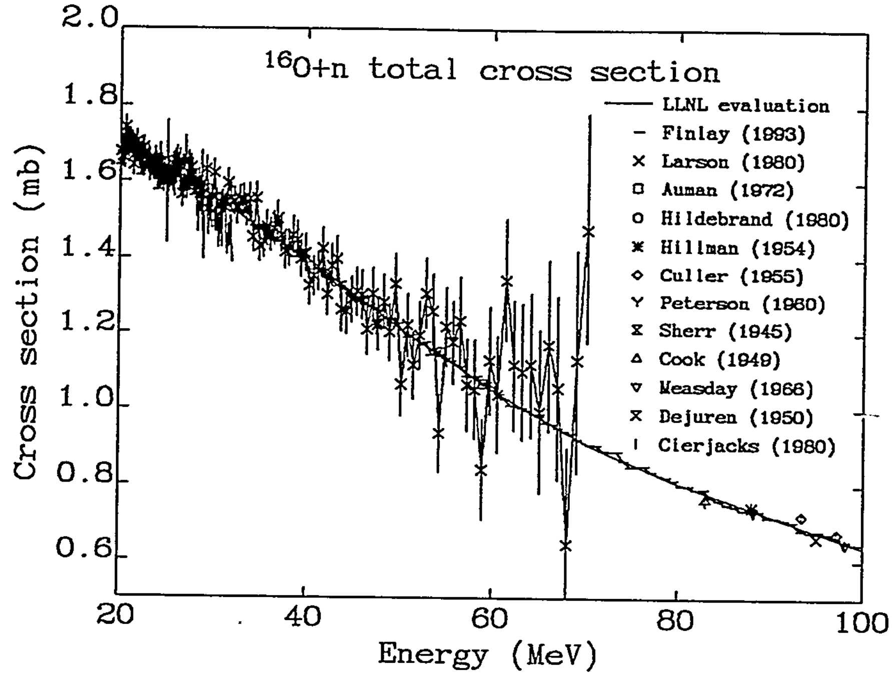

Fig. 4. Total cross section for neutrons on oxygen. The experimental data were taken from the Brookhaven NNDC CSISRS file.

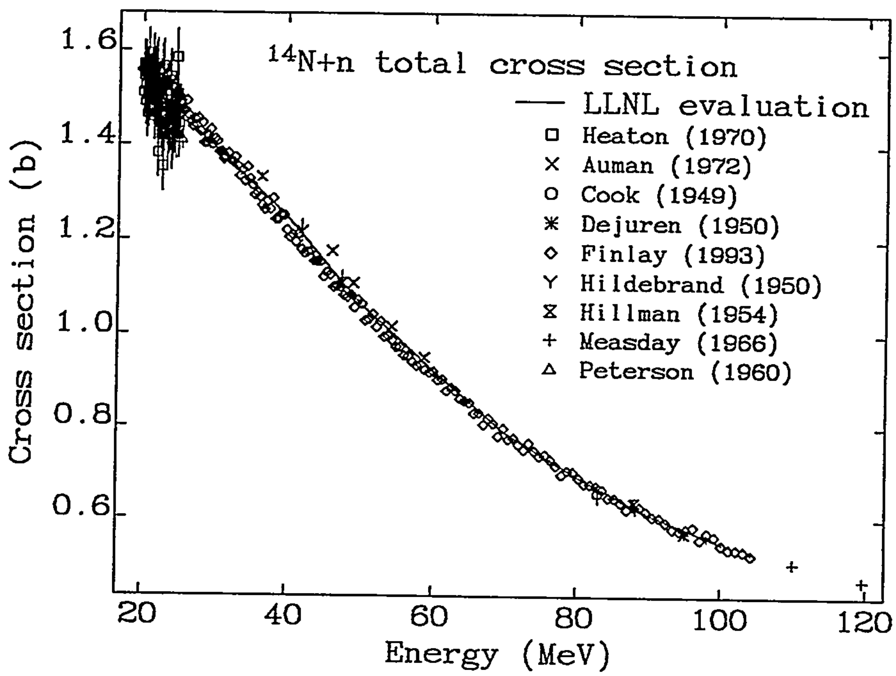

Fig. 5. Total cross section for neutrons on nitrogen. The experimental data were taken from the Brookhaven NNDC CSISRS file.

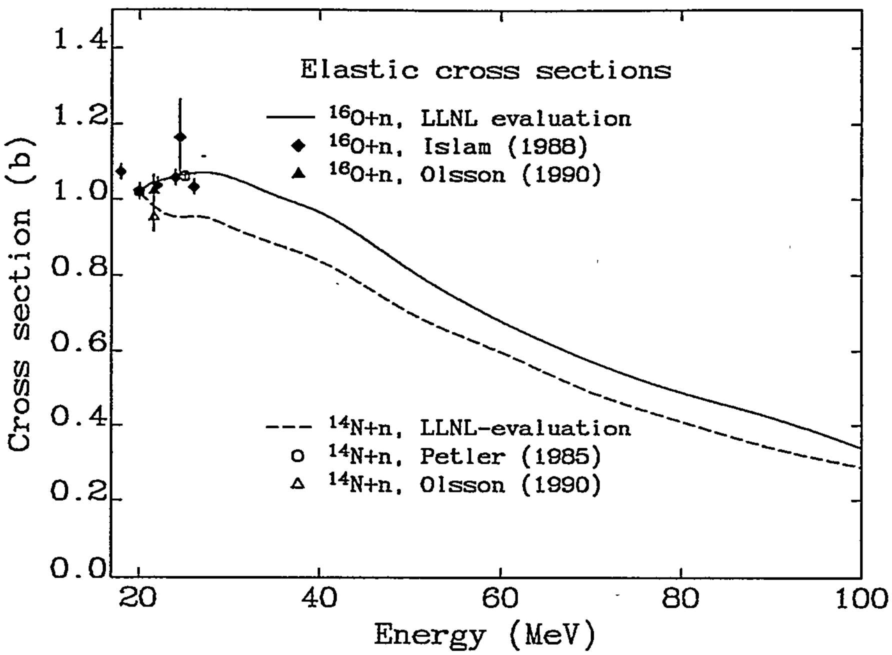

Fig. 6. Elastic cross section for neutrons on oxygen and nitrogen. The experimental data were taken from the Brookhaven NNDC CSISRS file.

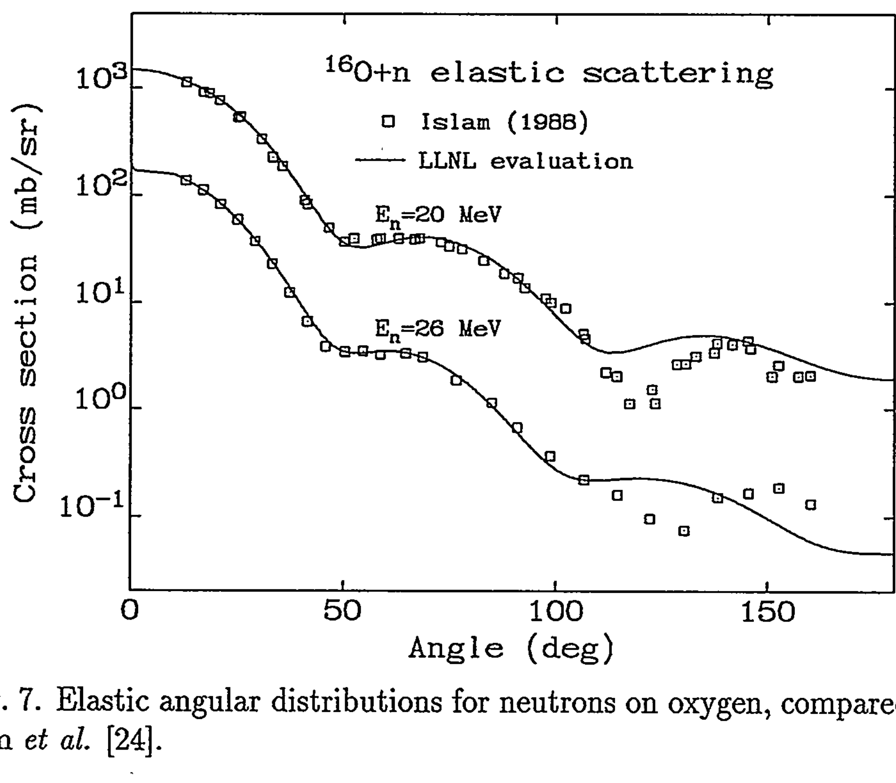

Fig. 7. Elastic angular distributions for neutrons on oxygen, compared with data of Islam *et al.* [24].

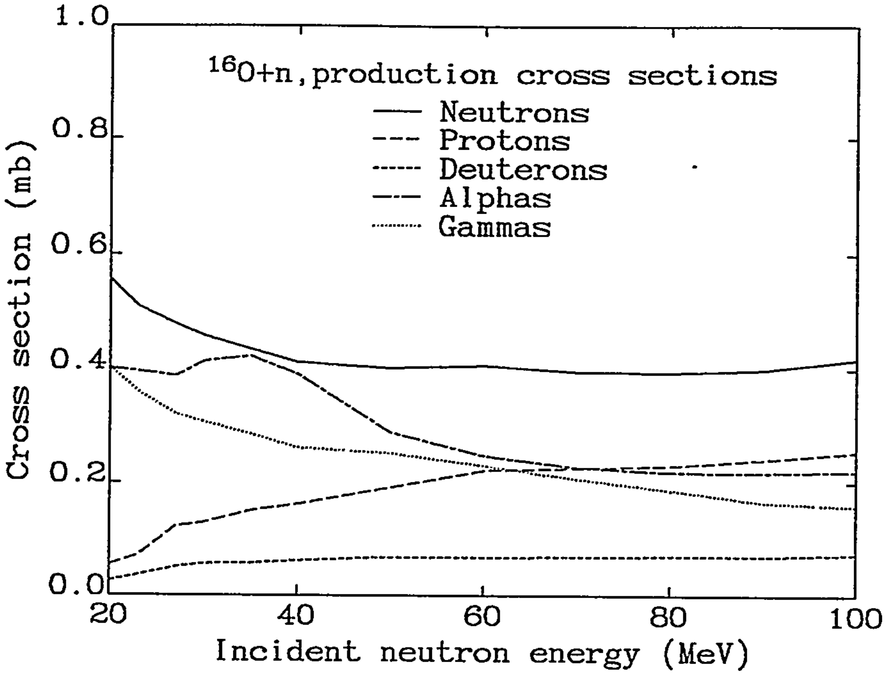

Fig. 8. Production cross sections of secondary particles with $A \leq 4$ for neutrons on oxygen.

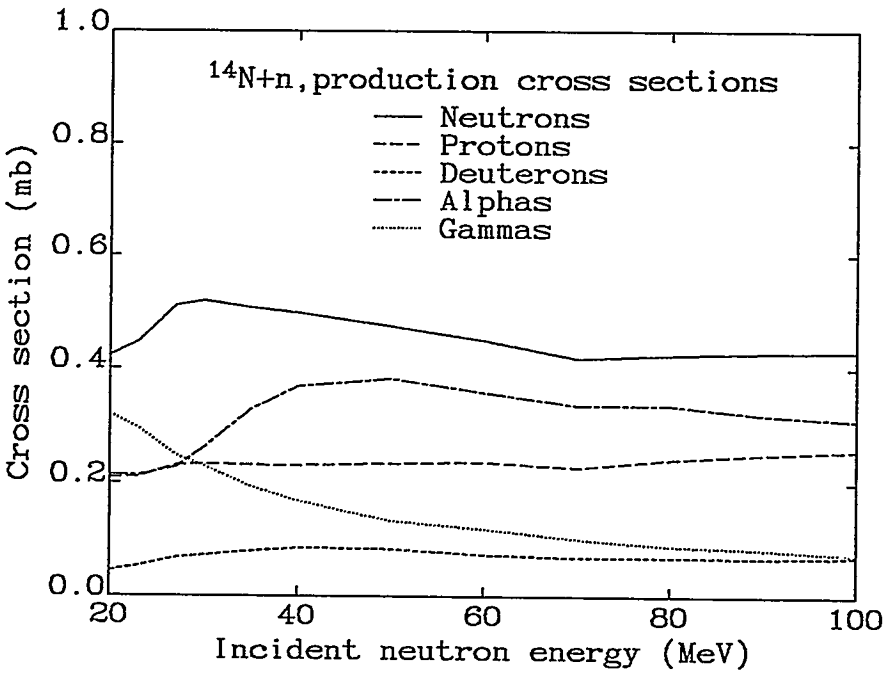

Fig. 9. Production cross sections of secondary particles with $A \leq 4$ for neutrons on nitrogen.

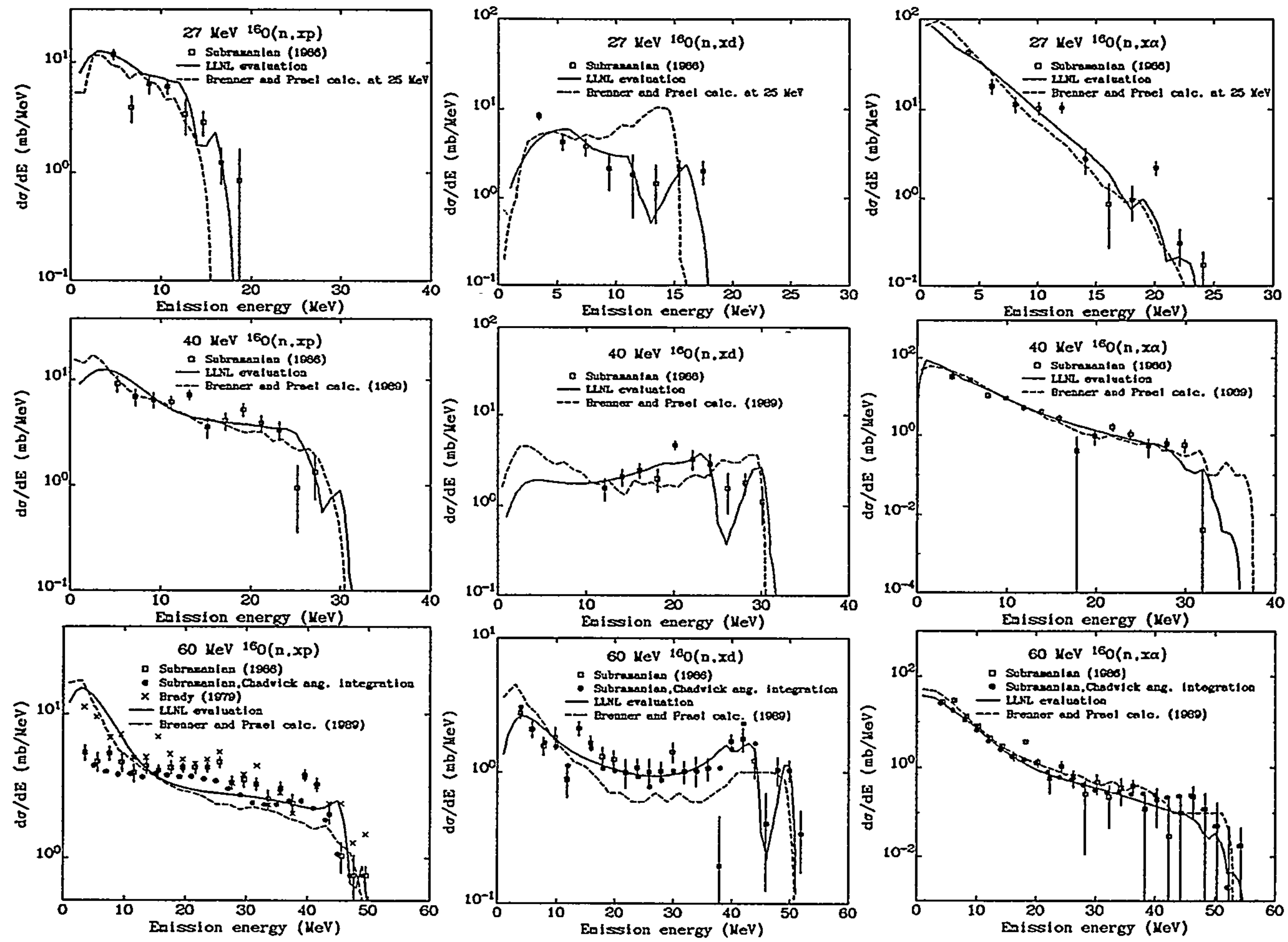

Fig. 10. Calculated angle-integrated proton, deuteron, and alpha emission spectra (lab frame) for neutrons on oxygen, compared with the data of Subramanian *et al.* [2]. Model calculations of Brenner and Prael [16] are also shown for comparison.

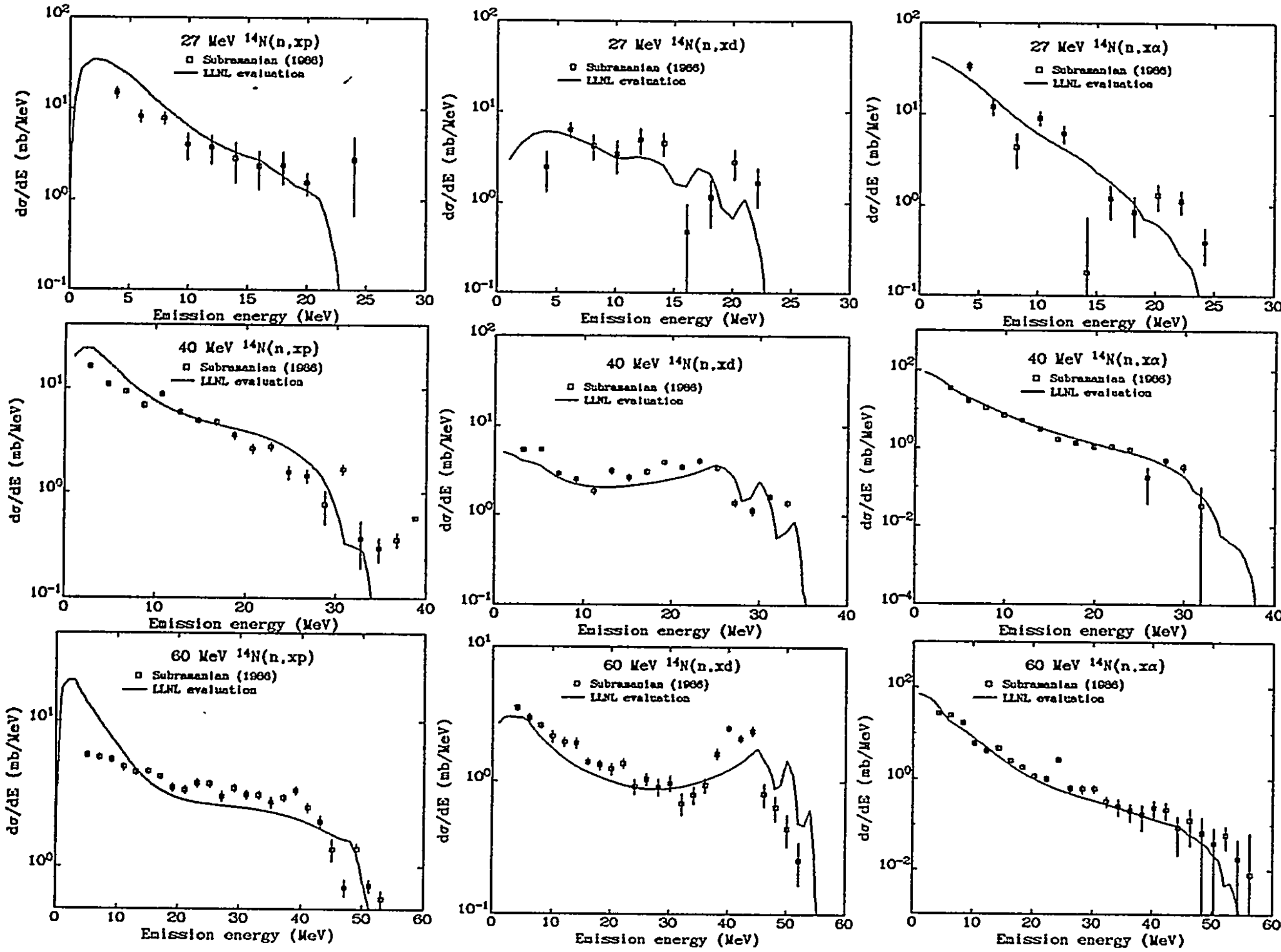

Fig. 11. Calculated angle-integrated proton, deuteron, and alpha emission spectra (lab frame) for neutrons on nitrogen, compared with the data of Subramanian *et al.* [2].

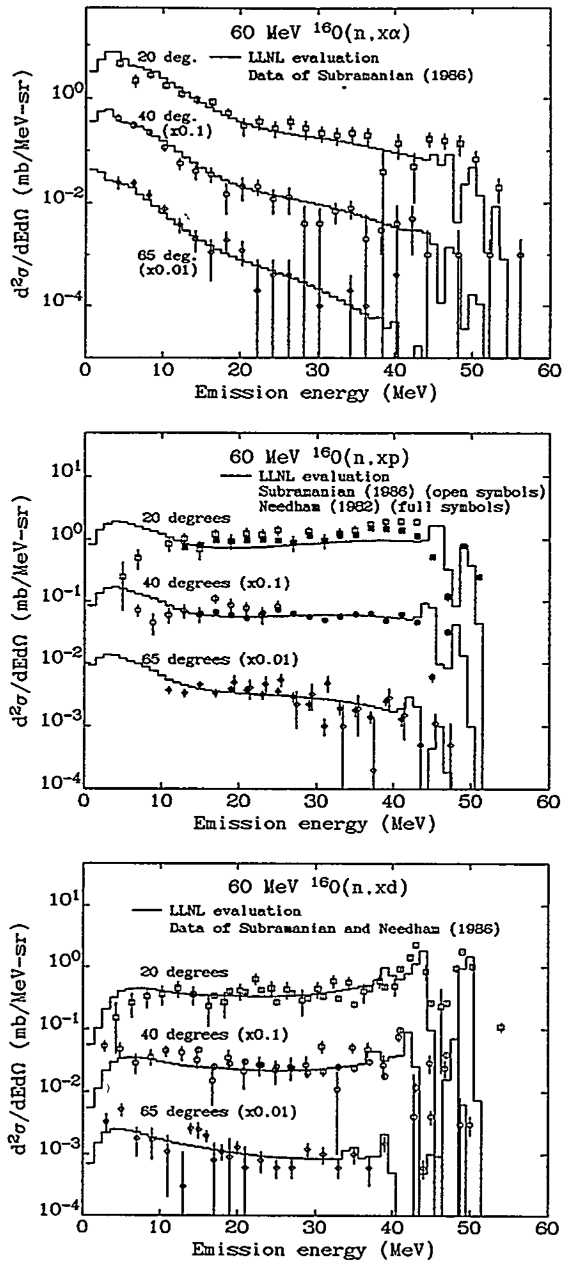

Fig. 12. Calculated double-differential spectra (lab frame) for alphas, protons, and deuterons following 60 MeV neutrons on oxygen, compared with the data of Subramanian *et al.* [2].

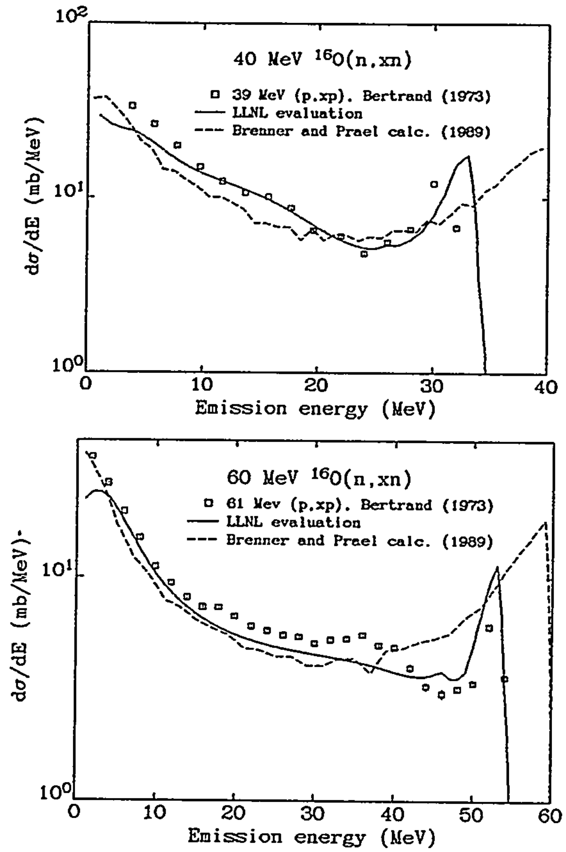

Fig. 13. Calculated $^{16}O(n, xn)$ angle-integrated spectra (lab frame) at 40 and 60 MeV compared with the Bertrand and Peelle $^{16}O(p, xp)$ measurements [42]. Brenner and Prael $^{16}O(n, xn)$ calculations are also shown for comparison [16].

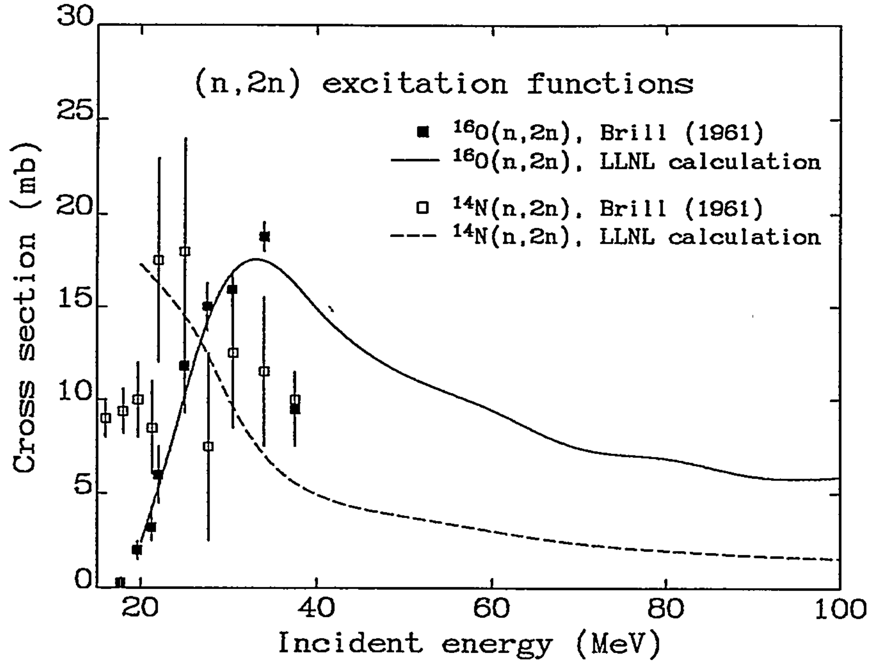

Fig. 14. The $^{16}O(n,2n)^{15}O$ and $^{14}N(n,2n)^{13}N$ calculated excitation functions compared with data of Brill *et al.* [44].

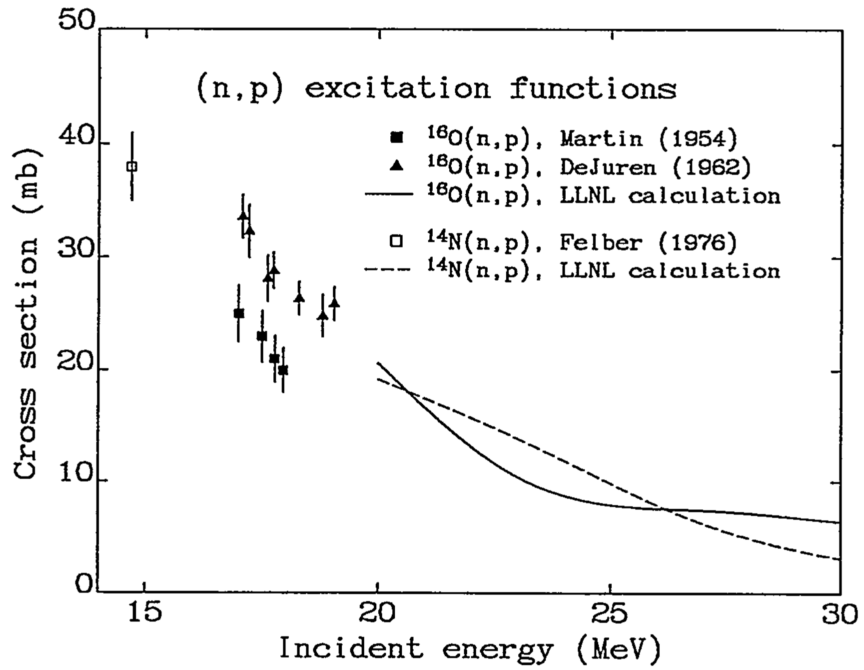

Fig. 15. The calculated $^{16}O(n,p)^{16}N$ excitation function compared with experimental data taken from the Brookhaven NNDC CSISRS file.

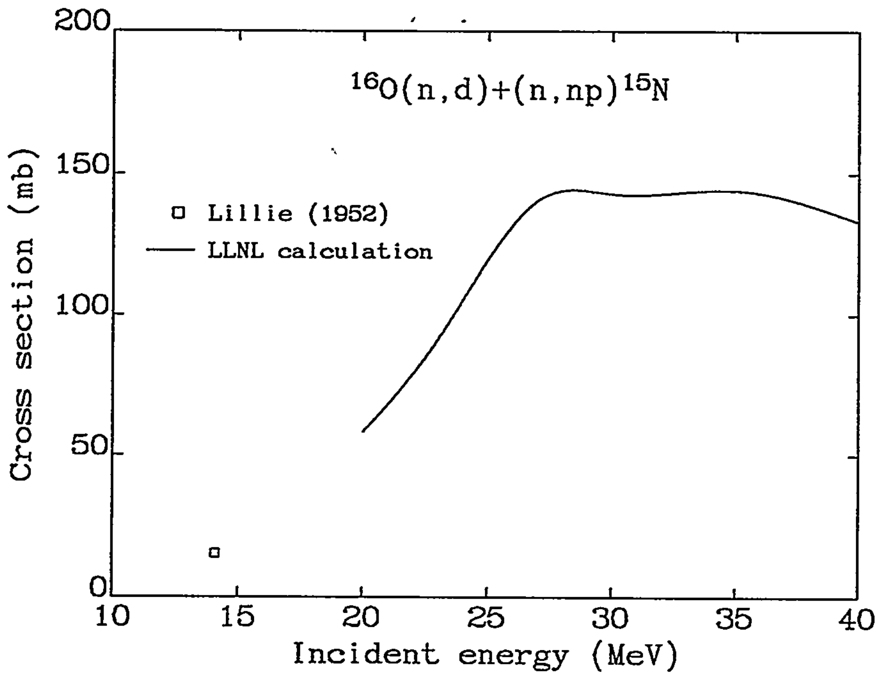

Fig. 16. The $^{16}O(n,d) + (n,np)^{15}N$ calculated excitation function compared with data of Lillie *et al.* taken from the Brookhaven NNDC CSISRS file.

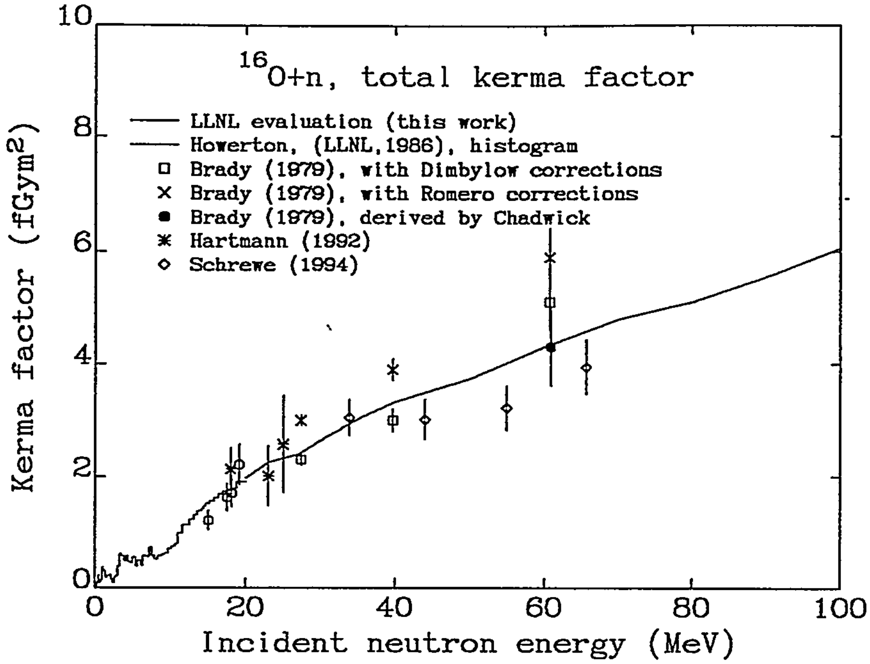

Fig. 17. Total calculated kerma factor for neutrons on oxygen compared with experimental measurements [13, 41, 45, 46].

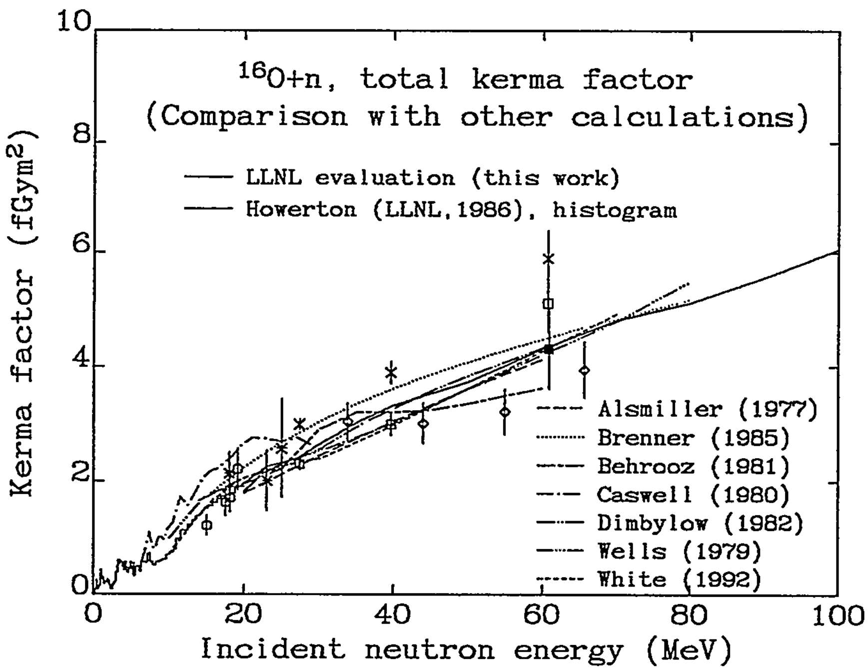

Fig. 18. Total calculated kerma factor for neutrons on oxygen compared with other calculations and evaluations [17, 47, 18, 23, 13, 3, 20, 48]. For key to experimental points, see Fig. 17.

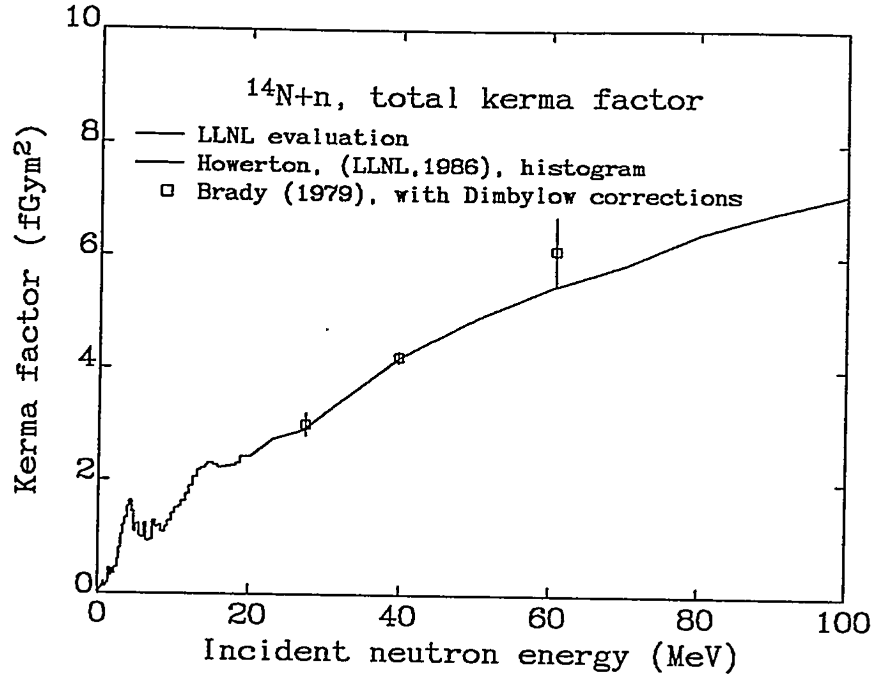

Fig. 19. Total calculated kerma factor for neutrons on nitrogen compared with experimental measurements of Brady *et al.* [13].

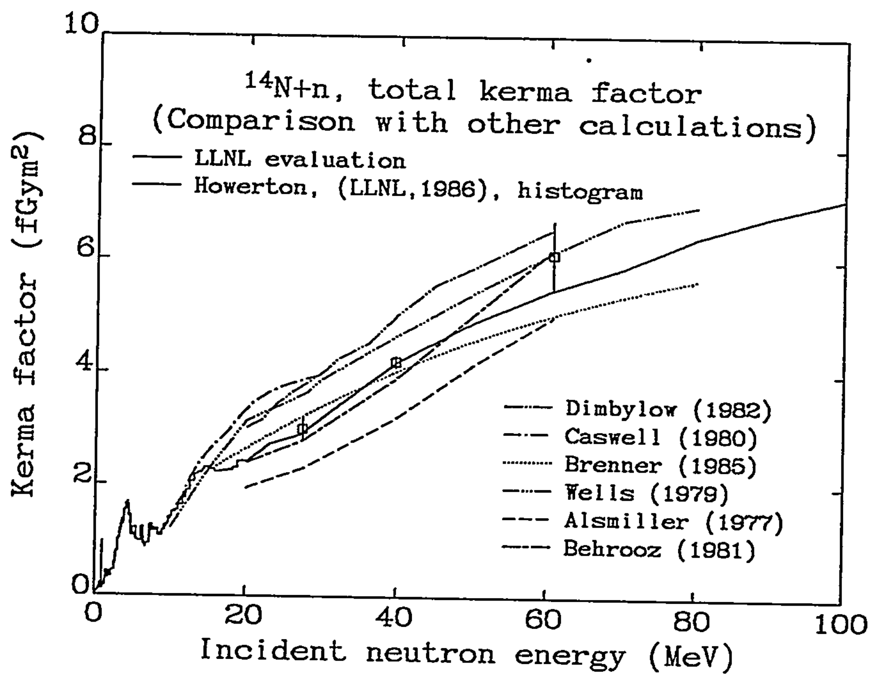

Fig. 20. Total calculated kerma factor for neutrons on nitrogen compared with other calculations and evaluations [17, 47, 18, 23, 13, 3, 20]. For key to experimental points, see Fig. 19.

8 Appendix 1 : Tabulations and Figures of Libraries for Oxygen

In the appendix we show the following figures and tables:

1. A figure (Fig. 21) showing the oxygen library angle-integrated emission spectra for $A \leq 4$ ejectiles, for incident energies of 20, 23, 27, 30, 35, 40, 50, 60, 70, 80, 90, and 100 MeV.

2. Tables (Table. VII) giving numerical values for the oxygen angle-integrated emission spectra for $A \leq 4$ ejectiles, for incident energies of 20, 23, 27, 30, 35, 40, 50, 60, 70, 80, 90, and 100 MeV. For completeness, at the end of each emission spectrum we also indicate the production cross section, the average kinetic energy, and the partial kerma factors. These are then combined with the elastic and recoil nonelastic kerma factors to give the total kerma factor.

3. Figures (Figs. 22-33) showing the oxygen library double-differential emission spectra for $A \leq 4$ ejectiles, for angles every 10-degrees between 0 and 180 degrees, and for incident energies of 20, 23, 27, 30, 35, 40, 50, 60, 70, 80, 90, and 100 MeV. Generally the higher lines correspond to forward angles and the lower lines to the backward angles.

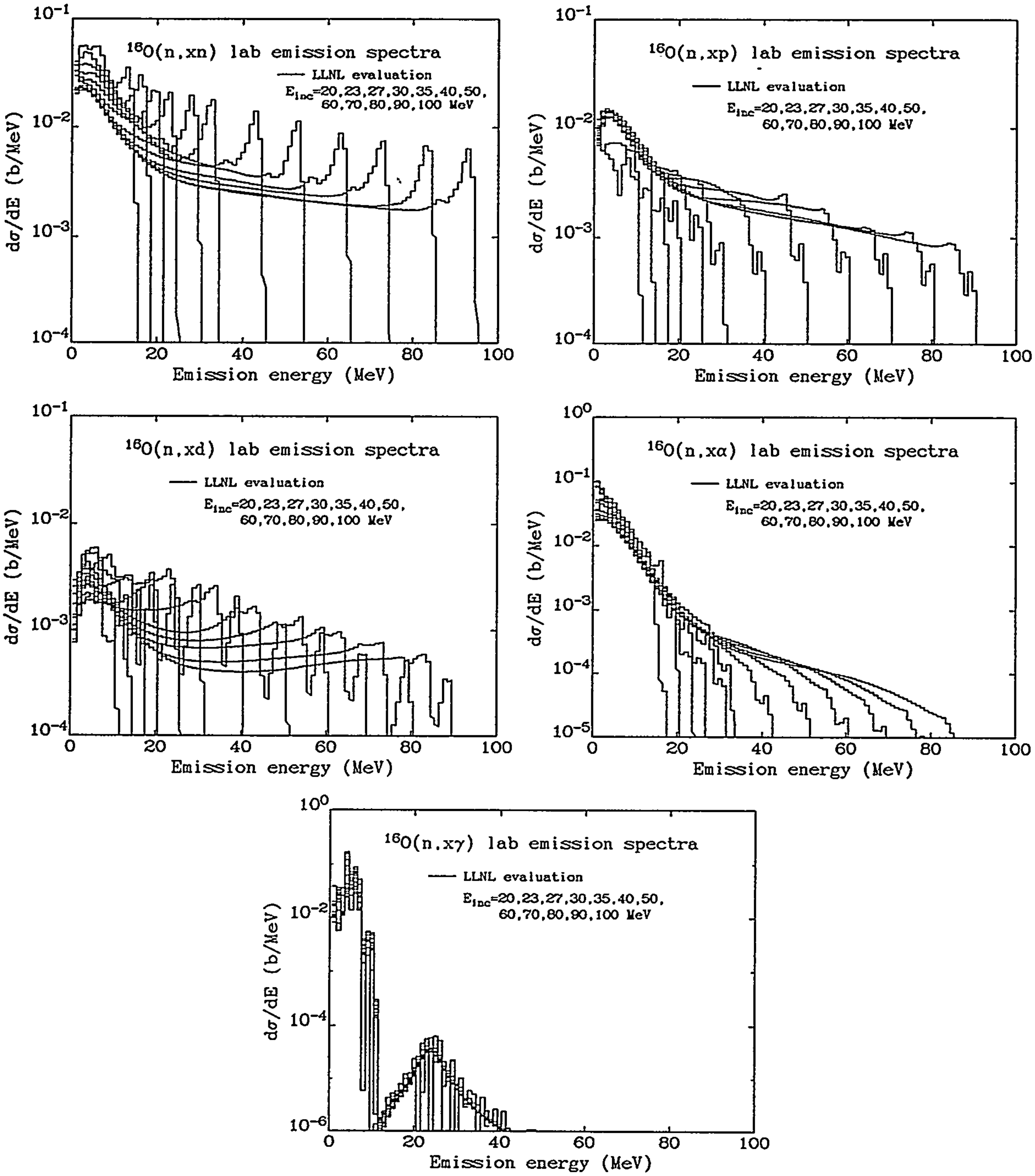

Figure 21: Angle-integrated evaluated emission spectra (lab frame) for incident neutron energies between 20 and 100 MeV on oxygen

The following pages contain tabulations of the evaluated angle-integrated emission spectra from ^{16}O+n reactions. Tabulations of the double-differential spectra can be obtained from the authors. Kerma factors are also shown.

Table VII: Tabulations of oxygen angle-integrated emission spectra

Incident Energy: $E_n = 20.00$MeV

Energy (MeV)	Lab angle–integrated emission spectra: (mb/MeV)				
	$d\sigma_n/dE$	$d\sigma_p/dE$	$d\sigma_d/dE$	$d\sigma_\alpha/dE$	$d\sigma_\gamma/dE$
1.00	4.01E+01	8.49E+00	7.52E-01	3.64E+01	3.86E+01
2.00	5.60E+01	6.22E+00	2.80E+00	5.45E+01	5.81E+00
3.00	5.67E+01	5.78E+00	5.08E+00	5.96E+01	3.64E+01
4.00	5.21E+01	5.21E+00	4.34E+00	5.57E+01	1.67E+02
5.00	5.50E+01	4.14E+00	2.50E+00	4.73E+01	1.38E+01
6.00	5.58E+01	2.44E+00	1.76E+00	3.66E+01	8.69E+01
7.00	4.55E+01	4.62E+00	2.22E+00	2.84E+01	5.14E+01
8.00	3.31E+01	6.33E+00	1.82E+00	2.43E+01	5.82E-03
9.00	2.67E+01	6.22E+00	2.14E+00	1.83E+01	1.96E+00
10.00	2.32E+01	4.01E+00	1.78E+00	1.31E+01	9.99E-04
11.00	2.56E+01	2.83E-01	1.77E-01	8.55E+00	1.35E-03
12.00	2.83E+01	2.16E-03	1.76E-03	6.91E+00	1.78E-03
13.00	3.53E+01	—	—	8.01E+00	1.49E-03
14.00	2.26E+01	—	—	4.33E+00	4.35E-03
15.00	2.02E+00	—	—	5.91E-01	5.27E-03
16.00	2.64E-02	—	—	7.44E-02	5.68E-03
17.00	2.02E-02	—	—	5.16E-02	7.62E-03
18.00	3.27E-02	—	—	2.58E-03	1.20E-02
19.00	5.87E-02	—	—	—	8.60E-03
20.00	5.70E-02	—	—	—	2.34E-02
21.00	5.93E-03	—	—	—	—
22.00	—	—	—	—	4.58E-02
23.00	—	—	—	—	3.37E-02
24.00	—	—	—	—	—
25.00	—	—	—	—	—
σ_{prod} (b)	5.58E-01	5.38E-02	2.54E-02	4.03E-01	4.02E-01
E_{av} (MeV)	6.53E+00	5.17E+00	5.20E+00	5.13E+00	4.47E+00
K (fGy· m^2)	—	1.67E-01	7.96E-02	1.24E+00	—
$\Sigma_{A<4}K_A$					1.49E+00
K_{recoil} non-elastic ($A > 4$)					2.20E-01
K_{recoil} elastic					2.81E-01
K_{total}					1.99E+00

Incident Energy: $E_n = 23.00$MeV

Energy (MeV)	Lab angle–integrated emission spectra: (mb/MeV)				
	$d\sigma_n/dE$	$d\sigma_p/dE$	$d\sigma_d/dE$	$d\sigma_\alpha/dE$	$d\sigma_\gamma/dE$
1.00	3.27E+01	6.99E+00	1.29E+00	4.81E+01	2.01E+01
2.00	4.36E+01	6.24E+00	2.42E+00	5.17E+01	7.87E+00
3.00	4.92E+01	7.12E+00	3.90E+00	5.02E+01	2.57E+01
4.00	4.75E+01	7.34E+00	5.46E+00	4.85E+01	1.56E+02
5.00	4.20E+01	7.28E+00	5.19E+00	4.08E+01	2.60E+01
6.00	3.69E+01	7.35E+00	5.24E+00	3.31E+01	7.89E+01
7.00	3.31E+01	6.97E+00	3.63E+00	2.59E+01	4.18E+01
8.00	2.94E+01	5.39E+00	8.60E-01	1.97E+01	1.43E+00
9.00	2.55E+01	3.63E+00	7.60E-01	1.66E+01	2.71E+00
10.00	2.15E+01	3.40E+00	7.76E-01	1.32E+01	1.04E+00
11.00	1.85E+01	2.33E+00	1.08E+00	1.17E+01	2.08E-03
12.00	1.57E+01	2.85E+00	1.81E+00	9.12E+00	1.75E-03
13.00	1.76E+01	2.71E+00	2.11E+00	6.70E+00	2.37E-03
14.00	1.95E+01	3.73E-01	3.56E-01	4.92E+00	3.19E-03
15.00	2.21E+01	2.53E-03	3.15E-03	4.93E+00	4.53E-03
16.00	2.98E+01	—	—	5.86E+00	4.14E-03
17.00	2.36E+01	—	—	2.29E+00	7.98E-03
18.00	3.60E+00	—	—	1.82E+00	1.01E-02
19.00	2.92E-02	—	—	1.58E+00	1.26E-02

Incident Energy: $E_n = 23.00$MeV: cont.

Energy (MeV)	Lab angle–integrated emission spectra: (mb/MeV)				
	$d\sigma_n/dE$	$d\sigma_p/dE$	$d\sigma_d/dE$	$d\sigma_\alpha/dE$	$d\sigma_\gamma/dE$
20.00	6.23E-03	—	—	1.13E-01	1.62E-02
21.00	1.04E-02	—	—	2.27E-03	2.59E-02
22.00	1.91E-02	—	—	—	2.30E-02
23.00	2.35E-02	—	—	—	5.51E-02
24.00	4.19E-03	—	—	—	—
25.00	—	—	—	—	6.33E-02
26.00	—	—	—	—	2.25E-02
27.00	—	—	—	—	—
28.00	—	—	—	—	—
σ_{prod} (b)	5.12E-01	7.00E-02	3.49E-02	3.97E-01	3.61E-01
E_{av} (MeV)	7.80E+00	5.88E+00	6.07E+00	5.55E+00	4.66E+00
K (fGy· m^2)	—	2.48E-01	1.28E-01	1.33E+00	—
$\Sigma_{A<4}K_A$					1.70E+00
K_{recoil} non-elastic ($A > 4$)					2.90E-01
K_{recoil} elastic					2.73E-01
K_{total}					2.27E+00

Incident Energy: $E_n = 27.00$MeV

Energy (MeV)	Lab angle–integrated emission spectra: (mb/MeV)				
	$d\sigma_n/dE$	$d\sigma_p/dE$	$d\sigma_d/dE$	$d\sigma_\alpha/dE$	$d\sigma_\gamma/dE$
1.00	3.70E+01	8.03E+00	1.30E+00	8.39E+01	1.27E+01
2.00	3.73E+01	1.11E+01	2.54E+00	6.51E+01	1.37E+01
3.00	3.79E+01	1.27E+01	4.08E+00	4.87E+01	1.24E+01
4.00	3.73E+01	1.24E+01	5.19E+00	4.07E+01	1.20E+02
5.00	3.53E+01	1.14E+01	5.84E+00	3.40E+01	5.13E+01
6.00	3.28E+01	1.03E+01	5.93E+00	2.69E+01	7.22E+01
7.00	2.96E+01	9.02E+00	4.69E+00	2.09E+01	2.98E+01
8.00	2.61E+01	7.87E+00	3.59E+00	1.64E+01	2.18E+00
9.00	2.29E+01	7.53E+00	3.24E+00	1.26E+01	3.96E+00
10.00	2.04E+01	7.28E+00	2.98E+00	9.53E+00	3.31E+00
11.00	1.82E+01	6.76E+00	2.91E+00	7.47E+00	1.57E-01
12.00	1.64E+01	6.58E+00	1.09E+00	5.75E+00	1.64E-03
13.00	1.47E+01	4.53E+00	5.19E-01	4.49E+00	2.19E-03
14.00	1.18E+01	1.79E+00	8.86E-01	3.52E+00	3.11E-03
15.00	1.10E+01	1.75E+00	1.61E+00	2.68E+00	4.11E-03
16.00	1.17E+01	2.32E+00	2.37E+00	2.00E+00	5.10E-03
17.00	1.37E+01	8.62E-01	7.31E-01	1.17E+00	6.05E-03
18.00	1.74E+01	8.85E-02	6.35E-03	7.59E-01	7.65E-03
19.00	2.18E+01	—	—	9.84E-01	1.04E-02
20.00	2.12E+01	—	—	5.97E-01	1.53E-02
21.00	5.76E+00	—	—	1.98E-01	2.25E-02
22.00	4.30E-02	—	—	2.15E-01	3.45E-02
23.00	4.32E-03	—	—	1.83E-01	3.06E-02
24.00	7.43E-03	—	—	1.09E-02	5.80E-02
25.00	1.41E-02	—	—	—	2.04E-02
26.00	2.19E-02	—	—	—	5.23E-02
27.00	7.30E-03	—	—	—	—
28.00	—	—	—	—	—
29.00	—	—	—	—	2.13E-02
30.00	—	—	—	—	5.98E-03
31.00	—	—	—	—	—
32.00	—	—	—	—	—
σ_{prod} (b)	4.80E-01	1.22E-01	4.95E-02	3.89E-01	3.22E-01
E_{av} (MeV)	8.78E+00	6.75E+00	7.40E+00	4.54E+00	4.82E+00
K (fGy· m^2)	—	4.98E-01	2.21E-01	1.06E+00	—
$\Sigma_{A<4}K_A$					1.78E+00
K_{recoil} non-elastic ($A > 4$)					3.60E-01
K_{recoil} elastic					2.68E-01
K_{total}					2.41E+00

Incident Energy: $E_n = 30.00$MeV

Energy (MeV)	Lab angle–integrated emission spectra: (mb/MeV)				
	$d\sigma_n/dE$	$d\sigma_p/dE$	$d\sigma_d/dE$	$d\sigma_\alpha/dE$	$d\sigma_\gamma/dE$
1.00	3.66E+01	7.32E+00	9.83E-01	1.01E+02	1.15E+01
2.00	3.18E+01	1.03E+01	1.76E+00	7.59E+01	1.92E+01
3.00	3.07E+01	1.23E+01	2.54E+00	5.44E+01	1.18E+01
4.00	3.14E+01	1.23E+01	3.15E+00	4.03E+01	9.23E+01
5.00	3.09E+01	1.15E+01	3.77E+00	3.16E+01	6.32E+01
6.00	2.89E+01	1.04E+01	4.20E+00	2.43E+01	6.92E+01
7.00	2.58E+01	9.19E+00	4.45E+00	1.86E+01	2.83E+01
8.00	2.26E+01	7.98E+00	4.72E+00	1.44E+01	2.62E+00
9.00	2.00E+01	6.88E+00	5.02E+00	1.12E+01	4.78E+00
10.00	1.79E+01	6.01E+00	3.89E+00	8.80E+00	4.09E+00
11.00	1.61E+01	5.43E+00	3.09E+00	6.97E+00	2.03E-01
12.00	1.49E+01	5.21E+00	3.11E+00	5.62E+00	1.55E-03
13.00	1.38E+01	4.85E+00	3.21E+00	4.60E+00	2.12E-03
14.00	1.30E+01	4.52E+00	3.22E+00	3.74E+00	3.03E-03
15.00	1.25E+01	4.33E+00	1.52E+00	3.12E+00	4.03E-03
16.00	1.20E+01	3.88E+00	4.65E-01	2.58E+00	5.04E-03
17.00	9.82E+00	1.86E+00	8.19E-01	2.15E+00	5.92E-03
18.00	1.00E+01	1.41E+00	1.56E+00	1.71E+00	7.42E-03
19.00	1.05E+01	2.19E+00	2.61E+00	1.24E+00	1.00E-02
20.00	1.14E+01	9.89E-01	1.18E+00	6.98E-01	1.42E-02
21.00	1.25E+01	5.07E-02	1.82E-02	5.01E-01	2.04E-02
22.00	1.79E+01	—	—	6.93E-01	5.42E-03
23.00	2.09E+01	—	—	4.33E-01	4.13E-02
24.00	8.28E+00	—	—	1.47E-01	3.60E-02
25.00	1.41E-01	—	—	1.75E-01	3.71E-02
26.00	3.42E-03	—	—	1.45E-01	2.72E-02
27.00	2.04E-03	—	—	7.64E-03	2.08E-02
28.00	4.05E-03	—	—	—	8.95E-03
29.00	7.19E-03	—	—	—	2.26E-02
30.00	3.63E-03	—	—	—	—
31.00	—	—	—	—	1.03E-02
32.00	—	—	—	—	2.87E-03
33.00	—	—	—	—	—
34.00	—	—	—	—	—
35.00	—	—	—	—	—
σ_{prod} (b)	4.60E-01	1.29E-01	5.53E-02	4.15E-01	3.08E-01
E_{av} (MeV)	1.00E+01	7.66E+00	9.59E+00	4.40E+00	4.87E+00
K (fGy· m^2)	—	5.95E-01	3.19E-01	1.10E+00	—
$\Sigma_{A<4}K_A$					2.02E+00
K_{recoil} non-elastic ($A > 4$)					3.90E-01
K_{recoil} elastic					2.59E-01
K_{total}					2.67E+00

Incident Energy: $E_n = 35.00$MeV

Energy (MeV)	Lab angle–integrated emission spectra: (mb/MeV)				
	$d\sigma_n/dE$	$d\sigma_p/dE$	$d\sigma_d/dE$	$d\sigma_\alpha/dE$	$d\sigma_\gamma/dE$
1.00	3.31E+01	7.75E+00	8.00E-01	1.03E+02	1.04E+01
2.00	2.84E+01	1.07E+01	1.37E+00	8.04E+01	2.73E+01
3.00	2.70E+01	1.25E+01	1.80E+00	6.03E+01	1.09E+01
4.00	2.72E+01	1.25E+01	2.02E+00	4.09E+01	6.16E+01
5.00	2.61E+01	1.16E+01	2.15E+00	2.99E+01	7.13E+01
6.00	2.41E+01	1.05E+01	2.26E+00	2.36E+01	6.51E+01
7.00	2.18E+01	9.35E+00	2.37E+00	1.80E+01	2.58E+01
8.00	1.96E+01	8.14E+00	2.52E+00	1.38E+01	2.95E+00
9.00	1.77E+01	7.03E+00	2.64E+00	1.06E+01	5.53E+00

Incident Energy: $E_n = 35.00$MeV: cont.

Energy (MeV)	Lab angle–integrated emission spectra: (mb/MeV)				
	$d\sigma_n/dE$	$d\sigma_p/dE$	$d\sigma_d/dE$	$d\sigma_\alpha/dE$	$d\sigma_\gamma/dE$
10.00	1.59E+01	6.13E+00	2.74E+00	8.14E+00	5.23E+00
11.00	1.45E+01	5.50E+00	2.82E+00	6.36E+00	2.98E-01
12.00	1.32E+01	5.06E+00	2.94E+00	5.08E+00	1.43E-03
13.00	1.21E+01	4.76E+00	3.07E+00	4.14E+00	2.01E-03
14.00	1.12E+01	4.56E+00	2.93E+00	3.39E+00	2.89E-03
15.00	1.03E+01	4.43E+00	2.70E+00	2.81E+00	3.85E-03
16.00	9.62E+00	4.34E+00	2.70E+00	2.34E+00	4.89E-03
17.00	8.97E+00	4.20E+00	2.70E+00	1.95E+00	5.81E-03
18.00	8.34E+00	4.08E+00	2.90E+00	1.66E+00	7.25E-03
19.00	7.93E+00	4.12E+00	3.42E+00	1.43E+00	9.71E-03
20.00	7.73E+00	3.71E+00	2.36E+00	1.24E+00	1.36E-02
21.00	7.85E+00	3.07E+00	5.13E-01	1.11E+00	1.96E-02
22.00	7.03E+00	1.83E+00	7.21E-01	1.01E+00	2.77E-02
23.00	5.96E+00	9.46E-01	1.41E+00	8.73E-01	3.53E-02
24.00	6.72E+00	1.61E+00	2.65E+00	6.18E-01	3.73E-02
25.00	7.85E+00	1.24E+00	1.98E+00	3.30E-01	3.21E-02
26.00	9.36E+00	7.84E-02	1.03E-01	2.90E-01	2.45E-02
27.00	1.42E+01	1.13E-03	2.08E-03	4.15E-01	7.14E-03
28.00	1.97E+01	—	—	2.40E-01	1.38E-02
29.00	1.27E+01	—	—	6.81E-02	1.11E-02
30.00	8.73E-01	—	—	8.19E-02	7.77E-03
31.00	1.27E-02	—	—	6.28E-02	6.79E-03
32.00	—	—	—	2.60E-03	3.91E-03
33.00	1.20E-03	—	—	—	5.89E-03
34.00	2.40E-03	—	—	—	5.07E-03
35.00	2.11E-03	—	—	—	—
36.00	—	—	—	—	4.38E-03
37.00	—	—	—	—	1.24E-03
38.00	—	—	—	—	—
39.00	—	—	—	—	—
40.00	—	—	—	—	—
σ_{prod} (b)	4.37E-01	1.50E-01	5.66E-02	4.24E-01	2.87E-01
E_{av} (MeV)	1.18E+01	9.24E+00	1.33E+01	4.43E+00	4.91E+00
K (fGy· m^2)	—	8.35E-01	4.53E-01	1.13E+00	—
$\Sigma_{A<4}K_A$					2.42E+00
K_{recoil} non-elastic ($A > 4$)					3.90E-01
K_{recoil} elastic					2.42E-01
K_{total}					3.05E+00

Incident Energy: $E_n = 40.00$MeV

Energy (MeV)	Lab angle–integrated emission spectra: (mb/MeV)				
	$d\sigma_n/dE$	$d\sigma_p/dE$	$d\sigma_d/dE$	$d\sigma_\alpha/dE$	$d\sigma_\gamma/dE$
1.00	2.95E+01	8.94E+00	7.53E-01	8.67E+01	8.20E+00
2.00	2.64E+01	1.09E+01	1.34E+00	7.02E+01	3.18E+01
3.00	2.51E+01	1.23E+01	1.74E+00	5.61E+01	1.09E+01
4.00	2.43E+01	1.24E+01	1.89E+00	3.91E+01	4.24E+01
5.00	2.23E+01	1.18E+01	1.89E+00	2.80E+01	7.00E+01
6.00	2.01E+01	1.06E+01	1.83E+00	2.26E+01	6.16E+01
7.00	1.79E+01	9.30E+00	1.78E+00	1.79E+01	2.44E+01
8.00	1.62E+01	8.02E+00	1.74E+00	1.39E+01	3.04E+00
9.00	1.49E+01	6.88E+00	1.73E+00	1.08E+01	5.50E+00
10.00	1.38E+01	5.94E+00	1.74E+00	8.44E+00	5.14E+00
11.00	1.30E+01	5.25E+00	1.78E+00	6.63E+00	3.05E-01
12.00	1.23E+01	4.78E+00	1.85E+00	5.26E+00	1.41E-03
13.00	1.16E+01	4.46E+00	1.93E+00	4.22E+00	1.87E-03

Incident Energy: $E_n = 40.00$MeV: cont.

Energy (MeV)	Lab angle–integrated emission spectra: (mb/MeV)				
	$d\sigma_n/dE$	$d\sigma_p/dE$	$d\sigma_d/dE$	$d\sigma_\alpha/dE$	$d\sigma_\gamma/dE$
14.00	1.09E+01	4.25E+00	2.02E+00	3.44E+00	2.63E-03
15.00	1.02E+01	4.10E+00	2.18E+00	2.85E+00	3.68E-03
16.00	9.48E+00	3.98E+00	2.33E+00	2.39E+00	4.70E-03
17.00	8.72E+00	3.89E+00	2.49E+00	2.02E+00	5.62E-03
18.00	7.98E+00	3.81E+00	2.73E+00	1.74E+00	6.99E-03
19.00	7.26E+00	3.76E+00	2.93E+00	1.50E+00	9.34E-03
20.00	6.62E+00	3.68E+00	2.89E+00	1.30E+00	1.32E-02
21.00	6.06E+00	3.58E+00	2.99E+00	1.14E+00	1.89E-02
22.00	5.62E+00	3.47E+00	3.18E+00	9.94E-01	2.67E-02
23.00	5.29E+00	3.40E+00	3.71E+00	8.72E-01	3.39E-02
24.00	5.06E+00	3.38E+00	3.02E+00	7.69E-01	3.55E-02
25.00	5.05E+00	3.10E+00	6.48E-01	6.85E-01	3.04E-02
26.00	5.27E+00	2.21E+00	3.77E-01	6.19E-01	2.31E-02
27.00	5.27E+00	1.39E+00	6.96E-01	5.79E-01	1.68E-02
28.00	5.67E+00	5.59E-01	1.32E+00	4.41E-01	1.24E-02
29.00	6.35E+00	7.57E-01	2.48E+00	2.71E-01	9.32E-03
30.00	7.80E+00	8.95E-01	2.64E+00	1.41E-01	7.23E-03
31.00	1.06E+01	1.50E-01	3.20E-01	1.10E-01	5.75E-03
32.00	1.58E+01	1.79E-03	5.76E-03	1.37E-01	3.28E-03
33.00	1.79E+01	—	—	2.63E-02	4.19E-03
34.00	3.23E+00	—	—	4.47E-03	3.40E-03
35.00	6.05E-02	—	—	3.19E-03	3.20E-03
36.00	—	—	—	—	2.16E-03
37.00	—	—	—	—	2.44E-03
38.00	—	—	—	—	1.48E-03
39.00	—	—	—	—	2.61E-03
40.00	—	—	—	—	—
41.00	—	—	—	—	2.38E-03
42.00	—	—	—	—	6.67E-04
43.00	—	—	—	—	—
44.00	—	—	—	—	—
45.00	—	—	—	—	—
σ_{prod} (b)	4.13E-01	1.62E-01	6.10E-02	3.92E-01	2.64E-01
E_{av} (MeV)	1.34E+01	1.05E+01	1.65E+01	4.77E+00	4.93E+00
K (fGy· m^2)	—	1.02E+00	6.08E-01	1.13E+00	—
$\Sigma_{A<4}K_A$					2.76E+00
K_{recoil} non-elastic ($A > 4$)					3.70E-01
K_{recoil} elastic					2.29E-01
K_{total}					3.36E+00

Incident Energy: $E_n = 50.00$MeV

Energy (MeV)	Lab angle–integrated emission spectra: (mb/MeV)				
	$d\sigma_n/dE$	$d\sigma_p/dE$	$d\sigma_d/dE$	$d\sigma_\alpha/dE$	$d\sigma_\gamma/dE$
1.00	2.30E+01	9.71E+00	1.10E+00	5.22E+01	1.10E+01
2.00	2.27E+01	1.26E+01	1.71E+00	4.60E+01	3.60E+01
3.00	2.21E+01	1.41E+01	2.11E+00	4.11E+01	1.15E+01
4.00	2.13E+01	1.36E+01	2.21E+00	3.19E+01	3.64E+01
5.00	1.95E+01	1.24E+01	2.15E+00	2.33E+01	6.46E+01
6.00	1.75E+01	1.09E+01	2.03E+00	1.87E+01	5.47E+01
7.00	1.54E+01	9.46E+00	1.90E+00	1.51E+01	2.42E+01
8.00	1.35E+01	8.14E+00	1.80E+00	1.21E+01	3.16E+00
9.00	1.21E+01	6.97E+00	1.71E+00	9.41E+00	5.66E+00
10.00	1.10E+01	5.98E+00	1.65E+00	7.27E+00	4.72E+00
11.00	1.02E+01	5.20E+00	1.60E+00	5.71E+00	2.78E-01
12.00	9.53E+00	4.64E+00	1.57E+00	4.50E+00	1.23E-03

Incident Energy: $E_n = 50.00$MeV: cont.

Energy (MeV)	Lab angle–integrated emission spectra: (mb/MeV)				
	$d\sigma_n/dE$	$d\sigma_p/dE$	$d\sigma_d/dE$	$d\sigma_\alpha/dE$	$d\sigma_\gamma/dE$
13.00	8.97E+00	4.25E+00	1.55E+00	3.58E+00	1.74E-03
14.00	8.51E+00	3.98E+00	1.54E+00	2.89E+00	2.55E-03
15.00	8.12E+00	3.79E+00	1.53E+00	2.37E+00	3.52E-03
16.00	7.78E+00	3.67E+00	1.52E+00	1.96E+00	4.54E-03
17.00	7.47E+00	3.58E+00	1.52E+00	1.65E+00	5.41E-03
18.00	7.19E+00	3.53E+00	1.52E+00	1.40E+00	6.74E-03
19.00	6.93E+00	3.50E+00	1.53E+00	1.20E+00	9.04E-03
20.00	6.68E+00	3.48E+00	1.54E+00	1.04E+00	1.27E-02
21.00	6.44E+00	3.47E+00	1.55E+00	9.07E-01	1.76E-02
22.00	6.21E+00	3.45E+00	1.57E+00	7.93E-01	2.48E-02
23.00	5.99E+00	3.43E+00	1.59E+00	6.96E-01	3.15E-02
24.00	5.77E+00	3.39E+00	1.62E+00	6.14E-01	3.29E-02
25.00	5.56E+00	3.34E+00	1.66E+00	5.42E-01	2.80E-02
26.00	5.37E+00	3.26E+00	1.71E+00	4.79E-01	2.12E-02
27.00	5.18E+00	3.16E+00	1.78E+00	4.22E-01	1.54E-02
28.00	5.02E+00	3.05E+00	1.86E+00	3.72E-01	1.13E-02
29.00	4.85E+00	2.91E+00	1.86E+00	3.26E-01	8.45E-03
30.00	4.71E+00	2.77E+00	1.80E+00	2.86E-01	6.52E-03
31.00	4.58E+00	2.62E+00	1.94E+00	2.50E-01	5.16E-03
32.00	4.48E+00	2.48E+00	2.25E+00	2.19E-01	4.18E-03
33.00	4.44E+00	2.37E+00	2.44E+00	1.91E-01	3.46E-03
34.00	4.51E+00	2.29E+00	2.58E+00	1.67E-01	2.91E-03
35.00	4.68E+00	1.98E+00	1.40E+00	1.48E-01	2.48E-03
36.00	4.98E+00	1.56E+00	4.58E-01	1.34E-01	2.15E-03
37.00	4.78E+00	8.52E-01	7.43E-01	1.11E-01	1.89E-03
38.00	4.56E+00	4.51E-01	1.31E+00	7.42E-02	1.67E-03
39.00	5.14E+00	7.40E-01	2.06E+00	3.82E-02	1.50E-03
40.00	5.92E+00	4.84E-01	9.20E-01	3.37E-02	1.35E-03
41.00	7.10E+00	2.21E-02	1.96E-02	4.44E-02	5.05E-04
42.00	1.06E+01	—	—	2.27E-02	1.13E-03
43.00	1.40E+01	—	—	6.48E-03	1.00E-03
44.00	7.82E+00	—	—	7.63E-03	9.89E-04
45.00	3.78E-01	—	—	4.70E-03	9.56E-04
46.00	8.17E-03	—	—	—	6.08E-04
47.00	—	—	—	—	1.08E-03
48.00	—	—	—	—	1.08E-03
49.00	—	—	—	—	—
50.00	—	—	—	—	1.04E-03
51.00	—	—	—	—	2.94E-04
52.00	—	—	—	—	—
53.00	—	—	—	—	—
54.00	—	—	—	—	—
55.00	—	—	—	—	—
σ_{prod} (b)	4.03E-01	1.92E-01	6.69E-02	2.90E-01	2.53E-01
E_{av} (MeV)	1.73E+01	1.30E+01	2.02E+01	5.34E+00	4.82E+00
K (fGy$\cdot$ m^2)	—	1.51E+00	8.15E-01	9.35E-01	—
$\Sigma_{A<4}K_A$					3.26E+00
K_{recoil} non-elastic ($A > 4$)					3.30E-01
K_{recoil} elastic					1.89E-01
K_{total}					3.78E+00

Incident Energy: $E_n = 60.00$MeV

Energy (MeV)	Lab angle–integrated emission spectra: (mb/MeV)				
	$d\sigma_n/dE$	$d\sigma_p/dE$	$d\sigma_d/dE$	$d\sigma_\alpha/dE$	$d\sigma_\gamma/dE$
1.00	2.23E+01	1.19E+01	1.37E+00	3.75E+01	1.65E+01
2.00	2.39E+01	1.42E+01	2.00E+00	3.53E+01	3.27E+01
3.00	2.39E+01	1.51E+01	2.45E+00	3.31E+01	1.27E+01
4.00	2.26E+01	1.44E+01	2.62E+00	2.77E+01	3.39E+01
5.00	2.00E+01	1.31E+01	2.60E+00	2.18E+01	5.58E+01
6.00	1.75E+01	1.16E+01	2.46E+00	1.76E+01	4.58E+01
7.00	1.52E+01	1.02E+01	2.28E+00	1.45E+01	1.97E+01
8.00	1.31E+01	8.79E+00	2.10E+00	1.17E+01	3.71E+00
9.00	1.14E+01	7.57E+00	1.92E+00	9.32E+00	5.30E+00
10.00	1.02E+01	6.50E+00	1.75E+00	7.19E+00	4.04E+00
11.00	9.19E+00	5.63E+00	1.61E+00	5.61E+00	2.34E-01
12.00	8.41E+00	4.96E+00	1.49E+00	4.38E+00	1.11E-03
13.00	7.78E+00	4.46E+00	1.40E+00	3.42E+00	1.58E-03
14.00	7.26E+00	4.09E+00	1.33E+00	2.70E+00	2.32E-03
15.00	6.83E+00	3.81E+00	1.26E+00	2.16E+00	3.25E-03
16.00	6.47E+00	3.59E+00	1.21E+00	1.76E+00	4.25E-03
17.00	6.16E+00	3.42E+00	1.16E+00	1.46E+00	5.12E-03
18.00	5.89E+00	3.28E+00	1.12E+00	1.23E+00	6.45E-03
19.00	5.67E+00	3.18E+00	1.08E+00	1.05E+00	8.69E-03
20.00	5.48E+00	3.09E+00	1.05E+00	9.11E-01	1.24E-02
21.00	5.32E+00	3.03E+00	1.02E+00	8.02E-01	1.80E-02
22.00	5.18E+00	2.97E+00	9.93E-01	7.14E-01	2.55E-02
23.00	5.06E+00	2.93E+00	9.72E-01	6.43E-01	3.22E-02
24.00	4.95E+00	2.89E+00	9.57E-01	5.85E-01	3.33E-02
25.00	4.86E+00	2.86E+00	9.46E-01	5.35E-01	2.82E-02
26.00	4.78E+00	2.83E+00	9.39E-01	4.92E-01	2.11E-02
27.00	4.70E+00	2.81E+00	9.37E-01	4.53E-01	1.53E-02
28.00	4.63E+00	2.78E+00	9.40E-01	4.18E-01	1.11E-02
29.00	4.56E+00	2.76E+00	9.48E-01	3.86E-01	8.32E-03
30.00	4.49E+00	2.73E+00	9.61E-01	3.57E-01	6.26E-03
31.00	4.43E+00	2.69E+00	9.80E-01	3.29E-01	4.94E-03
32.00	4.37E+00	2.66E+00	1.01E+00	3.03E-01	3.98E-03
33.00	4.31E+00	2.62E+00	1.04E+00	2.77E-01	3.28E-03
34.00	4.24E+00	2.58E+00	1.09E+00	2.53E-01	2.74E-03
35.00	4.17E+00	2.53E+00	1.15E+00	2.30E-01	2.33E-03
36.00	4.10E+00	2.48E+00	1.23E+00	2.09E-01	2.01E-03
37.00	4.02E+00	2.43E+00	1.33E+00	1.90E-01	1.75E-03
38.00	3.93E+00	2.37E+00	1.48E+00	1.73E-01	1.54E-03
39.00	3.84E+00	2.32E+00	1.60E+00	1.56E-01	1.37E-03
40.00	3.75E+00	2.27E+00	1.47E+00	1.41E-01	1.23E-03
41.00	3.67E+00	2.24E+00	1.45E+00	1.28E-01	1.11E-03
42.00	3.61E+00	2.24E+00	1.58E+00	1.16E-01	1.01E-03
43.00	3.58E+00	2.28E+00	1.65E+00	1.06E-01	9.23E-04
44.00	3.59E+00	2.43E+00	1.44E+00	9.79E-02	8.50E-04
45.00	3.68E+00	2.54E+00	3.66E-01	9.13E-02	7.86E-04
46.00	3.77E+00	1.79E+00	2.23E-01	7.59E-02	7.31E-04
47.00	3.52E+00	6.73E-01	3.86E-01	6.23E-02	6.83E-04
48.00	3.52E+00	6.14E-01	6.58E-01	3.53E-02	6.40E-04
49.00	3.76E+00	8.79E-01	1.13E+00	2.61E-02	6.03E-04
50.00	4.94E+00	3.76E-01	1.12E+00	3.40E-02	5.69E-04
51.00	6.75E+00	4.93E-02	1.30E-01	1.96E-02	5.22E-04
52.00	9.24E+00	—	3.51E-03	4.60E-03	4.74E-04

Incident Energy: $E_n = 60.00$MeV: cont.

Energy (MeV)	Lab angle–integrated emission spectra: (mb/MeV)				
	$d\sigma_n/dE$	$d\sigma_p/dE$	$d\sigma_d/dE$	$d\sigma_\alpha/dE$	$d\sigma_\gamma/dE$
53.00	1.13E+01	—	—	4.51E-03	5.24E-04
54.00	3.20E+00	—	—	2.65E-03	4.31E-04
55.00	4.78E-02	—	—	—	5.95E-04
56.00	—	—	—	—	2.67E-04
57.00	—	—	—	—	3.14E-04
58.00	—	—	—	—	5.99E-04
59.00	—	—	—	—	—
60.00	—	—	—	—	5.87E-04
61.00	—	—	—	—	1.64E-04
62.00	—	—	—	—	—
63.00	—	—	—	—	—
64.00	—	—	—	—	—
65.00	—	—	—	—	—
σ_{prod} (b)	4.07E-01	2.23E-01	6.64E-02	2.49E-01	2.31E-01
E_{av} (MeV)	1.97E+01	1.58E+01	2.22E+01	5.98E+00	4.66E+00
K (fGy· m^2)	—	2.12E+00	8.87E-01	8.97E-01	—
$\Sigma_{A<4}K_A$					3.90E+00
K_{recoil} non-elastic ($A > 4$)					3.00E-01
K_{recoil} elastic					1.48E-01
K_{total}					4.35E+00

Incident Energy: $E_n = 70.00$MeV

Energy (MeV)	Lab angle–integrated emission spectra: (mb/MeV)				
	$d\sigma_n/dE$	$d\sigma_p/dE$	$d\sigma_d/dE$	$d\sigma_\alpha/dE$	$d\sigma_\gamma/dE$
1.00	2.17E+01	1.00E+01	1.75E+00	3.22E+01	1.82E+01
2.00	2.29E+01	1.28E+01	2.27E+00	3.04E+01	2.91E+01
3.00	2.28E+01	1.43E+01	2.59E+00	2.90E+01	1.29E+01
4.00	2.17E+01	1.41E+01	2.69E+00	2.51E+01	3.03E+01
5.00	1.94E+01	1.31E+01	2.61E+00	2.03E+01	4.80E+01
6.00	1.70E+01	1.18E+01	2.40E+00	1.63E+01	3.83E+01
7.00	1.48E+01	1.03E+01	2.15E+00	1.35E+01	1.91E+01
8.00	1.27E+01	8.96E+00	1.94E+00	1.11E+01	2.70E+00
9.00	1.09E+01	7.77E+00	1.76E+00	8.88E+00	4.73E+00
10.00	9.58E+00	6.70E+00	1.59E+00	6.96E+00	3.52E+00
11.00	8.51E+00	5.78E+00	1.45E+00	5.44E+00	2.00E-01
12.00	7.66E+00	5.04E+00	1.33E+00	4.28E+00	9.80E-04
13.00	6.98E+00	4.47E+00	1.23E+00	3.38E+00	1.41E-03
14.00	6.43E+00	4.03E+00	1.15E+00	2.67E+00	2.10E-03
15.00	5.97E+00	3.68E+00	1.08E+00	2.14E+00	2.96E-03
16.00	5.59E+00	3.40E+00	1.03E+00	1.73E+00	3.91E-03
17.00	5.28E+00	3.17E+00	9.81E-01	1.43E+00	4.76E-03
18.00	5.01E+00	2.97E+00	9.43E-01	1.20E+00	6.01E-03
19.00	4.79E+00	2.82E+00	9.11E-01	1.02E+00	8.15E-03
20.00	4.61E+00	2.69E+00	8.85E-01	8.78E-01	1.17E-02
21.00	4.46E+00	2.59E+00	8.63E-01	7.68E-01	1.71E-02
22.00	4.33E+00	2.51E+00	8.45E-01	6.81E-01	2.44E-02
23.00	4.21E+00	2.45E+00	8.29E-01	6.13E-01	3.11E-02
24.00	4.11E+00	2.40E+00	8.16E-01	5.58E-01	3.21E-02
25.00	4.02E+00	2.36E+00	8.05E-01	5.14E-01	2.71E-02
26.00	3.94E+00	2.33E+00	7.97E-01	4.77E-01	2.04E-02
27.00	3.87E+00	2.31E+00	7.90E-01	4.46E-01	1.48E-02
28.00	3.81E+00	2.29E+00	7.86E-01	4.19E-01	1.08E-02
29.00	3.75E+00	2.28E+00	7.83E-01	3.96E-01	8.06E-03
30.00	3.69E+00	2.26E+00	7.83E-01	3.75E-01	6.18E-03
31.00	3.64E+00	2.25E+00	7.85E-01	3.56E-01	4.86E-03

Incident Energy: $E_n = 70.00$MeV: cont.

Energy (MeV)	Lab angle–integrated emission spectra: (mb/MeV)				
	$d\sigma_n/dE$	$d\sigma_p/dE$	$d\sigma_d/dE$	$d\sigma_\alpha/dE$	$d\sigma_\gamma/dE$
32.00	3.58E+00	2.24E+00	7.89E-01	3.39E-01	3.91E-03
33.00	3.53E+00	2.23E+00	7.95E-01	3.22E-01	3.20E-03
34.00	3.48E+00	2.21E+00	8.03E-01	3.07E-01	2.66E-03
35.00	3.42E+00	2.20E+00	8.12E-01	2.92E-01	2.25E-03
36.00	3.37E+00	2.18E+00	8.23E-01	2.78E-01	1.93E-03
37.00	3.32E+00	2.17E+00	8.36E-01	2.64E-01	1.67E-03
38.00	3.28E+00	2.15E+00	8.50E-01	2.50E-01	1.46E-03
39.00	3.23E+00	2.13E+00	8.67E-01	2.36E-01	1.27E-03
40.00	3.17E+00	2.11E+00	8.85E-01	2.22E-01	1.14E-03
41.00	3.12E+00	2.09E+00	9.06E-01	2.08E-01	1.02E-03
42.00	3.07E+00	2.07E+00	9.30E-01	1.94E-01	9.22E-04
43.00	3.02E+00	2.05E+00	9.56E-01	1.80E-01	8.39E-04
44.00	2.97E+00	2.03E+00	9.86E-01	1.66E-01	7.68E-04
45.00	2.93E+00	2.00E+00	1.02E+00	1.53E-01	7.07E-04
46.00	2.88E+00	1.98E+00	1.06E+00	1.39E-01	6.54E-04
47.00	2.84E+00	1.95E+00	1.11E+00	1.26E-01	6.07E-04
48.00	2.80E+00	1.92E+00	1.18E+00	1.14E-01	5.66E-04
49.00	2.77E+00	1.89E+00	1.12E+00	1.02E-01	5.29E-04
50.00	2.76E+00	1.86E+00	1.06E+00	9.07E-02	4.97E-04
51.00	2.75E+00	1.83E+00	1.10E+00	8.09E-02	4.69E-04
52.00	2.77E+00	1.81E+00	1.11E+00	7.26E-02	4.43E-04
53.00	2.84E+00	1.82E+00	1.21E+00	6.56E-02	4.20E-04
54.00	2.95E+00	1.86E+00	1.33E+00	6.07E-02	3.99E-04
55.00	3.16E+00	1.69E+00	7.23E-01	5.71E-02	3.80E-04
56.00	3.52E+00	1.35E+00	2.47E-01	4.16E-02	3.63E-04
57.00	3.45E+00	9.64E-01	3.68E-01	2.81E-02	3.48E-04
58.00	3.09E+00	4.72E-01	6.25E-01	1.61E-02	3.34E-04
59.00	3.34E+00	7.34E-01	9.37E-01	1.71E-02	3.21E-04
60.00	3.70E+00	6.58E-01	3.96E-01	2.00E-02	1.74E-04
61.00	4.53E+00	6.37E-02	1.01E-02	9.33E-03	2.90E-04
62.00	6.32E+00	1.54E-03	—	3.30E-03	2.92E-04
63.00	8.89E+00	—	—	4.28E-03	2.41E-04
64.00	6.39E+00	—	—	1.85E-03	2.90E-04
65.00	6.21E-01	—	—	—	3.51E-04
66.00	1.49E-02	—	—	—	1.90E-04
67.00	—	—	—	—	3.67E-04
68.00	—	—	—	—	—
69.00	—	—	—	—	3.64E-04
70.00	—	—	—	—	1.02E-04
71.00	—	—	—	—	—
72.00	—	—	—	—	—
73.00	—	—	—	—	—
74.00	—	—	—	—	—
75.00	—	—	—	—	—
σ_{prod} (b)	3.96E-01	2.27E-01	6.75E-02	2.28E-01	2.07E-01
E_{av} (MeV)	2.23E+01	1.84E+01	2.54E+01	6.51E+00	4.57E+00
K (fGy· m^2)	—	2.52E+00	1.03E+00	8.94E-01	—
$\Sigma_{A<4}K_A$					4.45E+00
K_{recoil} non-elastic ($A > 4$)					2.90E-01
K_{recoil} elastic					1.20E-01
K_{total}					4.86E+00

Incident Energy: $E_n = 80.00$MeV

Energy (MeV)	Lab angle–integrated emission spectra: (mb/MeV)				
	$d\sigma_n/dE$	$d\sigma_p/dE$	$d\sigma_d/dE$	$d\sigma_\alpha/dE$	$d\sigma_\gamma/dE$
1.00	2.03E+01	1.01E+01	2.16E+00	2.88E+01	1.81E+01
2.00	2.16E+01	1.27E+01	2.62E+00	2.76E+01	2.61E+01
3.00	2.18E+01	1.42E+01	2.86E+00	2.67E+01	1.26E+01
4.00	2.09E+01	1.39E+01	2.88E+00	2.34E+01	2.80E+01
5.00	1.90E+01	1.30E+01	2.78E+00	1.95E+01	4.10E+01
6.00	1.68E+01	1.18E+01	2.53E+00	1.60E+01	3.38E+01
7.00	1.48E+01	1.04E+01	2.22E+00	1.34E+01	1.54E+01
8.00	1.28E+01	9.12E+00	1.94E+00	1.11E+01	4.04E+00
9.00	1.11E+01	7.98E+00	1.70E+00	9.05E+00	4.20E+00
10.00	9.67E+00	6.94E+00	1.50E+00	7.26E+00	3.01E+00
11.00	8.56E+00	6.03E+00	1.34E+00	5.74E+00	1.70E-01
12.00	7.66E+00	5.27E+00	1.20E+00	4.57E+00	9.05E-04
13.00	6.93E+00	4.68E+00	1.09E+00	3.63E+00	1.30E-03
14.00	6.33E+00	4.23E+00	1.00E+00	2.89E+00	1.95E-03
15.00	5.83E+00	3.86E+00	9.34E-01	2.30E+00	2.79E-03
16.00	5.41E+00	3.55E+00	8.78E-01	1.86E+00	3.73E-03
17.00	5.04E+00	3.30E+00	8.34E-01	1.52E+00	4.56E-03
18.00	4.74E+00	3.08E+00	7.99E-01	1.26E+00	5.77E-03
19.00	4.49E+00	2.90E+00	7.71E-01	1.06E+00	7.85E-03
20.00	4.28E+00	2.75E+00	7.49E-01	9.04E-01	1.13E-02
21.00	4.10E+00	2.62E+00	7.32E-01	7.78E-01	1.67E-02
22.00	3.95E+00	2.51E+00	7.18E-01	6.78E-01	2.39E-02
23.00	3.82E+00	2.42E+00	7.06E-01	5.99E-01	3.04E-02
24.00	3.70E+00	2.34E+00	6.97E-01	5.35E-01	3.14E-02
25.00	3.60E+00	2.27E+00	6.90E-01	4.85E-01	2.64E-02
26.00	3.51E+00	2.21E+00	6.84E-01	4.44E-01	1.99E-02
27.00	3.44E+00	2.16E+00	6.79E-01	4.11E-01	1.44E-02
28.00	3.37E+00	2.12E+00	6.76E-01	3.83E-01	1.06E-02
29.00	3.31E+00	2.08E+00	6.73E-01	3.60E-01	7.91E-03
30.00	3.25E+00	2.04E+00	6.71E-01	3.39E-01	6.08E-03
31.00	3.20E+00	2.01E+00	6.71E-01	3.22E-01	4.79E-03
32.00	3.16E+00	1.98E+00	6.71E-01	3.07E-01	3.85E-03
33.00	3.11E+00	1.95E+00	6.72E-01	2.93E-01	3.16E-03
34.00	3.07E+00	1.92E+00	6.74E-01	2.80E-01	2.63E-03
35.00	3.03E+00	1.89E+00	6.76E-01	2.68E-01	2.22E-03
36.00	2.99E+00	1.87E+00	6.79E-01	2.57E-01	1.90E-03
37.00	2.95E+00	1.84E+00	6.83E-01	2.46E-01	1.64E-03
38.00	2.91E+00	1.81E+00	6.87E-01	2.35E-01	1.43E-03
39.00	2.88E+00	1.78E+00	6.92E-01	2.25E-01	1.26E-03
40.00	2.84E+00	1.76E+00	6.97E-01	2.16E-01	1.11E-03
41.00	2.81E+00	1.73E+00	7.02E-01	2.06E-01	9.95E-04
42.00	2.78E+00	1.70E+00	7.08E-01	1.97E-01	8.94E-04
43.00	2.75E+00	1.68E+00	7.14E-01	1.88E-01	8.09E-04
44.00	2.72E+00	1.65E+00	7.21E-01	1.79E-01	7.36E-04
45.00	2.68E+00	1.63E+00	7.27E-01	1.71E-01	6.73E-04
46.00	2.66E+00	1.60E+00	7.34E-01	1.62E-01	6.19E-04
47.00	2.63E+00	1.57E+00	7.41E-01	1.54E-01	5.71E-04
48.00	2.60E+00	1.55E+00	7.48E-01	1.46E-01	5.30E-04
49.00	2.57E+00	1.52E+00	7.56E-01	1.37E-01	4.91E-04
50.00	2.55E+00	1.50E+00	7.65E-01	1.29E-01	4.59E-04
51.00	2.52E+00	1.47E+00	7.75E-01	1.21E-01	4.31E-04
52.00	2.50E+00	1.45E+00	7.86E-01	1.13E-01	4.05E-04

Incident Energy: $E_n = 80.00$MeV: cont.

Energy (MeV)	Lab angle–integrated emission spectra: (mb/MeV)				
	$d\sigma_n/dE$	$d\sigma_p/dE$	$d\sigma_d/dE$	$d\sigma_\alpha/dE$	$d\sigma_\gamma/dE$
53.00	2.48E+00	1.42E+00	8.00E-01	1.05E-01	3.82E-04
54.00	2.46E+00	1.39E+00	8.18E-01	9.72E-02	3.62E-04
55.00	2.44E+00	1.37E+00	8.42E-01	8.96E-02	3.43E-04
56.00	2.42E+00	1.35E+00	8.77E-01	8.22E-02	3.26E-04
57.00	2.40E+00	1.32E+00	9.28E-01	7.50E-02	3.11E-04
58.00	2.39E+00	1.30E+00	1.00E+00	6.80E-02	2.97E-04
59.00	2.38E+00	1.28E+00	1.06E+00	6.14E-02	2.84E-04
60.00	2.38E+00	1.26E+00	9.08E-01	5.56E-02	2.73E-04
61.00	2.38E+00	1.24E+00	8.82E-01	5.04E-02	2.62E-04
62.00	2.40E+00	1.24E+00	9.30E-01	4.58E-02	2.52E-04
63.00	2.45E+00	1.24E+00	9.60E-01	4.19E-02	2.43E-04
64.00	2.53E+00	1.25E+00	8.40E-01	3.90E-02	2.34E-04
65.00	2.69E+00	1.22E+00	2.60E-01	3.18E-02	2.26E-04
66.00	2.88E+00	1.18E+00	2.16E-01	2.38E-02	2.19E-04
67.00	2.71E+00	6.22E-01	3.61E-01	1.29E-02	2.12E-04
68.00	2.83E+00	4.54E-01	5.90E-01	1.28E-02	2.06E-04
69.00	3.18E+00	7.09E-01	5.80E-01	1.49E-02	1.97E-05
70.00	3.82E+00	3.34E-01	7.06E-02	6.91E-03	1.94E-04
71.00	4.41E+00	1.81E-02	2.41E-03	2.44E-03	2.04E-04
72.00	6.43E+00	—	—	3.02E-03	1.74E-04
73.00	7.53E+00	—	—	1.28E-03	1.83E-04
74.00	2.99E+00	—	—	—	1.91E-04
75.00	7.72E-02	—	—	—	1.08E-04
76.00	1.98E-03	—	—	—	3.75E-04
77.00	—	—	—	—	—
78.00	—	—	—	—	—
79.00	—	—	—	—	3.83E-04
80.00	—	—	—	—	—
81.00	—	—	—	—	—
82.00	—	—	—	—	—
83.00	—	—	—	—	—
84.00	—	—	—	—	—
85.00	—	—	—	—	—
σ_{prod} (b)	3.95E-01	2.31E-01	6.83E-02	2.19E-01	1.87E-01
E_{av} (MeV)	2.48E+01	1.97E+01	2.77E+01	6.92E+00	4.53E+00
K (fGy· m^2)	—	2.74E+00	1.14E+00	9.14E-01	—
$\Sigma_{A<4}K_A$					4.80E+00
K_{recoil} non-elastic ($A > 4$)					2.70E-01
K_{recoil} elastic					1.00E-01
K_{total}					5.17E+00

Incident Energy: $E_n = 90.00$MeV

Energy (MeV)	Lab angle–integrated emission spectra: (mb/MeV)				
	$d\sigma_n/dE$	$d\sigma_p/dE$	$d\sigma_d/dE$	$d\sigma_\alpha/dE$	$d\sigma_\gamma/dE$
1.00	2.03E+01	1.04E+01	2.55E+00	2.67E+01	1.72E+01
2.00	2.18E+01	1.24E+01	3.07E+00	2.60E+01	2.27E+01
3.00	2.20E+01	1.36E+01	3.32E+00	2.56E+01	1.18E+01
4.00	2.13E+01	1.36E+01	3.32E+00	2.28E+01	2.45E+01
5.00	1.95E+01	1.30E+01	3.23E+00	1.93E+01	3.60E+01
6.00	1.73E+01	1.20E+01	2.96E+00	1.61E+01	2.99E+01
7.00	1.53E+01	1.08E+01	2.59E+00	1.36E+01	1.37E+01
8.00	1.34E+01	9.59E+00	2.22E+00	1.15E+01	2.19E+00
9.00	1.16E+01	8.48E+00	1.93E+00	9.56E+00	3.74E+00
10.00	1.01E+01	7.45E+00	1.67E+00	7.81E+00	2.65E+00
11.00	8.88E+00	6.50E+00	1.46E+00	6.26E+00	1.47E-01

Incident Energy: $E_n = 90.00$MeV: cont.

Energy (MeV)	Lab angle-integrated emission spectra: (mb/MeV)				
	$d\sigma_n/dE$	$d\sigma_p/dE$	$d\sigma_d/dE$	$d\sigma_\alpha/dE$	$d\sigma_\gamma/dE$
12.00	7.88E+00	5.69E+00	1.28E+00	5.02E+00	8.50E-04
13.00	7.06E+00	5.05E+00	1.13E+00	4.05E+00	1.22E-03
14.00	6.38E+00	4.54E+00	1.01E+00	3.26E+00	1.80E-03
15.00	5.81E+00	4.12E+00	9.09E-01	2.62E+00	2.65E-03
16.00	5.32E+00	3.78E+00	8.28E-01	2.12E+00	3.58E-03
17.00	4.90E+00	3.49E+00	7.63E-01	1.74E+00	4.43E-03
18.00	4.55E+00	3.25E+00	7.11E-01	1.44E+00	5.63E-03
19.00	4.26E+00	3.03E+00	6.68E-01	1.20E+00	7.67E-03
20.00	4.02E+00	2.85E+00	6.34E-01	1.01E+00	1.11E-02
21.00	3.82E+00	2.70E+00	6.06E-01	8.62E-01	1.65E-02
22.00	3.65E+00	2.56E+00	5.83E-01	7.41E-01	2.38E-02
23.00	3.50E+00	2.45E+00	5.64E-01	6.43E-01	3.03E-02
24.00	3.38E+00	2.35E+00	5.49E-01	5.63E-01	3.13E-02
25.00	3.28E+00	2.26E+00	5.37E-01	4.98E-01	2.63E-02
26.00	3.19E+00	2.19E+00	5.27E-01	4.46E-01	1.97E-02
27.00	3.11E+00	2.12E+00	5.18E-01	4.04E-01	1.43E-02
28.00	3.05E+00	2.07E+00	5.11E-01	3.69E-01	1.05E-02
29.00	2.99E+00	2.02E+00	5.06E-01	3.40E-01	7.90E-03
30.00	2.94E+00	1.97E+00	5.02E-01	3.16E-01	6.09E-03
31.00	2.89E+00	1.93E+00	4.98E-01	2.95E-01	4.80E-03
32.00	2.85E+00	1.89E+00	4.96E-01	2.77E-01	3.86E-03
33.00	2.81E+00	1.85E+00	4.94E-01	2.62E-01	3.16E-03
34.00	2.77E+00	1.82E+00	4.94E-01	2.49E-01	2.63E-03
35.00	2.74E+00	1.78E+00	4.94E-01	2.38E-01	2.22E-03
36.00	2.70E+00	1.75E+00	4.94E-01	2.27E-01	1.90E-03
37.00	2.67E+00	1.72E+00	4.96E-01	2.18E-01	1.64E-03
38.00	2.64E+00	1.69E+00	4.97E-01	2.09E-01	1.43E-03
39.00	2.61E+00	1.66E+00	5.00E-01	2.01E-01	1.25E-03
40.00	2.58E+00	1.64E+00	5.02E-01	1.94E-01	1.11E-03
41.00	2.55E+00	1.61E+00	5.05E-01	1.87E-01	9.87E-04
42.00	2.52E+00	1.58E+00	5.08E-01	1.80E-01	8.86E-04
43.00	2.49E+00	1.56E+00	5.11E-01	1.74E-01	7.99E-04
44.00	2.46E+00	1.53E+00	5.15E-01	1.68E-01	7.25E-04
45.00	2.43E+00	1.51E+00	5.19E-01	1.62E-01	6.61E-04
46.00	2.41E+00	1.49E+00	5.23E-01	1.56E-01	6.05E-04
47.00	2.38E+00	1.47E+00	5.27E-01	1.51E-01	5.57E-04
48.00	2.35E+00	1.45E+00	5.31E-01	1.45E-01	5.14E-04
49.00	2.32E+00	1.43E+00	5.36E-01	1.40E-01	4.77E-04
50.00	2.30E+00	1.41E+00	5.40E-01	1.34E-01	4.44E-04
51.00	2.27E+00	1.39E+00	5.45E-01	1.29E-01	4.14E-04
52.00	2.24E+00	1.37E+00	5.49E-01	1.23E-01	3.88E-04
53.00	2.22E+00	1.35E+00	5.54E-01	1.18E-01	3.65E-04
54.00	2.19E+00	1.33E+00	5.58E-01	1.12E-01	3.44E-04
55.00	2.17E+00	1.32E+00	5.63E-01	1.07E-01	3.25E-04
56.00	2.15E+00	1.30E+00	5.68E-01	1.01E-01	3.07E-04
57.00	2.12E+00	1.28E+00	5.72E-01	9.56E-02	2.92E-04
58.00	2.10E+00	1.27E+00	5.77E-01	9.02E-02	2.77E-04
59.00	2.08E+00	1.25E+00	5.82E-01	8.50E-02	2.64E-04
60.00	2.06E+00	1.23E+00	5.88E-01	7.97E-02	2.52E-04
61.00	2.04E+00	1.22E+00	5.94E-01	7.45E-02	2.42E-04
62.00	2.02E+00	1.20E+00	6.01E-01	6.93E-02	2.32E-04
63.00	2.01E+00	1.18E+00	6.10E-01	6.44E-02	2.22E-04

Incident Energy: $E_n = 90.00$MeV: cont.

Energy (MeV)	Lab angle–integrated emission spectra: (mb/MeV)				
	$d\sigma_n/dE$	$d\sigma_p/dE$	$d\sigma_d/dE$	$d\sigma_\alpha/dE$	$d\sigma_\gamma/dE$
64.00	1.99E+00	1.17E+00	6.21E-01	5.96E-02	2.14E-04
65.00	1.98E+00	1.15E+00	6.36E-01	5.47E-02	2.06E-04
66.00	1.97E+00	1.13E+00	6.60E-01	5.02E-02	1.99E-04
67.00	1.95E+00	1.11E+00	6.89E-01	4.60E-02	1.92E-04
68.00	1.94E+00	1.09E+00	7.37E-01	4.16E-02	1.86E-04
69.00	1.93E+00	1.08E+00	7.22E-01	3.77E-02	1.80E-04
70.00	1.93E+00	1.07E+00	7.20E-01	3.46E-02	1.74E-04
71.00	1.92E+00	1.06E+00	7.23E-01	3.18E-02	1.69E-04
72.00	1.92E+00	1.06E+00	7.42E-01	2.92E-02	1.64E-04
73.00	1.93E+00	1.08E+00	7.58E-01	2.78E-02	1.60E-04
74.00	1.95E+00	1.13E+00	3.77E-01	2.66E-02	1.55E-04
75.00	1.99E+00	1.11E+00	8.99E-02	1.89E-02	1.51E-04
76.00	2.02E+00	9.10E-01	1.27E-01	1.37E-02	1.48E-04
77.00	2.03E+00	7.46E-01	2.09E-01	8.44E-03	1.44E-04
78.00	2.16E+00	3.56E-01	3.54E-01	1.07E-02	1.41E-04
79.00	2.31E+00	4.83E-01	5.18E-01	8.97E-03	9.86E-05
80.00	2.65E+00	5.66E-01	2.08E-01	2.03E-03	1.39E-04
81.00	3.30E+00	9.79E-02	6.33E-03	2.10E-03	1.29E-04
82.00	4.55E+00	2.54E-03	—	—	1.48E-04
83.00	6.82E+00	—	—	—	1.08E-04
84.00	6.12E+00	—	—	—	1.37E-04
85.00	1.02E+00	—	—	—	9.16E-05
86.00	2.62E-02	—	—	—	1.78E-04
87.00	—	—	—	—	—
88.00	—	—	—	—	1.79E-04
89.00	—	—	—	—	5.05E-05
90.00	—	—	—	—	—
91.00	—	—	—	—	—
92.00	—	—	—	—	—
93.00	—	—	—	—	—
94.00	—	—	—	—	—
95.00	—	—	—	—	—
σ_{prod} (b)	4.00E-01	2.42E-01	6.82E-02	2.19E-01	1.65E-01
E_{av} (MeV)	2.66E+01	2.17E+01	2.78E+01	7.31E+00	4.48E+00
K (fGy· m^2)	—	3.17E+00	1.14E+00	9.64E-01	—
$\Sigma_{A<4}K_A$					5.28E+00
K_{recoil} non-elastic ($A > 4$)					2.60E-01
K_{recoil} elastic					8.51E-02
K_{total}					5.63E+00

Incident Energy: $E_n = 100.00$MeV

Energy (MeV)	Lab angle–integrated emission spectra: (mb/MeV)				
	$d\sigma_n/dE$	$d\sigma_p/dE$	$d\sigma_d/dE$	$d\sigma_\alpha/dE$	$d\sigma_\gamma/dE$
1.00	2.03E+01	9.41E+00	2.92E+00	2.53E+01	1.67E+01
2.00	2.18E+01	1.21E+01	3.45E+00	2.51E+01	2.20E+01
3.00	2.23E+01	1.39E+01	3.72E+00	2.52E+01	1.15E+01
4.00	2.16E+01	1.42E+01	3.70E+00	2.28E+01	2.39E+01
5.00	2.00E+01	1.37E+01	3.62E+00	1.95E+01	3.40E+01
6.00	1.79E+01	1.27E+01	3.38E+00	1.65E+01	2.76E+01
7.00	1.60E+01	1.15E+01	3.00E+00	1.40E+01	1.42E+01
8.00	1.41E+01	1.02E+01	2.59E+00	1.20E+01	2.03E+00
9.00	1.23E+01	9.08E+00	2.25E+00	1.01E+01	3.55E+00
10.00	1.07E+01	8.03E+00	1.95E+00	8.34E+00	2.51E+00
11.00	9.41E+00	7.04E+00	1.69E+00	6.79E+00	1.39E-01
12.00	8.34E+00	6.18E+00	1.48E+00	5.48E+00	8.21E-04

Incident Energy: $E_n = 100.00$MeV: cont.

Energy (MeV)	Lab angle-integrated emission spectra: (mb/MeV)				
	$d\sigma_n/dE$	$d\sigma_p/dE$	$d\sigma_d/dE$	$d\sigma_\alpha/dE$	$d\sigma_\gamma/dE$
13.00	7.46E+00	5.47E+00	1.29E+00	4.44E+00	1.20E-03
14.00	6.72E+00	4.90E+00	1.14E+00	3.59E+00	1.81E-03
15.00	6.09E+00	4.44E+00	1.01E+00	2.91E+00	2.64E-03
16.00	5.56E+00	4.05E+00	9.03E-01	2.35E+00	3.60E-03
17.00	5.09E+00	3.72E+00	8.15E-01	1.92E+00	4.46E-03
18.00	4.70E+00	3.44E+00	7.41E-01	1.58E+00	5.66E-03
19.00	4.38E+00	3.19E+00	6.80E-01	1.31E+00	7.79E-03
20.00	4.10E+00	2.98E+00	6.30E-01	1.10E+00	1.13E-02
21.00	3.88E+00	2.79E+00	5.88E-01	9.24E-01	1.68E-02
22.00	3.69E+00	2.64E+00	5.53E-01	7.85E-01	2.44E-02
23.00	3.53E+00	2.50E+00	5.24E-01	6.73E-01	3.12E-02
24.00	3.39E+00	2.38E+00	5.00E-01	5.82E-01	3.21E-02
25.00	3.27E+00	2.28E+00	4.81E-01	5.07E-01	2.69E-02
26.00	3.17E+00	2.20E+00	4.65E-01	4.47E-01	2.02E-02
27.00	3.08E+00	2.13E+00	4.52E-01	3.97E-01	1.47E-02
28.00	3.01E+00	2.07E+00	4.41E-01	3.57E-01	1.08E-02
29.00	2.94E+00	2.02E+00	4.32E-01	3.24E-01	8.15E-03
30.00	2.89E+00	1.98E+00	4.25E-01	2.96E-01	6.29E-03
31.00	2.84E+00	1.94E+00	4.19E-01	2.73E-01	4.97E-03
32.00	2.79E+00	1.90E+00	4.14E-01	2.54E-01	4.01E-03
33.00	2.75E+00	1.86E+00	4.10E-01	2.38E-01	3.29E-03
34.00	2.71E+00	1.83E+00	4.07E-01	2.25E-01	2.74E-03
35.00	2.67E+00	1.80E+00	4.04E-01	2.13E-01	2.31E-03
36.00	2.64E+00	1.76E+00	4.02E-01	2.04E-01	1.97E-03
37.00	2.60E+00	1.73E+00	4.00E-01	1.95E-01	1.70E-03
38.00	2.57E+00	1.70E+00	3.99E-01	1.87E-01	1.48E-03
39.00	2.54E+00	1.67E+00	3.98E-01	1.79E-01	1.30E-03
40.00	2.50E+00	1.65E+00	3.98E-01	1.73E-01	1.15E-03
41.00	2.47E+00	1.62E+00	3.98E-01	1.67E-01	1.02E-03
42.00	2.45E+00	1.60E+00	3.99E-01	1.62E-01	9.12E-04
43.00	2.42E+00	1.57E+00	4.00E-01	1.56E-01	8.21E-04
44.00	2.39E+00	1.55E+00	4.01E-01	1.51E-01	7.43E-04
45.00	2.36E+00	1.53E+00	4.03E-01	1.47E-01	6.76E-04
46.00	2.34E+00	1.51E+00	4.06E-01	1.42E-01	6.18E-04
47.00	2.31E+00	1.48E+00	4.09E-01	1.38E-01	5.67E-04
48.00	2.29E+00	1.46E+00	4.12E-01	1.33E-01	5.22E-04
49.00	2.26E+00	1.44E+00	4.17E-01	1.29E-01	4.83E-04
50.00	2.24E+00	1.42E+00	4.21E-01	1.25E-01	4.48E-04
51.00	2.21E+00	1.40E+00	4.26E-01	1.21E-01	4.17E-04
52.00	2.19E+00	1.38E+00	4.32E-01	1.18E-01	3.90E-04
53.00	2.17E+00	1.36E+00	4.38E-01	1.14E-01	3.65E-04
54.00	2.15E+00	1.34E+00	4.44E-01	1.10E-01	3.43E-04
55.00	2.13E+00	1.31E+00	4.50E-01	1.07E-01	3.23E-04
56.00	2.10E+00	1.29E+00	4.56E-01	1.03E-01	3.05E-04
57.00	2.08E+00	1.27E+00	4.62E-01	9.99E-02	2.89E-04
58.00	2.06E+00	1.25E+00	4.68E-01	9.64E-02	2.74E-04
59.00	2.04E+00	1.23E+00	4.74E-01	9.29E-02	2.60E-04
60.00	2.02E+00	1.21E+00	4.81E-01	8.95E-02	2.48E-04
61.00	2.01E+00	1.19E+00	4.87E-01	8.59E-02	2.36E-04
62.00	1.99E+00	1.16E+00	4.93E-01	8.23E-02	2.26E-04
63.00	1.97E+00	1.14E+00	4.98E-01	7.87E-02	2.16E-04
64.00	1.95E+00	1.12E+00	5.04E-01	7.51E-02	2.07E-04

Incident Energy: $E_n = 100.00$MeV: cont.

	Lab angle–integrated emission spectra: (mb/MeV)				
Energy (MeV)	$d\sigma_n/dE$	$d\sigma_p/dE$	$d\sigma_d/dE$	$d\sigma_\alpha/dE$	$d\sigma_\gamma/dE$
65.00	1.93E+00	1.10E+00	5.09E-01	7.14E-02	1.99E-04
66.00	1.92E+00	1.08E+00	5.14E-01	6.78E-02	1.91E-04
67.00	1.90E+00	1.06E+00	5.18E-01	6.42E-02	1.84E-04
68.00	1.89E+00	1.04E+00	5.21E-01	6.06E-02	1.78E-04
69.00	1.87E+00	1.02E+00	5.24E-01	5.70E-02	1.72E-04
70.00	1.86E+00	1.00E+00	5.27E-01	5.35E-02	1.66E-04
71.00	1.84E+00	9.82E-01	5.29E-01	5.01E-02	1.60E-04
72.00	1.83E+00	9.63E-01	5.30E-01	4.67E-02	1.55E-04
73.00	1.82E+00	9.45E-01	5.32E-01	4.34E-02	1.51E-04
74.00	1.81E+00	9.28E-01	5.33E-01	4.03E-02	1.46E-04
75.00	1.79E+00	9.12E-01	5.36E-01	3.74E-02	1.42E-04
76.00	1.78E+00	8.95E-01	5.40E-01	3.44E-02	1.38E-04
77.00	1.78E+00	8.80E-01	5.46E-01	3.17E-02	1.35E-04
78.00	1.77E+00	8.66E-01	5.48E-01	2.92E-02	1.31E-04
79.00	1.76E+00	8.54E-01	5.12E-01	2.68E-02	1.28E-04
80.00	1.76E+00	8.44E-01	4.85E-01	2.48E-02	1.25E-04
81.00	1.77E+00	8.38E-01	5.32E-01	2.31E-02	1.22E-04
82.00	1.78E+00	8.41E-01	5.71E-01	2.17E-02	1.19E-04
83.00	1.82E+00	8.57E-01	5.86E-01	2.07E-02	1.16E-04
84.00	1.88E+00	8.89E-01	5.03E-01	1.69E-02	1.14E-04
85.00	2.01E+00	8.72E-01	1.50E-01	1.19E-02	1.12E-04
86.00	2.20E+00	7.78E-01	1.26E-01	6.94E-03	1.09E-04
87.00	2.17E+00	4.63E-01	2.06E-01	8.61E-03	1.07E-04
88.00	2.08E+00	2.89E-01	3.44E-01	8.90E-03	4.43E-05
89.00	2.38E+00	4.79E-01	3.29E-01	3.85E-03	8.36E-05
90.00	2.74E+00	3.17E-01	3.77E-02	1.76E-03	1.09E-04
91.00	3.19E+00	1.67E-02	1.61E-03	2.26E-03	1.11E-04
92.00	4.85E+00	—	—	—	8.77E-05
93.00	6.41E+00	—	—	—	8.67E-05
94.00	3.55E+00	—	—	—	1.30E-04
95.00	1.89E-01	—	—	—	1.38E-04
96.00	6.80E-03	—	—	—	—
97.00	—	—	—	—	1.39E-04
98.00	—	—	—	—	5.96E-05
99.00	—	—	—	—	—
100.00	—	—	—	—	—
101.00	—	—	—	—	—
102.00	—	—	—	—	—
103.00	—	—	—	—	—
104.00	—	—	—	—	—
105.00	—	—	—	—	—
σ_{prod} (b)	4.19E-01	2.56E-01	7.23E-02	2.21E-01	1.58E-01
E_{av} (MeV)	2.87E+01	2.32E+01	2.83E+01	7.60E+00	4.47E+00
K (fGy· m^2)	—	3.58E+00	1.23E+00	1.01E+00	—
$\Sigma_{A<4}K_A$					5.82E+00
K_{recoil} non-elastic ($A > 4$)					2.50E-01
K_{recoil} elastic					6.80E-02
K_{total}					6.14E+00

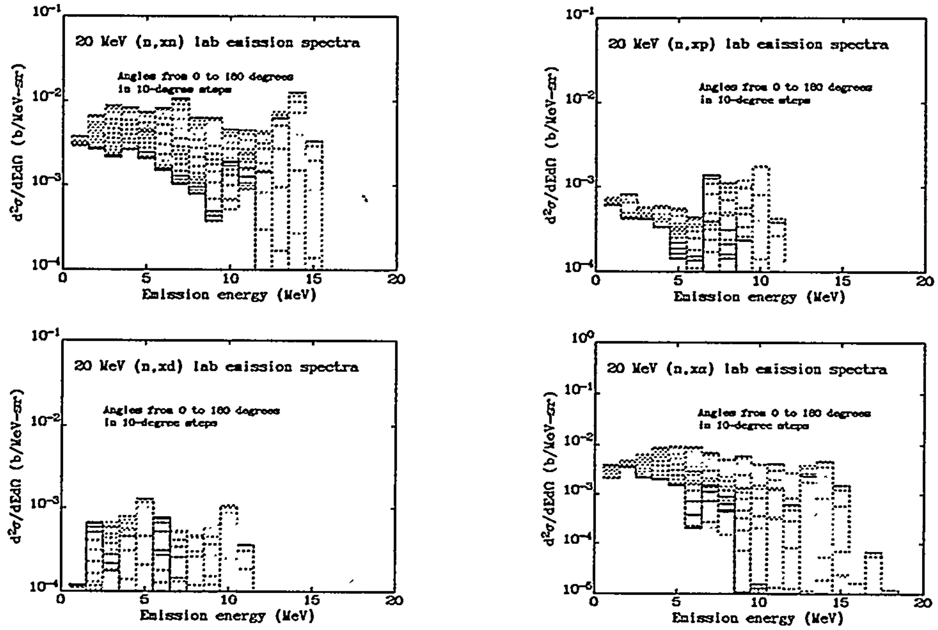

Figure 22: 20 MeV oxygen double-differential evaluated emission spectra. Rainbow colors indicate different angles, red being 0-degrees and purple 180-degrees.

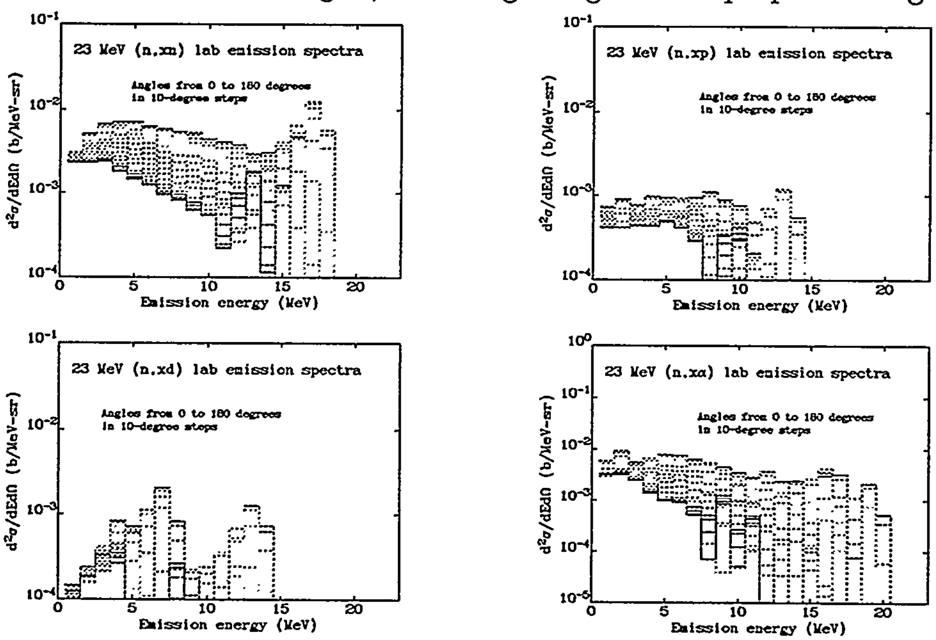

Figure 23: 23 MeV oxygen double-differential evaluated emission spectra. Rainbow colors indicate different angles, red being 0-degrees and purple 180-degrees.

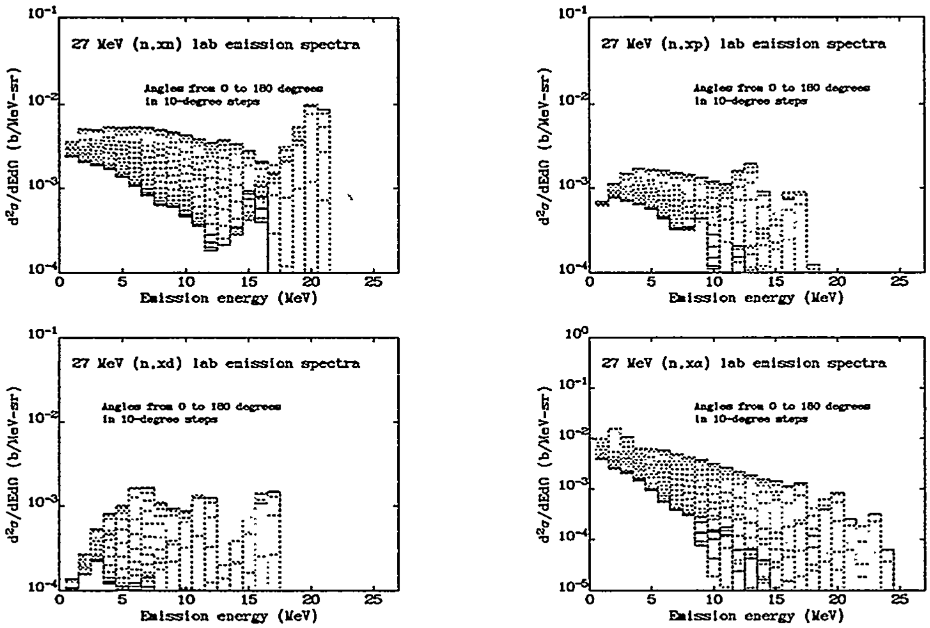

Figure 24: 27 MeV oxygen double-differential evaluated emission spectra. Rainbow colors indicate different angles, red being 0-degrees and purple 180-degrees.

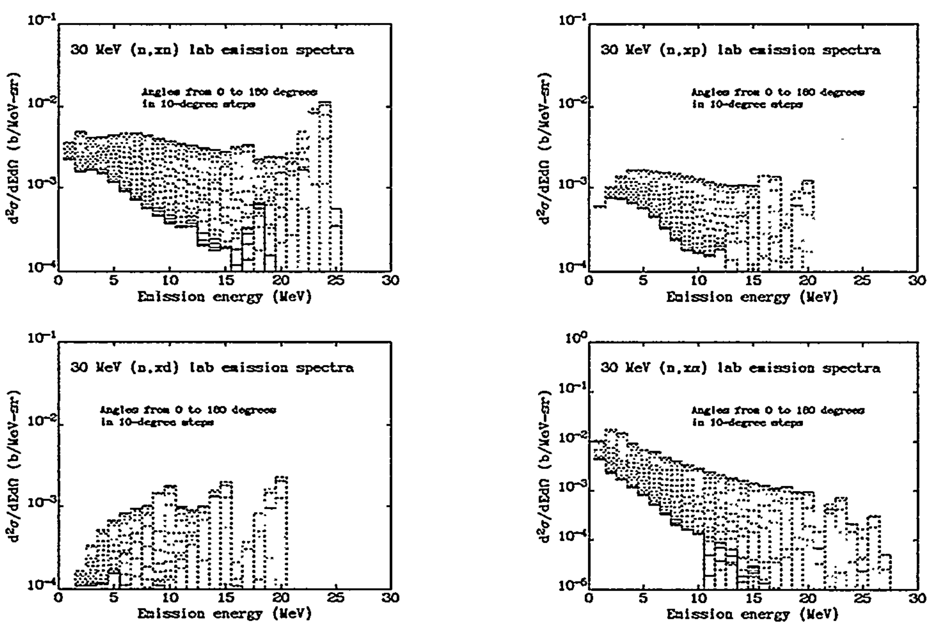

Figure 25: 30 MeV oxygen double-differential evaluated emission spectra. Rainbow colors indicate different angles, red being 0-degrees and purple 180-degrees.

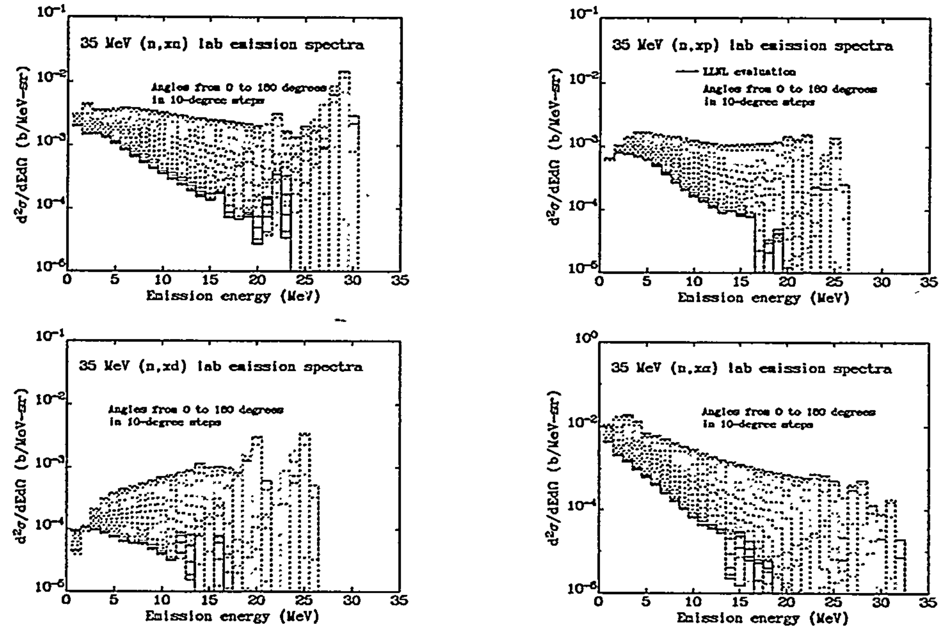

Figure 26: 35 MeV oxygen double-differential evaluated emission spectra. Rainbow colors indicate different angles, red being 0-degrees and purple 180-degrees.

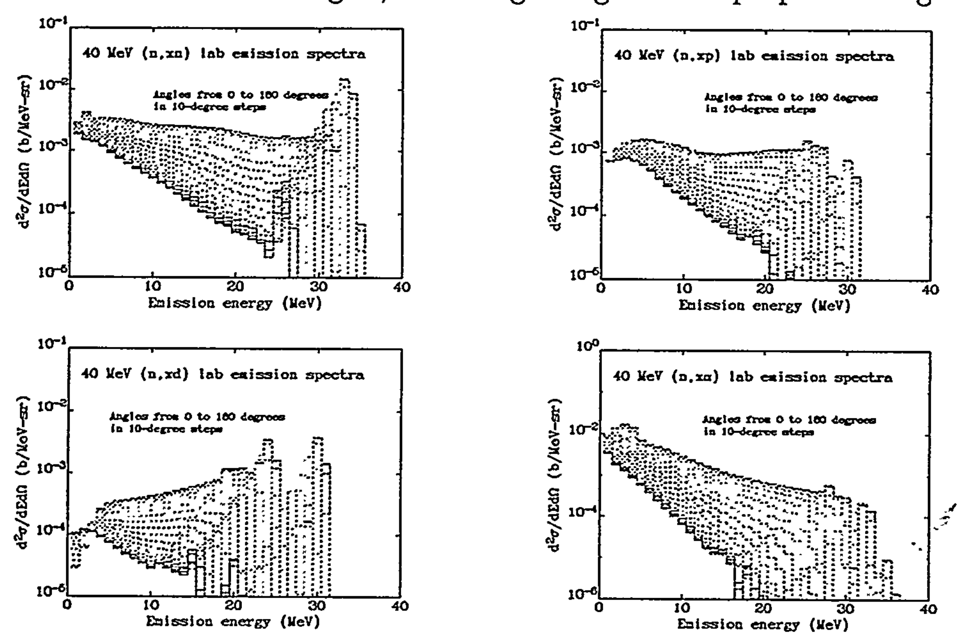

Figure 27: 40 MeV oxygen double-differential evaluated emission spectra. Rainbow colors indicate different angles, red being 0-degrees and purple 180-degrees.

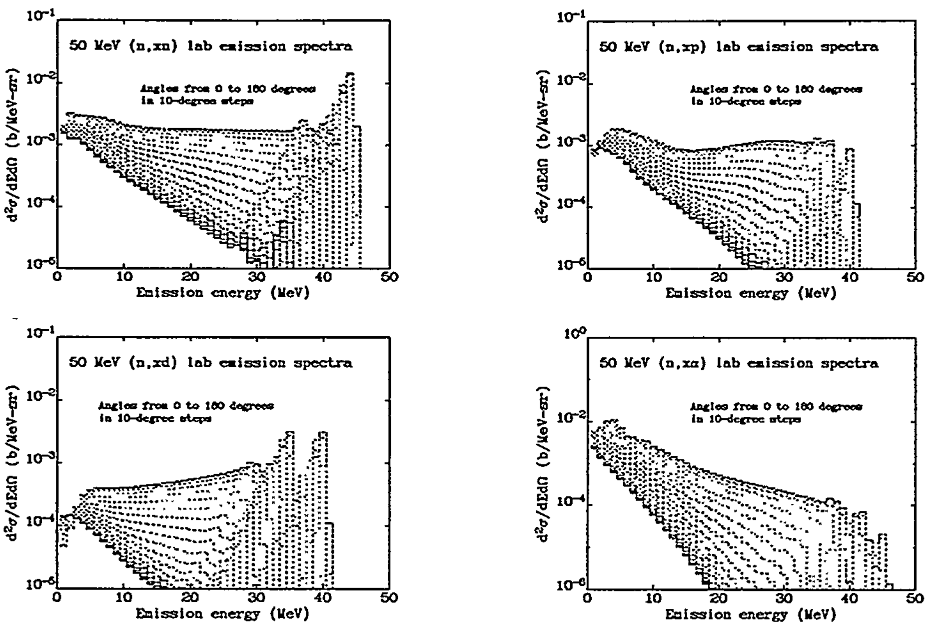

Figure 28: 50 MeV oxygen double-differential evaluated emission spectra. Rainbow colors indicate different angles, red being 0-degrees and purple 180-degrees.

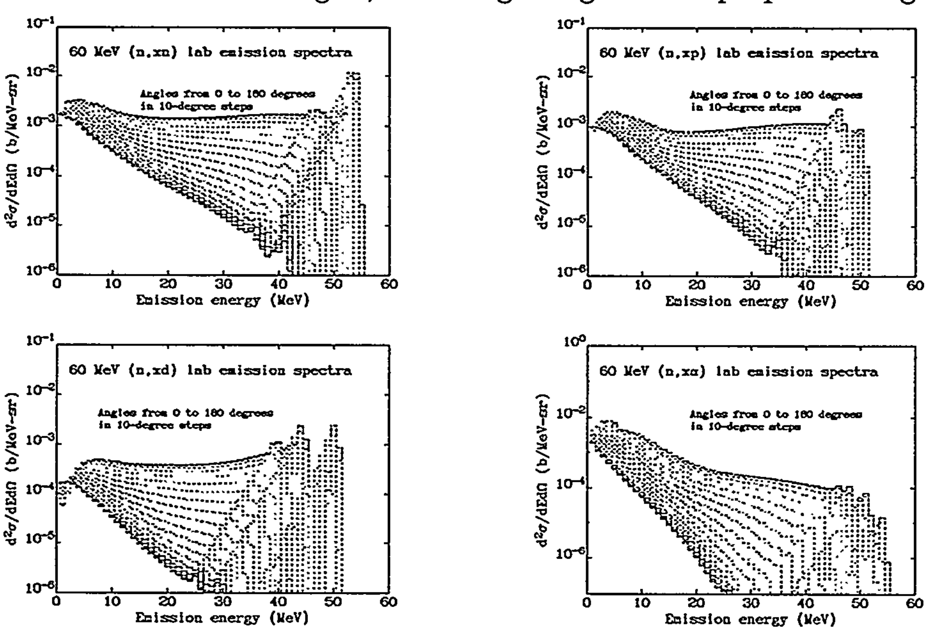

Figure 29: 60 MeV oxygen double-differential evaluated emission spectra. Rainbow colors indicate different angles, red being 0-degrees and purple 180-degrees.

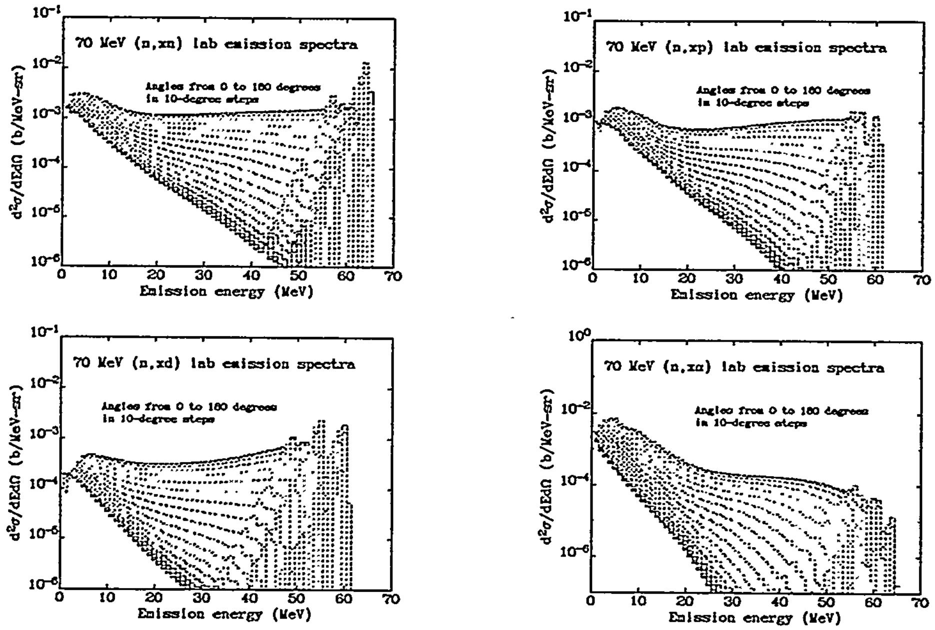

Figure 30: 70 MeV oxygen double-differential evaluated emission spectra. Rainbow colors indicate different angles, red being 0-degrees and purple 180-degrees.

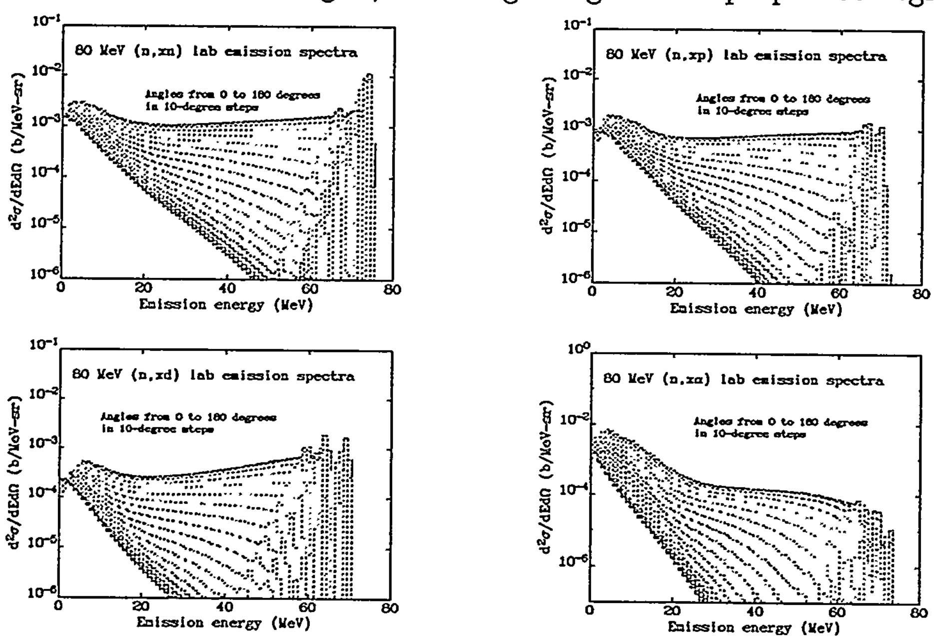

Figure 31: 80 MeV oxygen double-differential evaluated emission spectra. Rainbow colors indicate different angles, red being 0-degrees and purple 180-degrees.

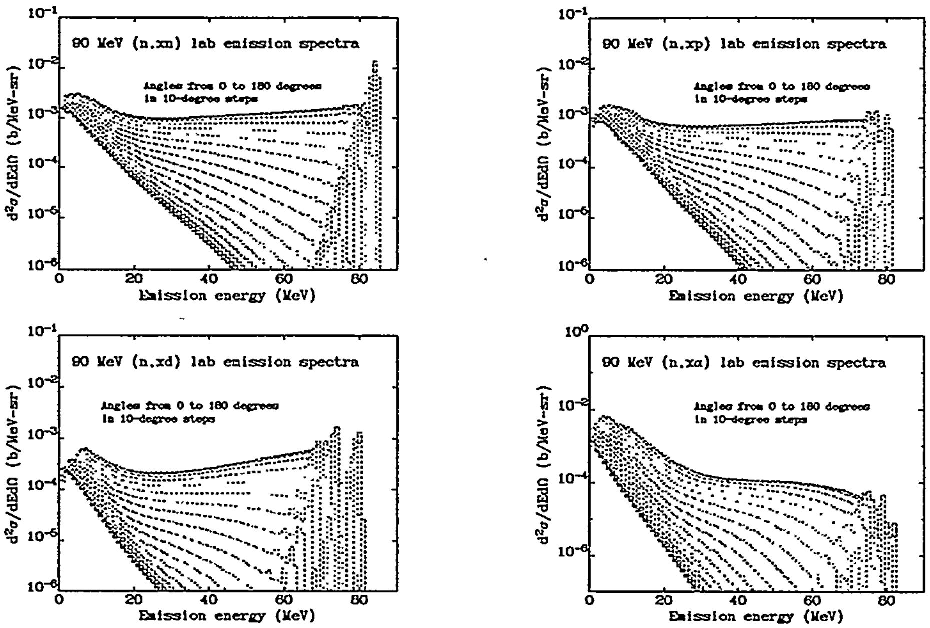

Figure 32: 90 MeV oxygen double-differential evaluated emission spectra. Rainbow colors indicate different angles, red being 0-degrees and purple 180-degrees.

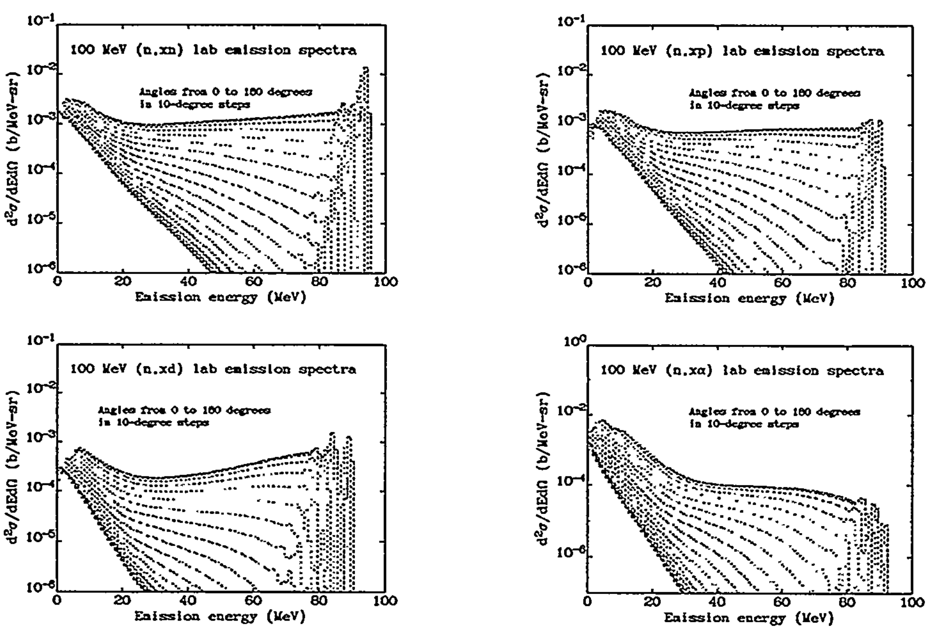

Figure 33: 100 MeV oxygen double-differential evaluated emission spectra. Rainbow colors indicate different angles, red being 0-degrees and purple 180-degrees.

9 Appendix 2 : Tabulations and Figures of Libraries for Nitrogen

In the appendix we show the following figures and tables:

1. A figure (Fig. 34) showing the nitrogen library angle-integrated emission spectra for $A \leq 4$ ejectiles, for incident energies of 20, 23, 27, 30, 35, 40, 50, 60, 70, 80, 90, and 100 MeV.

2. Tables (Table. VIII) giving numerical values for the nitrogen angle-integrated emission spectra for $A \leq 4$ ejectiles, for incident energies of 20, 23, 27, 30, 35, 40, 50, 60, 70, 80, 90, and 100 MeV. For completeness, at the end of each emission spectrum we also indicate the production cross section, the average kinetic energy, and the partial kerma factors. These are then combined with the elastic and recoil nonelastic kerma factors to give the total kerma factor.

3. Figures (Figs. 35-46) showing the nitrogen library double-differential emission spectra for $A \leq 4$ ejectiles, for angles every 10-degrees between 0 and 180 degrees, and for incident energies of 20, 23, 27, 30, 35, 40, 50, 60, 70, 80, 90, and 100 MeV. Generally the higher lines correspond to forward angles and the lower lines to the backward angles.

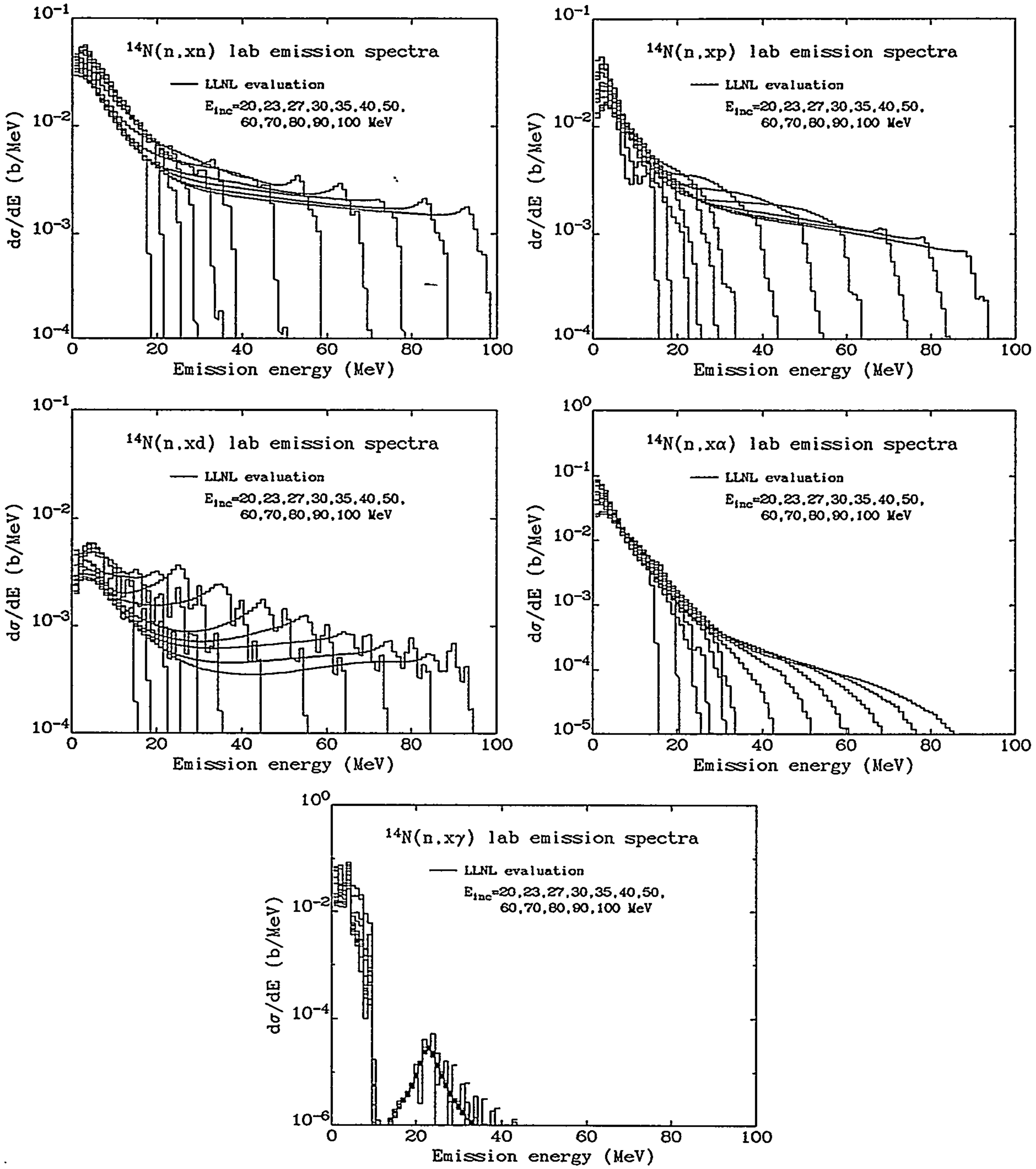

Figure 34: Angle-integrated evaluated emission spectra (lab frame) for incident neutron energies between 20 and 100 MeV on nitrogen

The following pages contain tabulations of the evaluated angle-integrated emission spectra from $^{14}N+n$ reactions. Tabulations of the double-differential spectra can be obtained from the authors. Kerma factors are also shown.

Table VIII: Tabulations of nitrogen angle-integrated emission spectra

Incident Energy: $E_n = 20.00$MeV

Energy (MeV)	Lab angle–integrated emission spectra: (mb/MeV)				
	$d\sigma_n/dE$	$d\sigma_p/dE$	$d\sigma_d/dE$	$d\sigma_\alpha/dE$	$d\sigma_\gamma/dE$
1.00	3.62E+01	4.13E+01	2.08E+00	2.57E+01	5.70E+01
2.00	4.72E+01	4.42E+01	3.69E+00	2.80E+01	7.40E+01
3.00	4.69E+01	3.79E+01	4.90E+00	2.78E+01	3.11E+01
4.00	4.09E+01	2.70E+01	5.71E+00	2.42E+01	6.45E+01
5.00	3.55E+01	1.68E+01	4.86E+00	2.08E+01	3.03E+01
6.00	3.16E+01	9.40E+00	4.45E+00	1.87E+01	2.73E+01
7.00	2.84E+01	5.40E+00	4.32E+00	1.57E+01	2.04E+01
8.00	2.54E+01	3.28E+00	2.16E+00	1.24E+01	9.07E+00
9.00	2.27E+01	2.90E+00	2.76E+00	1.06E+01	5.99E+00
10.00	2.06E+01	4.18E+00	3.46E+00	9.02E+00	5.46E-03
11.00	1.84E+01	4.72E+00	2.84E+00	8.01E+00	7.78E-04
12.00	1.71E+01	4.69E+00	1.15E+00	6.61E+00	7.13E-04
13.00	1.51E+01	4.64E+00	1.37E+00	4.49E+00	9.53E-04
14.00	1.16E+01	2.74E+00	1.47E+00	2.03E+00	1.31E-03
15.00	1.14E+01	3.63E-01	1.96E-01	2.58E-01	1.85E-03
16.00	9.51E+00	2.69E-03	2.08E-03	3.47E-03	2.58E-03
17.00	4.80E+00	—	—	—	3.35E-03
18.00	6.40E-01	—	—	—	4.40E-03
19.00	4.57E-03	—	—	—	6.39E-03
20.00	—	—	—	—	1.38E-02
21.00	—	—	—	—	1.45E-02
22.00	—	—	—	—	4.08E-02
23.00	—	—	—	—	2.69E-02
24.00	—	—	—	—	5.17E-02
25.00	—	—	—	—	—
σ_{prod} (b)	4.24E-01	2.09E-01	4.54E-02	2.14E-01	3.20E-01
E_{av} (MeV)	6.64E+00	4.01E+00	6.46E+00	5.33E+00	3.58E+00
K (fGy$\cdot$ m^2)	—	5.80E-01	2.02E-01	7.87E-01	—
$\Sigma_{A<4}K_A$					1.57E+00
K_{recoil} non-elastic ($A > 4$)					4.40E-01
K_{recoil} elastic					4.13E-01
K_{total}					2.42E+00

Incident Energy: $E_n = 23.00$MeV

Energy (MeV)	Lab angle–integrated emission spectra: (mb/MeV)				
	$d\sigma_n/dE$	$d\sigma_p/dE$	$d\sigma_d/dE$	$d\sigma_\alpha/dE$	$d\sigma_\gamma/dE$
1.00	3.19E+01	3.20E+01	1.99E+00	2.37E+01	6.66E+01
2.00	4.82E+01	3.82E+01	3.55E+00	2.58E+01	6.26E+01
3.00	5.14E+01	3.46E+01	4.68E+00	2.55E+01	3.05E+01
4.00	4.49E+01	2.66E+01	5.16E+00	2.22E+01	7.53E+01
5.00	3.78E+01	1.93E+01	5.23E+00	1.87E+01	1.94E+01
6.00	3.33E+01	1.29E+01	5.09E+00	1.60E+01	1.92E+01
7.00	2.91E+01	8.82E+00	4.62E+00	1.33E+01	1.68E+01
8.00	2.53E+01	6.36E+00	4.34E+00	1.14E+01	1.89E+00
9.00	2.18E+01	4.74E+00	3.59E+00	9.76E+00	3.66E+00
10.00	1.88E+01	3.53E+00	2.92E+00	8.48E+00	1.73E-02
11.00	1.63E+01	2.96E+00	1.75E+00	7.04E+00	1.25E-03
12.00	1.44E+01	3.46E+00	1.86E+00	6.10E+00	6.69E-04
13.00	1.29E+01	3.61E+00	2.67E+00	5.37E+00	9.22E-04
14.00	1.18E+01	3.14E+00	2.32E+00	4.85E+00	1.27E-03
15.00	1.13E+01	3.74E+00	1.03E+00	4.64E+00	1.78E-03
16.00	1.07E+01	3.77E+00	1.09E+00	4.15E+00	2.48E-03
17.00	8.34E+00	1.99E+00	1.44E+00	3.09E+00	3.23E-03
18.00	7.09E+00	3.64E-01	3.11E-01	1.92E+00	4.22E-03
19.00	7.04E+00	2.59E-03	3.20E-03	1.36E+00	6.10E-03

Incident Energy: $E_n = 23.00$MeV: cont.

Energy (MeV)	Lab angle–integrated emission spectra: (mb/MeV)				
	$d\sigma_n/dE$	$d\sigma_p/dE$	$d\sigma_d/dE$	$d\sigma_\alpha/dE$	$d\sigma_\gamma/dE$
20.00	4.60E+00	—	—	8.12E-02	9.70E-03
21.00	9.77E-01	—	—	1.92E-03	2.58E-03
22.00	6.89E-03	—	—	—	2.90E-02
23.00	—	—	—	—	3.10E-02
24.00	—	—	—	—	2.09E-02
25.00	—	—	—	—	2.24E-02
26.00	—	—	—	—	9.03E-03
27.00	—	—	—	—	1.62E-02
28.00	—	—	—	—	—
σ_{prod} (b)	4.48E-01	2.10E-01	5.36E-02	2.13E-01	2.96E-01
E_{av} (MeV)	7.16E+00	4.82E+00	7.54E+00	6.28E+00	3.26E+00
K (fGy· m^2)	—	6.98E-01	2.79E-01	9.24E-01	—
$\Sigma_{A<4}K_A$					1.90E+00
K_{recoil} non-elastic ($A > 4$)					4.70E-01
K_{recoil} elastic					3.67E-01
K_{total}					2.74E+00

Incident Energy: $E_n = 27.00$MeV

Energy (MeV)	Lab angle–integrated emission spectra: (mb/MeV)				
	$d\sigma_n/dE$	$d\sigma_p/dE$	$d\sigma_d/dE$	$d\sigma_\alpha/dE$	$d\sigma_\gamma/dE$
1.00	3.83E+01	2.77E+01	2.92E+00	4.18E+01	6.94E+01
2.00	5.41E+01	3.47E+01	4.38E+00	3.64E+01	3.31E+01
3.00	5.63E+01	3.32E+01	5.48E+00	3.02E+01	3.40E+01
4.00	4.89E+01	2.78E+01	5.93E+00	2.46E+01	8.44E+01
5.00	4.11E+01	2.28E+01	5.81E+00	1.98E+01	9.22E+00
6.00	3.74E+01	1.75E+01	5.33E+00	1.55E+01	9.61E+00
7.00	3.36E+01	1.31E+01	4.75E+00	1.20E+01	7.13E+00
8.00	2.95E+01	1.03E+01	4.20E+00	9.32E+00	6.11E-01
9.00	2.53E+01	8.08E+00	3.60E+00	7.37E+00	1.45E+00
10.00	2.14E+01	6.35E+00	3.10E+00	5.95E+00	5.96E-03
11.00	1.81E+01	5.14E+00	3.10E+00	4.99E+00	9.61E-04
12.00	1.55E+01	4.33E+00	3.19E+00	4.25E+00	6.74E-04
13.00	1.34E+01	3.72E+00	3.01E+00	3.62E+00	9.28E-04
14.00	1.17E+01	3.28E+00	2.63E+00	3.01E+00	1.29E-03
15.00	1.04E+01	2.97E+00	1.64E+00	2.32E+00	1.82E-03
16.00	9.34E+00	2.74E+00	1.51E+00	1.88E+00	2.52E-03
17.00	8.43E+00	2.22E+00	2.41E+00	1.45E+00	3.23E-03
18.00	7.68E+00	1.81E+00	2.12E+00	1.12E+00	4.15E-03
19.00	7.33E+00	1.44E+00	9.09E-01	7.27E-01	5.93E-03
20.00	7.14E+00	1.27E+00	6.78E-01	6.49E-01	9.41E-03
21.00	5.47E+00	1.04E+00	1.09E+00	4.93E-01	1.60E-02
22.00	3.98E+00	3.82E-01	4.18E-01	2.90E-01	2.60E-02
23.00	2.69E+00	1.01E-02	5.14E-03	2.10E-01	3.14E-02
24.00	2.52E+00	1.77E-03	—	5.55E-02	2.44E-02
25.00	1.27E+00	2.59E-03	—	2.13E-02	5.92E-03
26.00	6.41E-02	5.43E-03	—	—	1.03E-02
27.00	1.88E-02	1.08E-02	—	—	7.02E-03
28.00	—	6.18E-03	—	—	4.55E-03
29.00	—	—	—	—	2.76E-03
30.00	—	—	—	—	2.57E-03
31.00	—	—	—	—	5.96E-03
32.00	—	—	—	—	—
σ_{prod} (b)	5.11E-01	2.32E-01	6.82E-02	2.28E-01	2.49E-01
E_{av} (MeV)	7.51E+00	5.58E+00	8.62E+00	5.03E+00	3.01E+00
K (fGy· m^2)	—	8.91E-01	4.05E-01	7.90E-01	—
$\Sigma_{A<4}K_A$					2.09E+00
K_{recoil} non-elastic ($A > 4$)					4.70E-01
K_{recoil} elastic					3.48E-01
K_{total}					2.90E+00

Incident Energy: $E_n = 30.00$MeV

Energy (MeV)	Lab angle–integrated emission spectra: (mb/MeV)				
	$d\sigma_n/dE$	$d\sigma_p/dE$	$d\sigma_d/dE$	$d\sigma_\alpha/dE$	$d\sigma_\gamma/dE$
1.00	4.08E+01	2.97E+01	2.87E+00	5.73E+01	6.02E+01
2.00	5.32E+01	3.19E+01	3.75E+00	4.53E+01	3.09E+01
3.00	5.37E+01	2.90E+01	4.41E+00	3.43E+01	3.46E+01
4.00	4.64E+01	2.40E+01	4.78E+00	2.57E+01	8.26E+01
5.00	3.87E+01	2.02E+01	4.83E+00	2.02E+01	8.08E+00
6.00	3.48E+01	1.65E+01	4.76E+00	1.57E+01	6.44E+00
7.00	3.11E+01	1.30E+01	4.59E+00	1.21E+01	5.35E+00
8.00	2.73E+01	1.07E+01	4.32E+00	9.41E+00	4.20E-01
9.00	2.35E+01	8.90E+00	4.07E+00	7.37E+00	8.66E-01
10.00	2.04E+01	7.33E+00	3.75E+00	5.89E+00	2.44E-03
11.00	1.78E+01	6.10E+00	3.43E+00	4.85E+00	6.25E-04
12.00	1.57E+01	5.17E+00	3.12E+00	4.11E+00	6.52E-04
13.00	1.40E+01	4.49E+00	3.07E+00	3.53E+00	9.04E-04
14.00	1.25E+01	4.02E+00	3.14E+00	3.08E+00	1.26E-03
15.00	1.12E+01	3.67E+00	3.34E+00	2.70E+00	1.81E-03
16.00	1.00E+01	3.44E+00	3.01E+00	2.39E+00	2.53E-03
17.00	9.07E+00	3.31E+00	2.37E+00	2.03E+00	3.26E-03
18.00	8.30E+00	3.26E+00	1.64E+00	1.47E+00	4.17E-03
19.00	7.59E+00	2.74E+00	1.09E+00	1.20E+00	5.91E-03
20.00	6.99E+00	2.10E+00	1.82E+00	9.81E-01	9.31E-03
21.00	6.58E+00	1.67E+00	1.96E+00	7.94E-01	1.57E-02
22.00	6.40E+00	1.17E+00	9.66E-01	5.55E-01	2.54E-02
23.00	6.51E+00	8.41E-01	4.96E-01	5.00E-01	3.06E-02
24.00	5.49E+00	5.19E-01	8.70E-01	2.04E-01	2.37E-02
25.00	3.96E+00	1.38E-01	4.86E-01	2.23E-01	1.51E-02
26.00	2.93E+00	7.34E-03	1.21E-02	1.70E-01	9.57E-03
27.00	2.61E+00	—	—	3.12E-02	6.43E-03
28.00	1.85E+00	—	—	1.04E-02	2.83E-03
29.00	1.44E-01	2.02E-03	—	—	2.78E-03
30.00	2.94E-02	4.72E-03	—	—	2.90E-03
31.00	1.64E-03	4.12E-03	—	—	2.12E-03
32.00	—	—	—	—	2.74E-03
33.00	—	—	—	—	—
34.00	—	—	—	—	3.56E-03
35.00	—	—	—	—	—
σ_{prod} (b)	5.20E-01	2.34E-01	7.30E-02	2.62E-01	2.30E-01
E_{av} (MeV)	8.29E+00	6.33E+00	1.01E+01	4.87E+00	3.00E+00
K (fGy$\cdot$ m^2)	—	1.02E+00	5.06E-01	8.80E-01	—
$\Sigma_{A<4}K_A$					2.41E+00
K_{recoil} non-elastic ($A > 4$)					4.70E-01
K_{recoil} elastic					3.30E-01
K_{total}					3.21E+00

Incident Energy: $E_n = 35.00$MeV

Energy (MeV)	Lab angle–integrated emission spectra: (mb/MeV)				
	$d\sigma_n/dE$	$d\sigma_p/dE$	$d\sigma_d/dE$	$d\sigma_\alpha/dE$	$d\sigma_\gamma/dE$
1.00	4.29E+01	2.20E+01	4.53E+00	7.96E+01	4.40E+01
2.00	5.02E+01	2.56E+01	4.35E+00	6.16E+01	2.53E+01
3.00	4.96E+01	2.50E+01	4.03E+00	4.46E+01	3.41E+01
4.00	4.32E+01	2.14E+01	3.97E+00	3.04E+01	7.61E+01
5.00	3.49E+01	1.84E+01	3.71E+00	2.31E+01	6.00E+00
6.00	3.05E+01	1.55E+01	3.38E+00	1.80E+01	4.21E+00
7.00	2.74E+01	1.27E+01	3.17E+00	1.39E+01	1.37E+00
8.00	2.46E+01	1.09E+01	3.08E+00	1.09E+01	2.01E+00
9.00	2.17E+01	9.49E+00	3.01E+00	8.54E+00	4.13E-01

Incident Energy: $E_n = 35.00$MeV: cont.

Energy (MeV)	Lab angle–integrated emission spectra: (mb/MeV)				
	$d\sigma_n/dE$	$d\sigma_p/dE$	$d\sigma_d/dE$	$d\sigma_\alpha/dE$	$d\sigma_\gamma/dE$
10.00	1.91E+01	8.25E+00	2.96E+00	6.71E+00	1.14E-03
11.00	1.69E+01	7.24E+00	2.92E+00	5.39E+00	5.51E-04
12.00	1.50E+01	6.44E+00	2.88E+00	4.42E+00	6.34E-04
13.00	1.35E+01	5.74E+00	2.86E+00	3.68E+00	8.69E-04
14.00	1.22E+01	5.13E+00	2.82E+00	3.08E+00	1.23E-03
15.00	1.10E+01	4.62E+00	2.78E+00	2.57E+00	1.78E-03
16.00	9.95E+00	4.18E+00	2.81E+00	2.15E+00	2.51E-03
17.00	8.99E+00	3.84E+00	2.84E+00	1.81E+00	3.24E-03
18.00	8.11E+00	3.55E+00	2.94E+00	1.53E+00	4.13E-03
19.00	7.30E+00	3.29E+00	3.14E+00	1.30E+00	5.85E-03
20.00	6.59E+00	3.09E+00	3.20E+00	1.11E+00	9.21E-03
21.00	5.98E+00	2.96E+00	2.99E+00	9.31E-01	1.55E-02
22.00	5.45E+00	2.89E+00	2.78E+00	7.92E-01	2.50E-02
23.00	5.02E+00	2.90E+00	1.20E+00	6.93E-01	2.98E-02
24.00	4.72E+00	2.66E+00	1.63E+00	5.73E-01	2.29E-02
25.00	4.51E+00	1.69E+00	2.25E+00	5.03E-01	1.44E-02
26.00	4.39E+00	1.01E+00	1.49E+00	4.14E-01	9.13E-03
27.00	4.39E+00	8.32E-01	5.48E-01	2.99E-01	6.11E-03
28.00	4.19E+00	4.97E-01	8.44E-01	1.92E-01	4.32E-03
29.00	3.58E+00	1.35E-01	8.14E-01	1.07E-01	3.21E-03
30.00	3.90E+00	1.35E-02	7.03E-02	7.86E-02	2.48E-03
31.00	3.89E+00	—	1.50E-03	1.67E-02	1.97E-03
32.00	2.69E+00	—	—	6.32E-03	1.61E-03
33.00	4.88E-01	—	—	—	1.21E-03
34.00	1.55E-01	1.47E-03	—	—	1.39E-03
35.00	1.82E-01	2.20E-03	—	—	8.08E-04
36.00	3.21E-02	—	—	—	1.05E-03
37.00	—	—	—	—	6.67E-04
38.00	—	—	—	—	1.88E-03
39.00	—	—	—	—	—
40.00	—	—	—	—	—
σ_{prod} (b)	5.07E-01	2.32E-01	8.00E-02	3.29E-01	1.94E-01
E_{av} (MeV)	9.16E+00	7.94E+00	1.25E+01	4.60E+00	3.05E+00
K (fGy· m^2)	—	1.27E+00	6.88E-01	1.04E+00	—
$\Sigma_{A<4} K_A$					3.00E+00
K_{recoil} non-elastic ($A > 4$)					4.20E-01
K_{recoil} elastic					3.02E-01
K_{total}					3.72E+00

Incident Energy: $E_n = 40.00$MeV

Energy (MeV)	Lab angle–integrated emission spectra: (mb/MeV)				
	$d\sigma_n/dE$	$d\sigma_p/dE$	$d\sigma_d/dE$	$d\sigma_\alpha/dE$	$d\sigma_\gamma/dE$
1.00	4.60E+01	2.02E+01	5.02E+00	8.73E+01	3.39E+01
2.00	4.83E+01	2.38E+01	4.65E+00	7.05E+01	2.25E+01
3.00	4.48E+01	2.37E+01	4.06E+00	5.21E+01	2.97E+01
4.00	3.87E+01	2.00E+01	3.87E+00	3.39E+01	7.03E+01
5.00	3.11E+01	1.69E+01	3.58E+00	2.49E+01	5.63E+00
6.00	2.66E+01	1.41E+01	3.05E+00	1.96E+01	3.67E+00
7.00	2.36E+01	1.16E+01	2.62E+00	1.54E+01	2.44E+00
8.00	2.11E+01	9.88E+00	2.37E+00	1.21E+01	1.00E-01
9.00	1.89E+01	8.67E+00	2.20E+00	9.52E+00	2.28E-01
10.00	1.69E+01	7.64E+00	2.10E+00	7.49E+00	7.24E-04
11.00	1.54E+01	6.80E+00	2.04E+00	5.95E+00	4.94E-04
12.00	1.41E+01	6.18E+00	2.02E+00	4.80E+00	6.70E-04
13.00	1.30E+01	5.70E+00	2.02E+00	3.94E+00	9.60E-04

Incident Energy: $E_n = 40.00$MeV: cont.

Energy (MeV)	Lab angle–integrated emission spectra: (mb/MeV)				
	$d\sigma_n/dE$	$d\sigma_p/dE$	$d\sigma_d/dE$	$d\sigma_\alpha/dE$	$d\sigma_\gamma/dE$
14.00	1.20E+01	5.30E+00	2.03E+00	3.27E+00	1.38E-03
15.00	1.10E+01	4.96E+00	2.08E+00	2.75E+00	2.02E-03
16.00	1.01E+01	4.70E+00	2.14E+00	2.34E+00	2.86E-03
17.00	9.23E+00	4.47E+00	2.21E+00	2.00E+00	3.12E-03
18.00	8.37E+00	4.27E+00	2.29E+00	1.73E+00	3.97E-03
19.00	7.56E+00	4.08E+00	2.39E+00	1.50E+00	5.62E-03
20.00	6.83E+00	3.88E+00	2.50E+00	1.30E+00	8.87E-03
21.00	6.20E+00	3.67E+00	2.64E+00	1.14E+00	1.50E-02
22.00	5.68E+00	3.45E+00	2.81E+00	9.91E-01	2.42E-02
23.00	5.29E+00	3.20E+00	3.03E+00	8.67E-01	2.87E-02
24.00	4.99E+00	2.92E+00	3.33E+00	7.58E-01	2.19E-02
25.00	4.78E+00	2.60E+00	3.64E+00	6.63E-01	1.38E-02
26.00	4.62E+00	2.27E+00	3.38E+00	5.66E-01	8.71E-03
27.00	4.49E+00	1.94E+00	2.74E+00	4.49E-01	5.81E-03
28.00	4.39E+00	1.60E+00	1.45E+00	3.52E-01	4.10E-03
29.00	4.34E+00	1.15E+00	1.56E+00	2.65E-01	3.03E-03
30.00	4.33E+00	7.11E-01	2.35E+00	1.89E-01	2.32E-03
31.00	4.41E+00	3.35E-01	1.54E+00	8.18E-02	1.84E-03
32.00	4.62E+00	3.11E-01	5.70E-01	5.69E-02	1.50E-03
33.00	4.87E+00	2.81E-01	6.43E-01	2.63E-02	1.25E-03
34.00	4.12E+00	9.58E-02	8.46E-01	6.40E-03	1.05E-03
35.00	3.04E+00	6.90E-03	1.62E-01	4.16E-03	9.06E-04
36.00	1.85E+00	—	3.08E-03	2.89E-03	7.89E-04
37.00	1.80E+00	—	—	1.03E-03	1.79E-04
38.00	7.07E-01	—	—	—	7.02E-04
39.00	1.26E-02	—	—	—	3.82E-04
40.00	—	—	—	—	4.35E-04
41.00	—	—	—	—	5.70E-04
42.00	—	—	—	—	3.88E-04
43.00	—	—	—	—	1.15E-03
44.00	—	—	—	—	—
45.00	—	—	—	—	—
σ_{prod} (b)	4.98E-01	2.31E-01	8.59E-02	3.69E-01	1.69E-01
E_{av} (MeV)	1.04E+01	9.02E+00	1.52E+01	4.64E+00	3.10E+00
K (fGy· m^2)	—	1.44E+00	9.02E-01	1.18E+00	—
$\Sigma_{A<4} K_A$					3.52E+00
K_{recoil} non-elastic ($A > 4$)					4.10E-01
K_{recoil} elastic					2.80E-01
K_{total}					4.21E+00

Incident Energy: $E_n = 50.00$MeV

Energy (MeV)	Lab angle–integrated emission spectra: (mb/MeV)				
	$d\sigma_n/dE$	$d\sigma_p/dE$	$d\sigma_d/dE$	$d\sigma_\alpha/dE$	$d\sigma_\gamma/dE$
1.00	4.39E+01	1.81E+01	3.64E+00	8.41E+01	2.16E+01
2.00	4.26E+01	2.14E+01	3.75E+00	7.34E+01	2.06E+01
3.00	3.76E+01	2.13E+01	3.48E+00	5.96E+01	2.49E+01
4.00	3.26E+01	1.76E+01	3.32E+00	3.96E+01	5.70E+01
5.00	2.66E+01	1.47E+01	3.22E+00	2.59E+01	4.68E+00
6.00	2.22E+01	1.25E+01	2.84E+00	1.92E+01	2.80E+00
7.00	1.93E+01	1.06E+01	2.43E+00	1.56E+01	7.35E-01
8.00	1.70E+01	8.98E+00	2.17E+00	1.25E+01	1.48E+00
9.00	1.51E+01	7.80E+00	2.01E+00	9.88E+00	1.78E-01
10.00	1.34E+01	6.82E+00	1.89E+00	7.73E+00	4.60E-04
11.00	1.21E+01	5.98E+00	1.80E+00	6.10E+00	3.98E-04
12.00	1.10E+01	5.32E+00	1.73E+00	4.83E+00	5.74E-04

Incident Energy: $E_n = 50.00$MeV: cont.

Energy (MeV)	Lab angle–integrated emission spectra: (mb/MeV)				
	$d\sigma_n/dE$	$d\sigma_p/dE$	$d\sigma_d/dE$	$d\sigma_\alpha/dE$	$d\sigma_\gamma/dE$
13.00	1.01E+01	4.83E+00	1.68E+00	3.84E+00	7.98E-04
14.00	9.44E+00	4.45E+00	1.64E+00	3.09E+00	1.16E-03
15.00	8.87E+00	4.16E+00	1.61E+00	2.52E+00	1.72E-03
16.00	8.38E+00	3.96E+00	1.59E+00	2.08E+00	2.48E-03
17.00	7.97E+00	3.83E+00	1.57E+00	1.73E+00	3.20E-03
18.00	7.60E+00	3.73E+00	1.56E+00	1.46E+00	4.01E-03
19.00	7.26E+00	3.66E+00	1.55E+00	1.25E+00	5.61E-03
20.00	6.96E+00	3.61E+00	1.55E+00	1.07E+00	8.82E-03
21.00	6.67E+00	3.57E+00	1.55E+00	9.31E-01	1.49E-02
22.00	6.40E+00	3.54E+00	1.56E+00	8.11E-01	2.40E-02
23.00	6.15E+00	3.51E+00	1.58E+00	7.10E-01	2.82E-02
24.00	5.90E+00	3.47E+00	1.60E+00	6.23E-01	2.13E-02
25.00	5.67E+00	3.41E+00	1.62E+00	5.49E-01	1.33E-02
26.00	5.45E+00	3.33E+00	1.66E+00	4.83E-01	7.76E-03
27.00	5.24E+00	3.22E+00	1.70E+00	4.25E-01	5.18E-03
28.00	5.05E+00	3.10E+00	1.75E+00	3.73E-01	3.66E-03
29.00	4.86E+00	2.95E+00	1.81E+00	3.27E-01	2.70E-03
30.00	4.68E+00	2.79E+00	1.89E+00	2.85E-01	2.07E-03
31.00	4.51E+00	2.62E+00	1.98E+00	2.47E-01	1.64E-03
32.00	4.35E+00	2.43E+00	2.10E+00	2.14E-01	1.33E-03
33.00	4.19E+00	2.24E+00	2.24E+00	1.83E-01	1.10E-03
34.00	4.05E+00	2.05E+00	2.41E+00	1.55E-01	9.26E-04
35.00	3.91E+00	1.85E+00	2.43E+00	1.29E-01	7.91E-04
36.00	3.77E+00	1.67E+00	2.30E+00	1.05E-01	6.85E-04
37.00	3.65E+00	1.51E+00	1.96E+00	8.86E-02	6.00E-04
38.00	3.53E+00	1.41E+00	1.01E+00	7.08E-02	5.31E-04
39.00	3.43E+00	1.21E+00	1.45E+00	6.01E-02	4.74E-04
40.00	3.35E+00	7.09E-01	1.73E+00	4.56E-02	4.27E-04
41.00	3.31E+00	3.79E-01	1.02E+00	3.09E-02	3.87E-04
42.00	3.31E+00	2.88E-01	4.69E-01	1.78E-02	3.53E-04
43.00	3.15E+00	1.65E-01	7.17E-01	9.92E-03	3.25E-04
44.00	2.67E+00	4.22E-02	4.84E-01	5.71E-03	3.00E-04
45.00	2.86E+00	4.02E-03	2.31E-02	—	2.79E-04
46.00	2.80E+00	—	—	—	2.60E-04
47.00	1.92E+00	—	—	—	2.10E-04
48.00	3.62E-01	—	—	—	2.73E-04
49.00	1.14E-01	—	—	—	1.86E-04
50.00	1.27E-01	—	—	—	2.45E-04
51.00	2.29E-02	—	—	—	1.78E-04
52.00	—	—	—	—	5.58E-04
53.00	—	—	—	—	—
54.00	—	—	—	—	—
55.00	—	—	—	—	—
σ_{prod} (b)	4.75E-01	2.35E-01	8.40E-02	3.82E-01	1.34E-01
E_{av} (MeV)	1.32E+01	1.19E+01	1.95E+01	4.61E+00	3.19E+00
K (fGy· m^2)	—	1.93E+00	1.13E+00	1.21E+00	—
$\Sigma_{A<4}K_A$					4.27E+00
K_{recoil} non-elastic ($A > 4$)					4.00E-01
K_{recoil} elastic					2.31E-01
K_{total}					4.90E+00

Incident Energy: $E_n = 60.00$MeV

Energy (MeV)	Lab angle-integrated emission spectra: (mb/MeV)				
	$d\sigma_n/dE$	$d\sigma_p/dE$	$d\sigma_d/dE$	$d\sigma_\alpha/dE$	$d\sigma_\gamma/dE$
1.00	4.06E+01	1.68E+01	2.70E+00	7.12E+01	1.85E+01
2.00	3.85E+01	1.89E+01	3.00E+00	6.30E+01	2.04E+01
3.00	3.36E+01	1.88E+01	3.04E+00	5.49E+01	2.02E+01
4.00	2.89E+01	1.58E+01	2.99E+00	3.99E+01	4.88E+01
5.00	2.42E+01	1.34E+01	2.99E+00	2.66E+01	5.33E+00
6.00	2.03E+01	1.18E+01	2.76E+00	1.85E+01	3.04E+00
7.00	1.75E+01	1.03E+01	2.42E+00	1.52E+01	2.84E+00
8.00	1.51E+01	8.88E+00	2.14E+00	1.27E+01	2.38E-01
9.00	1.33E+01	7.79E+00	1.94E+00	1.03E+01	4.69E-01
10.00	1.16E+01	6.87E+00	1.77E+00	8.23E+00	3.35E-04
11.00	1.02E+01	6.06E+00	1.62E+00	6.55E+00	3.38E-04
12.00	9.13E+00	5.30E+00	1.49E+00	5.27E+00	4.81E-04
13.00	8.25E+00	4.71E+00	1.39E+00	4.17E+00	7.06E-04
14.00	7.55E+00	4.26E+00	1.31E+00	3.29E+00	1.03E-03
15.00	6.98E+00	3.89E+00	1.24E+00	2.64E+00	1.54E-03
16.00	6.52E+00	3.61E+00	1.18E+00	2.14E+00	2.24E-03
17.00	6.15E+00	3.39E+00	1.13E+00	1.76E+00	2.93E-03
18.00	5.83E+00	3.21E+00	1.09E+00	1.46E+00	3.73E-03
19.00	5.57E+00	3.07E+00	1.04E+00	1.22E+00	5.23E-03
20.00	5.35E+00	2.96E+00	1.01E+00	1.03E+00	8.24E-03
21.00	5.16E+00	2.87E+00	9.75E-01	8.87E-01	1.40E-02
22.00	5.01E+00	2.81E+00	9.47E-01	7.72E-01	2.27E-02
23.00	4.88E+00	2.76E+00	9.24E-01	6.77E-01	2.67E-02
24.00	4.76E+00	2.72E+00	9.06E-01	6.02E-01	2.02E-02
25.00	4.66E+00	2.69E+00	8.92E-01	5.41E-01	1.27E-02
26.00	4.57E+00	2.67E+00	8.83E-01	4.89E-01	8.01E-03
27.00	4.49E+00	2.64E+00	8.78E-01	4.45E-01	5.34E-03
28.00	4.41E+00	2.62E+00	8.78E-01	4.06E-01	3.75E-03
29.00	4.34E+00	2.59E+00	8.81E-01	3.72E-01	2.75E-03
30.00	4.27E+00	2.56E+00	8.89E-01	3.42E-01	2.10E-03
31.00	4.20E+00	2.53E+00	9.01E-01	3.14E-01	1.65E-03
32.00	4.14E+00	2.50E+00	9.17E-01	2.88E-01	1.32E-03
33.00	4.07E+00	2.47E+00	9.38E-01	2.63E-01	1.08E-03
34.00	4.01E+00	2.43E+00	9.63E-01	2.39E-01	9.03E-04
35.00	3.94E+00	2.38E+00	9.93E-01	2.17E-01	7.64E-04
36.00	3.86E+00	2.34E+00	1.03E+00	1.98E-01	6.26E-04
37.00	3.78E+00	2.28E+00	1.07E+00	1.80E-01	5.46E-04
38.00	3.69E+00	2.22E+00	1.11E+00	1.63E-01	4.81E-04
39.00	3.60E+00	2.16E+00	1.16E+00	1.48E-01	4.27E-04
40.00	3.50E+00	2.09E+00	1.22E+00	1.34E-01	3.82E-04
41.00	3.40E+00	2.01E+00	1.30E+00	1.22E-01	3.45E-04
42.00	3.29E+00	1.93E+00	1.38E+00	1.12E-01	3.13E-04
43.00	3.19E+00	1.85E+00	1.48E+00	1.04E-01	2.86E-04
44.00	3.10E+00	1.76E+00	1.62E+00	9.70E-02	2.62E-04
45.00	3.02E+00	1.68E+00	1.76E+00	8.35E-02	2.42E-04
46.00	2.94E+00	1.60E+00	1.47E+00	6.20E-02	2.24E-04
47.00	2.88E+00	1.55E+00	1.27E+00	5.41E-02	2.09E-04
48.00	2.84E+00	1.52E+00	8.97E-01	4.36E-02	1.95E-04
49.00	2.84E+00	1.23E+00	9.65E-01	3.56E-02	1.83E-04
50.00	2.88E+00	8.09E-01	1.43E+00	2.28E-02	1.73E-04
51.00	3.00E+00	5.35E-01	1.14E+00	1.80E-02	1.63E-04
52.00	3.18E+00	2.87E-01	5.03E-01	4.73E-03	1.55E-04

Technical Information Department • Lawrence Livermore National Laboratory
University of California • Livermore, California 94550